UNIVERSITÄT FÜR BODENKULTUR WIEN
University of Natural Resources
and Life Sciences, Vienna

Master Thesis

Three recombinant proteins one challenge: Stabilization of CHO clones and evaluation of the production capacity

submitted by

Lukas PRANTER, BSc

in the framework of the Master programme

Biotechnology

in partial fulfilment of the requirements for the academic degree

Diplom-Ingenieur

Vienna, April 2022

Supervisor:

Univ.Prof Dipl.-Ing. Dr.nat.techn. Renate Kunert
Institute of Animal Cell Technology and System Biology
Department of Biotechnology

Affidavit

I hereby declare that I have authored this master thesis independently, and that I have not used any assistance other than that which is permitted. The work contained herein is my own except where explicitly stated otherwise. All ideas taken in wording or in basic content from unpublished sources or from published literature are duly identified and cited, and the precise references included.

I further declare that this master thesis has not been submitted, in whole or in part, in the same or a similar form, to any other educational institution as part of the requirements for an academic degree.

I hereby confirm that I am familiar with the standards of Scientific Integrity and with the guidelines of Good Scientific Practice, and that this work fully complies with these standards and guidelines.

Vienna, 13.04.2022 Lukas PRANTER

Acknowledgments

I would like to thank Prof. Renate Kunert for giving me the opportunity to work in her research group and for being a resourceful, wise, patient and dedicated teacher. She and others made the laboratory feel like a second home to me. I would like to thank co-supervisor Patrick Mayrhofer for guiding me with his exceptional knowledge, competence, immense motivation and always trying to laugh at my jokes. I would like to thank Willibald Steinfellner for his unwavering support in my first steps at the lab, teaching me everything there is to know. Furthermore, I would like to thank my friend and lab colleague Thomas Holzer for helping and supporting me every way he could. Last but not least, I would like to thank my parents for always believing in me and their support.

Abstract

The development of recombinant protein production clones in animal cell culture technology is a time consuming and labor-intensive process. Especially, the nature of the individual protein can cause unexpected challenges and therefore the methodological platforms need to be developed carefully. The aim of this thesis was to generate stable CHO clones valid for the production of recombinant proteins in high quality and proof of concept for the production of several mg-amounts. The proteins of choice were the SARS-COV2 spike protein, its receptor binding domain (RBD) and a CD19-Albumin-domain2 (CD19-AD2) fusion construct. Starting with the early transfection pools stable cell lines were generated by limiting dilution subcloning. The performance in simple batch or semi-perfusion setting was studied. In routine batch culture the performance of all final subclones improved significantly over the parental clones. The CD19-AD2 expressing subclones showed higher vitality than the parental clone, which had problems in that regard. One clone expressing the SARS-COV2 spike protein was used in a fed-batch bioprocess mode. Mild hypothermia improved productivity massively compared to a control reactor, while valproic acid addition used for expression enhancer had no effect on productivity. Western blot experiments suggest correct expression of all proteins produced by the subclones. Fluorescence-activated-cell-sorting (FACS) stained for internal protein content affirmed subcloning success from one singular cell. To confirm biological activity of the SARS-COV2 construct, FACS and Western blot binding experiments with purified IgG of SARS-COV2 patient sera were performed. Multi angle light scattering (MALS) of purified reactor supernatant revealed a slight variation of homotrimer and aggregate formation between the different reactors.

Kurzfassung

Die Entwicklung rekombinanter Proteinproduktionsklone in der Tierzellkulturtechnologie ist ein zeit- und arbeitsintensiver Prozess. Insbesondere die Beschaffenheit der einzelnen Proteine kann unerwartete Herausforderungen mit sich bringen, weshalb die methodischen Plattformen sorgfältig entwickelt werden müssen. Ziel dieser Arbeit war es, stabile CHO-Klone zu generieren, die für die Produktion rekombinanter Proteine in hoher Qualität geeignet sind, und einen Konzeptnachweis für die Produktion von mehreren mg-Mengen zu erbringen. Die Proteine der Wahl waren das SARS-COV2-Spike-Protein, seine Rezeptorbindungsdomäne (RBD) und ein CD19-Albumin-domain2 (CD19-AD2) Fusionskonstrukt. Ausgehend von den frühen Transfektionspools wurden durch Subklonierung in limitierender Verdünnung stabile Zelllinien erzeugt. Deren Performance wurde in einfachen Batch- oder Semi-Perfusionskulturen untersucht. In der routinemäßigen Batch-Kultur verbesserte sich die Leistung aller endgültigen Subklone gegenüber den parentalen Klonen erheblich. Die CD19-AD2 exprimierenden Subklone zeigten eine höhere Vitalität als der parentale Klon, der in dieser Hinsicht Probleme hatte. Ein Klon, der das SARS-COV2-Spike-Protein exprimiert, wurde in einem Bioprozess im Fed-Batch-Verfahren eingesetzt. Milde Hypothermie verbesserte die Produktivität im Vergleich zu einem Kontrollreaktor massiv, während die Zugabe von Valproinsäure als Expressionsverstärker keine Auswirkungen auf die Produktivität hatte. Western-Blot-Experimente deuten auf eine korrekte Expression aller von den Subklonen produzierten Proteine hin. Fluoreszenz-aktivierte Zellsortierung (FACS), gefärbt nach internem Proteingehalt, bestätigte den Erfolg der Subklonierung aus einer einzigen Zelle. Um die biologische Aktivität des SARS-COV2-Konstrukts zu bestätigen, wurden FACS- und Western-Blot-Bindungsexperimente mit gereinigtem IgG aus SARS-COV2-Patientenseren durchgeführt. Die Mehrwinkel-Lichtstreuung (MALS) des gereinigten Reaktorüberstands zeigte eine leichte Variation der Homotrimer- und Aggregatbildung zwischen den verschiedenen Reaktoren.

Index

1. Introduction

The production of biologically active proteins continues to break new all-time highs, with demand for high-quality biopharmaceuticals rising. Most of these high value products are preferably produced by fermentation of mammalian cell lines. The alternatives, microorganisms like bacteria or yeast, have difficulties expressing complex proteins due to complex post translational modifications. New production techniques, media development as well as cell line development pushed the previously notoriously low producing mammalian cells to new boundaries, realizing protein titers beyond 10 g/L[1]. The most used stable production cell lines are still the Chinese Hamster Ovary (CHO) lines, because of various reasons: Firstly, the glycosylation pattern of therein expressed proteins is strikingly similar to that of human proteins[2], which is not only important for bioactivity but also precludes immune reactions from patients. Secondly, human viruses cannot propagate in CHO cells, making the process safer to work with, decreasing downstream processing and safety testing. Thirdly, biopharmaceuticals produced in CHO cells have been approved by the FDA and other agencies for years, and the production processes were standardized, which facilitates getting the costly approval for a newly developed pharmaceutical based on the CHO. This might be an important reason for the continuous industrial use of CHO cell lines as production vehicles, as regulators might feel more at ease approving a protein produced in a very well-studied cell factory, therefore reducing the cost to develop new products.

One of the most important, albeit time-consuming steps in cell line development is the subcloning process. It can improve productivity and quality of the desired protein and to assure consistent product quality it is necessary for an industrial production strain to come from a single cell subclone. To achieve single-cell descendance (proof of which is also required by regulators), various methods to ease the process are nowadays available. The most important of these are fluorescence assisted cell sorting, simple dilution and sometimes cell printing. General advancement in automatic processes as well as new developments in single cell imaging and microfluidics greatly reduced the time it takes for the sorting process and the isolation of single cells. Even though methods for cell sorting and singling out cells have drastically improved over the last decades, the growth of a single cell to a culture ready to be expanded is still the most time-consuming step[3]. In our experiments we subcloned 3 cell lines expressing 3 different proteins, 2 of which are difficult to express and have notoriously low production titers, namely the SARS-COV-2 envelope protein, often called Covid Spike soluble (CSs) and the extracellular part of the cluster of differentiation 19 (CD19). The power of subcloning to generate high-performance cell lines comes from epigenetic changes, like DNA-methylation and chromatin-packaging[4]. These arise by the stress induced when the cells miss cell-to-cell communication, which is the case when the cells get singled out in the subcloning process[4].

CHO fermentation is commonly performed in either of three modi operandi, batch, fed-batch and continuous process. The batch process basically defines the cultivation of the cells with a fixed supply of nutrients only at the initial seeding. As soon as the carbon or nitrogen source in the media runs out, cells have to be harvested or transferred. In a fed-batch on the other hand, low volumes of concentrated nutrient solution are added regularly by a distinct feeding scheme to enhance the longevity of the process. Thereby, the nutrient and metabolite content of the reactor can be controlled, or the feeding can be adjusted according to metabolite content. This can reduce the buildup of harmful cell metabolites like lactate and ammonia. In a continuous fermentation process, constant media exchange allows long processes and high cell densities. One example thereof is the perfusion process, which consist of a reactor with an outlet port outfitted with a membrane and an

inlet port for media supplementation. Cell retention is done mostly by membranes allowing a continuous media exchange. Semi-perfusion down scale models were developed to gather high quantities of supernatant and to observe cells in a high cell density setting. In this method, cells are cultivated in shaking tubes which can be centrifuged. Every 24 hours, a complete media exchange is achieved by centrifuging down the cells, harvesting the supernatant and replacing it with fresh media.

The top-performing subclone of our CSs expressing cell line was fermented under fed-batch conditions, with either one of two productivity-enhancing changes[5–9]: either valproic acid (VPA) addition or cultivation under mild hypothermia.

As fed-batch is still the most often used cultivation method for CHO cells in an industrial application[10], the performance of our top-clone in this setting might give an indication of the feasibility for a scale-up and production of the CSs.

To assess if our recombinant CSs and its receptor-binding domain (RBD) construct are biologically active, we performed Western blots and flow cytometry with HyperimmuneIgGs (Takeda), which are concentrated and purified IgGs from SARS-COV2 positive patients.

Covid Spike soluble (CSs)

The current global SARS-COV-2 coronavirus pandemic has put into spotlight one protein more than ever: the SARS-COV-2 spike protein (CS). This homotrimer decorates the membrane of the SARS-COV-2 beta coronavirus and mediates membrane fusion with epithelial lung cells by docking at the angiotensin-converting-enzyme-2 (ACE2). The CS changes its conformation from a prefusion state to a postfusion state upon ACE2 binding[11], providing energy for overcoming the kinetic barriers between two membranes, like repulsive hydration forces[12]. The CS in its prefusion state is the most abundant protein on the virion surface, a target for humoral immune response and therefore a prime vaccine candidate as well as used extensively for immunological assays[13].

The CS monomer has a molecular weight ranging between 180-200 kDa containing 1273 amino acids [14], with 22 potential N-linked glycosylation sites[15 ,16]and 15 disulfide bonds. The CS ectodomain contains 2 functional subunits, firstly S1, which mediates receptor binding and contains the receptor-binding-domain (RBD) and secondly S2, which contains a fusion loop peptide as well as two heptads repeat regions which together mediate the fusion of viral membrane with the host membrane[17,18]. To bind on the ACE2 receptor, the RBD on the S1 has to be in an accessible state, commonly referred to as the “up” conformation, contrary to the “down” formation, which has the RBD inaccessible but corresponds to a more stable state[19,20]. To achieve this, the S1 may temporarily undergo hinge-like conformational movements[20].

The chimeric Covid spike soluble protein (CSs) which we express in our CHO cells derives from the genetic construct (Genbank QJE37812.1) made by the laboratory of Prof. Krammer at the Mount Sinai School of Medicine. This construct features two stabilizing proline modifications at the S2 which favor the more stable prefusion conformation, as well as a modified and thereby deleted multibasic cleavage site which hinders the cleavage between S1 and S2 by furin-like proteases[20–22]. Cleavage at the multibasic cleavage site located at the S1/S2 boundaries is crucial for effective viral entry to the host cells[23]. To enhance trimerization, a T4 fold-on sequence was added right before a 6x His-tag at the C-terminus. The 6x His-tag was inserted to enable purification, detection and quantification.

We expressed the CSs in CHO-K1 cells, and our lab created the CSs expressing initial subclone 131A4. A high-producing subclone was selected by limited dilution subcloning in this master thesis. This

high-producing subclone named “C11” was further cultivated in a fed-batch process with one reactor featuring valproic acid (VPA) addition and the other under mild hypothermia conditions.

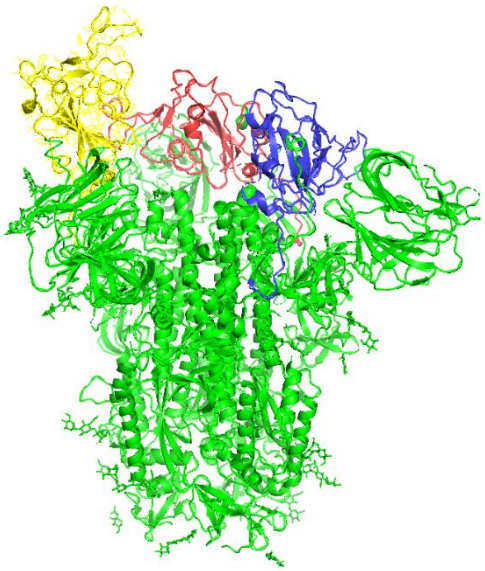

Figure 1: Covid spike homotrimer structure from PDB entry:6crz. The RBDs are colored yellow, red and blue; made with Pymol

Receptor binding domain (RBD)

The receptor binding domain (RBD) of the SARS-COV2 virus is located on the S1 subunit of the CS, namely from amino acids 331 to 524. It has a molecular weight of around 30 kDa. The binding between RBD and the ACE2 is very strong, with 13 hydrogen bonds and 2 salt bridges forming at the SARS-CoV-2 RBD–ACE2 interface[24]. Due to its highly conserved sequence[25] and strong binding of neutralizing antibodies, it can be considered a vaccine candidate more suitable for emerging future variants of the SARS-COV-2[26].

The RBD sequence we expressed in our CHO-K1 cells was provided by the laboratory of Prof. Krammer at the Mount Sinai School of Medicine. The RBD sequence carries the wild type amino-terminal signal peptide of the S protein, along with a C-terminal 6x His-Tag[21]. High titers of around 50 mg/L were already achieved by the laboratory of Prof. Krammer with Expi293F cells. The RBD expressing CHO-K1 clone 2P7 established by our laboratory was subcloned to generate a stable, high expressing clone for future experiments and assays.

Figure 2: RBD structure from PDB entry: 6crz; X-ray structure; made with Pymol

CD19-AD2

The cluster of differentiation 19 (CD19) is a glycoprotein expressed naturally only in B cells, where it functions as one of the most important signaling components[27]. It is therefore a prime candidate for cell type-specific immunotherapies, like chimeric antigen receptor (CAR)-T cell therapies. It is a type 1 transmembrane protein, containing a transmembrane domain with the C-terminus being located in the cytoplasm and the N-terminal end protruding from the cell surface and forming Ig-like domains[27]. It is a difficult-to-express (DTE) protein, due to low expression titers in culture and high amounts of misfolding as well as aggregation[28].

To enhance the stability and solubility of a protein, the addition of a fusion tag is common practice[29]. Our laboratory fused the domain 2 (AD2) of human serum albumin (HSA) to the C-terminus of the CD19 extracellular domain. The AD2 was chosen, instead of the full-length HSA, because of a greatly increased specific productivity in cell culture compared to the full-length albumin fusion tag[30]. With this enhancement and the usage of a bacterial artificial chromosome as a vector to minimize gene silencing[31], specific productivity could be amplified up to 1.4 pg/c/d with the help of the chemical chaperone VPA. To further improve productivity and, more importantly, the viability of the cell line (as the CD19 AD2 expressing clone had low μ of under 0.6 and takes a long time to recover from cryogenic storage), subcloning was performed.

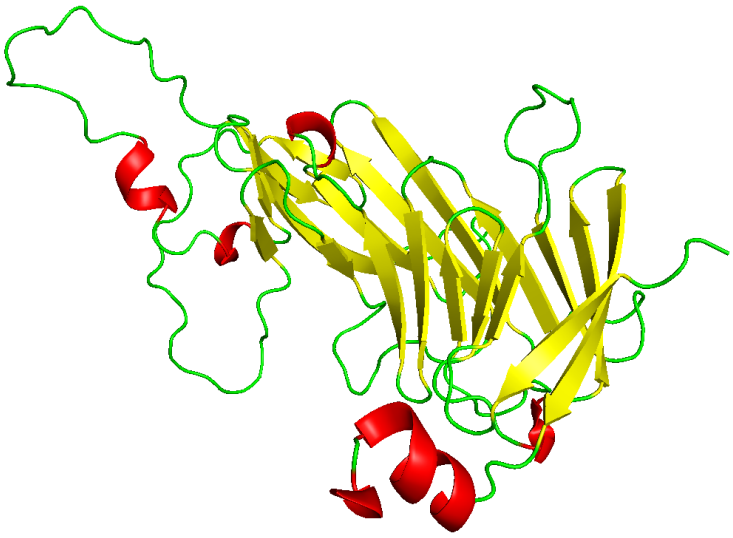

Figure 3: The CD19 extracellular domain, residues P20-K291, from UniProt ID:P15391; made in Pymol, structure from AlphaFold

2. Materials and Methods

2.1 Materials

Different recombinant proteins were used for stabilization of recombinant CHO-clones and their evaluation in upstream fermentation

Recombinant protein	RBD of SARS-COV2	CSs chimeric spike soluble of SARS-COV2	CD19-AD2 fusion protein of the extracellular domain of CD19 with the human albumin domain 2
Parental CHO-K1	2P7	131A4	D19
Cryopreserved subclones	G7; F3; F8	C11; G3; F4	C2; F9; E10
Best subclone	RBD F3	CSs C11	CD19-AD2 F9

2.1.1 Cell culture media

Subcloning medium:

CD CHO (Gibco; Ref:10743-029; Lot: 2095778)

+ 4 mM stable L-Glutamine (200 mM stock; Roti®cell; Ref: 9123; Charge 029279456)

+ 15 mg/L phenol red (5 g/L stock)

+ Human albumin 1 mg/mL (50mg/mL stock; Sigma Aldrich Cat. No. A7223)

+ Transferrin 20 µg/mL (20 mg/mL stock; Merck®, Cat.:9701-10)

+ rEGF 25 ng/mL (0.1 mg/mL stock)

Routine culture medium:

CD CHO (Gibco; Ref:10743-029)

+ 4 mM stable L-Glutamine (200mM stock; Roti®cell; Ref.: 9123; Charge 029279456)

+ 15 mg/L phenol red (5g/L stock)

+ 0.5 mg/mL G418 (50mg/mL stock; Roth; Ref.:2039.3)

+Anti clumping agent 1:500 (Ref.:01-0057AE; Lot:176630)

DOE medium

Cytiva ActiPro Liquid Medium

+ 12.55% Cytiva HyClone™ Cell Boost™ 3

+ 0.25% Cytiva HyClone™ Cell Boost 7b

+4 mM stable L-Glutamine (200mM stock; Roti®cell; Ref: 9123; Charge 029279456)

Fed-batch medium

HyClone™ CDM4HEK293™ (Cat: SH30858.02; Lot: AAG203879; expired: July 2016)

+ 6 mM L-glutamine (200 mM stock)

Feed medium

ActiCHO™ Feed-A Powder Base CD (Cat: 0069.3005; Lot: VC10252123; expired: October 2018)

FidCHO Feed-B CD Powder (Cat: G3137.3005; Lot: VC10688263; expired: July 2018)

Cryopreservation medium

Synth-a-Freeze™ Cryopreservation Medium (Gibco™; Cat: A1254201)

Metabolite contents of the media measured by Bioprofiler:

Table 1: Metabolite content of the different media used in the fermentation; Stable L-glutamine was not measurable in the case of the DoE medium

Metabolite	DoE Medium [mg/L]	CDM4HEK [mg/L]	Feed A [mg/L]	Feed B [mg/L]	CD CHO [mg/L]	Actipro [mg/L]
Glucose	14740	7780	66200	0	6900	6890
Lactate	0	0	0	0	0	0
Glutamine	584 (not measurable)	290	0	0	584 (not measurable)	584 (not measurable)
Glutamate	470	1100	7900	3400	310	400
Ammonium	39	15	0	0	8	41

2.1.2 ELISA, Gels and Western Blots

Nunc MaxiSorp™plate (Invitrogen™ Cat.: 11530627)

Nunc™ 96 well-plate (Thermo Fisher Scientific, Cat.: 167008)

TMB substrate solution (Thermo Scientific™, Cat.: 10301494)

10x PBS stock solution: 57.5 g Na_2HPO_4 * H_2O + 10 g KH_2PO_4 + 10 g KCl + 400 g NaCl, fill up to 5 L with dH_2O

Polyvinylpyrrolidone (PVP)

BSA (Bovine serum albumin, Sigma Aldrich® Cat.: A6283)

Tween® 20 (Roth® Polyoxyethylene-20-sorbitan monolaurate Cat.:9127.2)

Carbonate buffer: 8.4 g $NaHCO_3$ +4.2 g Na_2CO_3, fill up to 1 L with dH_2O

H_2SO_4 (Roth® Sulphuric acid 25% Cat. No. 0967.1)

RBD

Coating: CR3022 1mg/mL stock (Absolute antibody; CN: Ab01680-10.0; LN: T2015A01)

Conjugate: anti-6x-His-Tag monoclonal Antibody (HIS.H8), HRP (Ref.: MA1 21315-HRP; Lot: UJ283761)

CSS

Coating: ACE2wt-Fc (HEK 8.5 mg/mL)

Conjugate 1: anti 6x-His Tag Monoclonal Antibody (HIS.H8), Biotin (Cat: MA1-21315-BTIN)

Conjugate 2: Streptavidin-HRP 1:4000 (REF: 11089153001)

CD19:

Coating: Human Albumin Polyclonal Antibody (anti-HSA) 1 mg/mL (Bethyl Laboratories; CAT: A80-128A) in carbonate buffer (pH 9.6)

Blocking buffer:

PBS + 1% PVP

Wash buffer:

PBS + 0.1% Tween

Dilution buffer:

PBS +0.1% Tween + 1% PVP

Conjugate 1: HIB19, Biotin-anti-human CD19 antibody (0.5mg/mL; Biolegend; CAT:302204)

Conjugate 2: Streptavidin-HRP (Roche, REF: 11089153001)

BCA-assay

RIPA Lysis and Extraction Buffer (Thermo Scientific™ Cat: 89900)

QuantiPro™ working reagents (Sigma Aldrich Cat: NA.84)

Intracellular Protein content by flow cytometry

FACS buffer: 0.1M TrisHCl, 2mM $MgCl_2$, 0.1% Triton X-100, adjust to pH 7.4

FACS buffer + 20% fetal bovine serum (FCS): add 20% v/v FCS to the FACS buffer

Antibodies:

CR3022-biotin

6x-His-Tag Monoclonal Antibody (HIS.H8), Biotin (Cat: MA1-21315-BTIN) (1:100)

Hyperimmune-IgG (Takeda)

Streptavidin-Alexa 647 (Invitrogen Cat.:S21374)

LDS-PAGE

NuPAGE™ 4%-12% Bis-Tris, 15well, 15µL/well (Cat.: NP0323BOX)

NuPAGE™ LDS Sample Buffer (4X), (Cat.: NP0007)

DTT (dithiothreitol) Thermo Scientific™ (Cat.: R0861)

MOPS running buffer

Silver staining

Fixation solution: 50% Ethanol/10% acetic acid in water

Incubation Solution: 150 mL Ethanol

+ 1.75 g $Na_2S_2O_3*5H_2O$ (Sodiumthiosulfate pentahydrate)

+ 34 g $C_2H_3NaO_2$ (Sodium acetate)

Fill up to 500 mL with H_2O

+62.5 µl Glutaraldehyd / 25mL (prepare fresh)

Silver Solution: 0.25 g $AgNO_3$ in 500 mL H_2O

Develop Solution: 12.5 g Na_2CO_3 in 500 mL H_2O

Stop Solution: 0.05M EDTA in H_2O

Western blot

Roti-PVDF membrane, pore size 0.45 µm (Cat:307687458)

Methanol 20%

BSA (Bovine serum albumin) (Sigma Aldrich® Cat.: A6283PBS)

Tween® 20 Roth® Polyoxyethylene-20-sorbitan monolaurate (Cat.:9127.2)

Streptavidin-HRP (REF: 11089153001)

Chemiluminescence substrate: SuperSignal West Pico Plus substrate (Thermo Fisher).

HyperIgG-biotin (Takeda, biotin-fusion made in our lab)

6x-His-Tag Monoclonal Antibody (HIS.H8), Biotin (Cat: MA1-21315-BTIN)

Glutaraldehyde Sigma-Aldrich® Cat. No. G5882

2.1.3 Protein purification from culture supernatants

Tangential flow filtration

Column: Pellicon XL-Ultrafiltrationsmodul, Biomax 10 kDa, 0.005 m^2

Äkta system

Column: HisTrap HP (Cytiva)

Stripping buffer: dH_2O + 50 µM EDTA, + 20 mM phosphate, 500 mM NaCl

Running buffer: dH_2O + 20 mM imidazole, + 20 mM phosphate, 500 mM NaCl

Elution buffer: dH_2O + 500 mM imidazole, + 20 mM phosphate, 500 mM NaCl

Phosphate buffer, 10x stock: 22 g Na_2HPO_4, +6.25 g $NaH_2PO_4*H_2O$, + 117 NaCl

2.2 Methods

2.2.1 Cell culture

Subcloning with growth factors

Prepare the subcloning media. Measure viable cell density (VCD) of the to be subcloned culture with the ViCell XR. If the cells are taken from cryogenic storage, at least 2 passages are recommended before subcloning. Dilute to 10E3 cells/mL, prepare at least 8mL. This corresponds to 50 cells/50µL. Plate 5mL of this dilution (50 µL/well), which corresponds to ¼ of the 384 well plate. Prepare second dilution (at least 15mL) by diluting the rest of the first dilution 1:5. Plate 11mL of second dilution, corresponding to 10 cells/50µL. For the final dilution, dilute the second dilution 1:5. This corresponds to 2cells/50µL. Plate 20 mL on one additional whole 384-well plate. Due to dilution error and random distribution, some wells will only contain 1 cell/well. These are marked under the microscope and preferred for further selection. Incubate at 37°C with 7% CO_2. After 10-14 days each colonized well gets fed 50µL of RC-medium. Let the wells get colonized until a clear discoloration from the phenol red to orange/yellow is visible. Expand the growing wells by transferring from each 50µL of their cell suspension to 96 well plates. Add 150 µL of RC-medium to each well. After roughly 5 days the wells on the 96-well plate should be well colonized, and a semi-quantitative ELISA is done for further selection. Expand the best clones on 96-well plates, for each clone one row. After all wells on each row are well colonized make a quantitative ELISA. Of the best performers transfer each whole row, which should contain only one subclone, to a 50 mL shaking tube. Add 5mL of RC medium to the shaking tube, for a working volume of around 7 mL. After 4 passages make another final selection with quantitative ELISA, but also taking into account specific growth µ and specific productivity, which are calculated.

Cryopreservation of cells

Cool Mr. Frosty™ (Thermo Scientific™) and cryogenic tubes (Nunc™) at 4°C. The Measure VCD of the culture to be frozen. Aliquot to at least 5E6 cells/mL. Centrifuge the aliquots at 1000rpm for 6min. Discard the supernatant and subsequently dissolve the cell pellet. Add 1mL of Synth-a-Freeze™ (stored at 4°C) medium per 5E6 cells. Put the cryo-tubes in the Mr. Frosty, and let it cool down over night at -80°C. Next day the cryo-tubes can be put in liquid nitrogen storage.

Thawing of frozen cells

It is important to work as fast as possible, to minimize the damage done to the cells while thawing. Cool the culture medium to 4°C.As soon as the cryo-tubes are taken out of liquid nitrogen storage, drop them in ethanol. In the laminar flow hood warm the tubes with the palm of your hands. Give the liquid content of the cryo-tubes in 4°C cold culture medium. Centrifuge for 10 min at 1000rpm. Decant the supernatant, dissolve the cell pellet and fill up with 10 mL of pre-warmed cell culture medium.

Routine cell culture

Working sterile under the laminar flow hood required. Measure the viable cell density by ViCellXR, at least 0.7 mL required. If VCD is over 1E7 cells/mL, dilution with PBS is necessary to get accurate measurements. Calculate required volume of cell suspension for 3E5 cells/mL in with a total working volume of 10 mL in 50 mL shaking tubes. Transfer all the cell suspension in a sterile tube and transfer the required volume back into the old tube. Fill up with fresh, preheated medium to 10 mL. Put back into shaker. Passage every 3 to 4 days. Incubation in Kühner shaker at 37°C, 7% CO_2 and 220 rpm.

Semiperfusion culture

In our experiments, we used shaking tubes with a volume of 200 mL, and a working volume of 50 mL. These tubes were not designed for cell culture and therefore did not feature a sterile filtration system in the cap, which is normally the case. To allow oxygen flow, the cap was not screwed tightly. To speed up the VCD generation, we usually started with a VCD of at least 1-1.5E6 cells/mL. The medium used was the DoE-medium. After day 3, exactly every 24h the medium was fully exchanged (after measuring VCD in Vicell XR), by first centrifuging (1000 rpm /3 min) the tubes, discarding the old media, dissolving the pellet and finally resuspending it in fresh medium. The supernatant is kept. Incubation in Kühner shaker at 37°C, 7% CO_2 and 130 rpm.

2.2.2 Analytical methods

ELISA Protocols

Dilution plate for quantitative ELISA

On the Nunc dilution plate: First row used for blank, second and third row for standard (at least 150µL in column H). Fill remaining column H with samples. Add 75 µL of dilution buffer to the remaining wells. Dilute down in 1:2 steps by transferring 75 µL of the samples from column H to column G, repeat with remaining columns. Transfer 50 µL of each well to the Maxisorp plate.

Dilution plate for semi-quantitative ELISA

On the Nunc dilution plate: First row used for blank, second row for standard (at least 150µL on column H). Dilute standard down in 1:2 steps on the plate. Fill the remaining wells with diluted samples, one well for each sample.

RBD

Firstly, prepare the coating solution: 2.5µg/mL of CR3022 (1:400 of 1mg/mL stock) in carbonate buffer (pH 9.6). Coat the Maxisorp plate by applying 50 µL per well with the multipipette. Either coat over night or for at least 2h. Prepare TBS (0.1% Tween in PBS) by adding 0.1% w/v tween to the PBS solution. Prepare blocking solution by adding 2% w/v PVP in TPBS. Wash the plate in the plate washer and get rid of any droplets left by carefully smashing the plate on dry papers. Block the plate by applying 150µL/well blocking buffer for 1h. Prepare sample dilution buffer by adding 1% w/v BSA to TPBS and dilute the samples appropriately (not more than 1:10 dilution steps; 1:10 for semi-quantitative ELISA, 1:20 for supernatant of routine culture, 1:200 for SN of semi-perfusion) on a dilution plate. Wash the Maxisorp plate as before and transfer to each well 50µl from the dilution plate. Incubate for 1h. Prepare the conjugate solution by adding 10µL anti-His-HRP to 5 mL 1%BSA-TPBS. Repeat washing steps. Apply 50 µL of conjugate solution to every well and incubate it for 1h. Repeat washing steps. Add 100 µl TMB substrate per well and at least for 3min, maximum 10min, depending on the intensity of the coloring. Stop the reaction by applying 100 µL H_2SO_4. The OD450 at 620nm reference is measured.

CSs

Coat the Maxisorp plate by adding 50 µL of 5µg/mL ACE2 (ACE2 Ig fusion protein) in PBS (pH 7.4) per well. Incubate for 4h on the plate shaker or overnight at 4°C. Prepare wash buffer TPBS. To prepare the sample dilution buffer, add 1% w/v BSA to the TPBS. Prepare the dilution plate with the samples and the dilution buffer. Wash the Maxisorp plate and get rid of the last droplets by pounding the plate carefully on the table with papers. Dilute the samples appropriately (not more than 1:10 dilution steps; RBD-standard: 1:100 for supernatant of routine culture, 1:50 for semi-quantitative ELISA; CSs standard: 1:10 for SN of semi-perfusion and routine culture, 1:100 for fed-batch SN) on a dilution plate. Apply 50 µL of samples per well and incubate on the plate shaker for an hour. Repeat

washing steps. Prepare 1st conjugate solution by diluting anti-His-biotin in 1% w/v BSA-TPBS and apply 50 µL per well. Incubate on the plate shaker for one hour. Wash the plate in the plate washer. Prepare the 2nd conjugate solution by diluting Streptavidin-HRP 1:4000 in 1% w/v BSA-TPBS. Add 50 µL of the 2nd conjugate on each well and incubate on the plate shaker for 30min. Wash the plate again. Add 100 µL of TMB substrate and incubate on the desk for at least 3 min, with a maximum of 10 min. Stop the reaction by adding 100 µL H_2SO_4. The OD450 at 620nm reference is measured.

CD19

Coat the Maxisorp plate with 50µl of anti-HSA dilution (1:500) in carbonate buffer. Incubate for 4h on the plate shaker or overnight at 4°C. Prepare wash buffer TPBS and wash the plate and consequently knock it on a table with papers to get rid of eventually remaining droplets on the plate. Prepare blocking buffer by adding 1% w/v PVP to PBS. Block the plate by adding 150 µl of blocking buffer per well, incubate on the plate shaker for one hour. Dilute the samples appropriately on a Nunc dilution plate (not more than 1:10 steps; dilute to 1:5 for supernatant of routine culture and semi-quantitative ELISA, 1:50 for SN of semi-perfusion) with dilution buffer, made by adding 1%w/v PVP to TPBS. Prepare 1st conjugate solution by diluting Biotin-AntiHuCD19 1:500 in dilution buffer. Wash the plate. Add 50 µL of 1st conjugate solution to each well and incubate on the plate shaker for 1h. Repeat washing steps. Prepare 2nd conjugate solution by mixing Streptavidin-HRP 1:4000 in dilution buffer. Apply 50 µL per well of the second conjugate on the Maxisorp plate. Incubate for 1h on the plate shaker. Repeat washing steps. Apply 100 µL of TMB substrate per well and let it incubate at least for 5min, maximum 15min, depending on the intensity of the coloring. Stop the reaction by applying 100 µL H_2SO_4. The OD450 at 620nm reference is measured.

LDS-PAGE

Prepare samples: If no dilution required, transfer 13 µL of each sample to Eppendorf tubes. Add 2 µL of demineralized water if non-reducing conditions are requested. If a dilution is required, the proportions of sample to water are adjusted or the sample diluted beforehand with water. Add 5 µL of 4xLDS to each Eppendorf tube. For reducing conditions, add 2 µl of DTT. Incubate the non-reduced samples at 70°C for 10 min and the reduced samples for 98°C for 5min. Load 15 µL per lane on the 15-well gel. Let the gel run in the electrophoresis chamber for ca. 1.5h with around 100V.

Silver Staining

Carefully remove the gel from the glass tiles. Put it in fixation solution for 30 min, afterwards wash with H_2O. Transfer the gel into incubation solution and let it incubate for 15min. Wash the gel 3x 5min with water. Incubate the gel for 10 min in the silver solution and wash it briefly afterwards. Develop the plate in the developing solution while carefully watching for staining, stop the reaction with the stop solution after the gel is sufficiently stained.

Western blot

First cut out the PVDF membrane according to gel size. Activate the PVDF with MeOH for 1min, then wash it with water and subsequently transfer buffer (NuPAGE + MeOH). Blot the gel on the membrane for 1h at 10V and 3mA/cm^2, in our case 160 mA. Block the membrane for 1h in 5% BSA+TPBS under constant, slow shaking. Wash the membrane 3x for 5min in TPBS. Detect for 1h by putting the membrane in antibody (1:100 for HyperIgG-biotin; 1:500 for anti-His-biotin) + 0.5% BSA+TPBS solution. Wash 3x for 5min with TPBS. Incubate the membrane for 30min in Streptavidin-HRP (1:2000 in 0.5% BSA+TPBS). Wash 3x for 5min with TPBS. Develop with chemiluminescence substrate (300 µl+300 µl). Scan in fusion scanner.

Flow cytometry

Ethanol fixation of cells

Centrifuge the cell suspension with 1300 rpm for 5 min. Discard the supernatant if not needed and carefully dissolve the cell pellet by flicking the tube repeatedly. Add 5 mL PBS and vortex. Centrifuge again with 1300 rpm for 5 min. Discard the PBS and dissolve the cell pellet as before. Under constant vortexing, add dropwise 1-2 mL cold ethanol (4°C, 70% EthOH). Store at 4°C.

Sample preparation

Vortex the EthOH -fixated samples and put aliquots of 1.5E6 cells in Eppendorf tubes. Remove the EthOH by first centrifuging (1300 rpm / 7 min) and subsequently decanting the tubes. Wash the cell pellet with FACS-buffer by dissolving it and adding the buffer slowly and dropwise, under vortex. Remove the FACS buffer by centrifugation (1300 rpm / 7min) and subsequent decanting. Resuspend the pellet in 100µL FACS-buffer+20%FCS, again by adding the buffer dropwise under vortex. Incubate it at 37°C for 30min. Directly add 100 µL of 1st antibody, dropwise and under vortex. Dilute beforehand so that the final concentration corresponds to 1:100 (for CR3022 and Anti-His-biotin) or 1:20 (Hyperimmune IgG). Incubate at 37°C for 30 min. Directly add 0.8 mL FACS-buffer for washing and remove it by centrifugation (1300rpm / 7min). Resuspend the cell pellet in 200 µL of Streptavidin-Alexa 647 (1:100 diluted in FACS-buffer+20%FCS). Add the antibody solution dropwise under vortex to ensure no congregation of cells. Incubate at 37°C for 30min. Directly add 0.8 mL of FACS-buffer and then remove it by centrifugation (1300 rpm /7 min). Wash the pellet again in 1 mL FACS-buffer and centrifuge. Resuspend the pellet in 200 µl FACS- buffer. Samples measured in Beckman Coulter's Gallios^{TM}.

Flow cytometry data analysis

Data evaluation was performed by Kaluza software. The forward scatter (FCS), side scatter (SSC) and the fluorescence signal is measured. FCS gives information about the cell size, while SSC gives information about the internal complexity, or granularity, of the cells. In conjunction they allow to differentiate between cell population, even more so with the added measurement of fluorescence. To gate for single cells, FCS and SSC are plotted, and gate A placed (see figure 4). The gated cells are plotted for fluorescence on the x-axis and cell count on the y-axis.

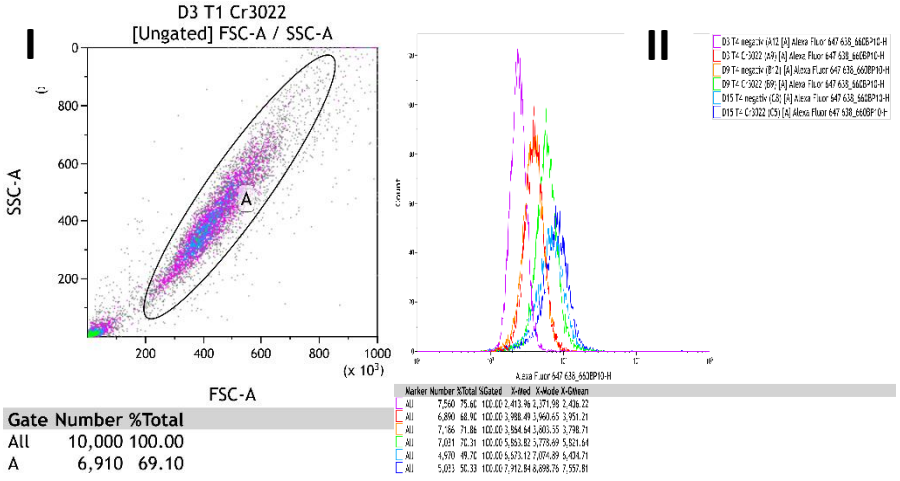

Figure 4.: I: Ungated cells plotted SSC vs FSC, gate A induced to differentiate; II: Gated cells plotted as count vs fluorescence

Cell lysis for protein content

Centrifuge supernatant containing at least 2E6 cells up to a maximum of 10E6 cells for 10 min at 1000 rpm. Discard the supernatant and wash the pellet with 1 mL PBS (4°C). Centrifuge again at 1000 rpm for 10 min. Discard the supernatant and repeat washing steps. Shock freeze the cell pellet in liquid nitrogen and store at -80°C.

Prepare RIPA-buffer: 1 tablet Complete Mini, EDTA-free Roche protease inhibitor in 10 mL RIPA buffer. Resuspend the cell pellet in RIPA-buffer (5E6 cells per mL of buffer) and incubate for 15 min at 4°C. Get rid of possible aggregates of nucleic acids. Centrifugate afterwards at 8000xg for 10min cooled to 4°C. The supernatant contains the cell lysate and can be stored at -20°C.

Protocol BCA assay

Prepare the QuantiPro™ working reagent solution, 150 µL per cell lysate sample: 25x QA + 25 QB +1 OC. Prepare BSA standard dilutions (30 µg, 20 µg, 10 µg, 5 µg, 0.5 µg). Dilute the samples, standard is 1:200. Mix 150 µL sample and 150 µL of Quantipro working reagent solution. Incubate for 1h at 60°C. Let the samples cool down and immediately measure the absorption at 562 nm.

2.2.3 Purification of culture supernatants

Tangential flow filtration (TFF)

The supernatant must be centrifuged and filtrated before being applied to the TFF. First, flush the column, which is stored in NaOH 2x with dH_2O. Apply the supernatant (around 400-500 mL) and concentrate at least 1:5. For our subsequent HisTrap we added 100 mL of running buffer. Keep an eye on the manometers, pressure at retentate should be 2 bar maximum and at the pump 3.5 bar maximum. The retentate is 0.22 µm filtrated and stored at 4°C.

Äkta HisTrap

If the column is dirty, strip the Ni^+ ions by applying stripping buffer. Wash the column with dH_2O and prime the column again by applying Ni^+solution. Flush again with water. Start a blank run, because imidazole absorbs at 280nm, same as proteins. TFF retentate is applied on the column with running buffer. Elute with elution buffer until a discernable difference in the UV signal from the blank run is discernable, at which point the fraction is collected and represents our eluate. Column is then stripped with stripping buffer and afterwards cleaned with 0.5 M NaOH.

Size exclusion chromatography (SEC)

SEC purification was performed using a HiLoad™ 16/600 Superdex™ 200 pg column (GE Healthcare) with the ÄKTA system. Firstly, the column was washed with one column volume dH_2O and then equilibrated with one column volume phosphate buffer. Then, the sample was injected through a loop with a flow rate of 1 mL/min. As soon as the UV signal started to increase, fractions of a volume of 1 mL were collected, sterile filtrated and stored at 4°C. The column was washed with one column volume dH_2O and afterwards column and system were stored in 20% EtOH.

2.2.4 Calculations

Growth rate µ [1/d]: $\mu = \frac{\ln(\frac{x2}{x1})}{t}$

x_2= VCD [cells/mL] after t

x_1= starting VCD [cells/mL]

t = time between x_1 and x_2 [d]

delta integral of viable cell density ΔIVCD [c x d]: $\frac{(x1*V1)-(x2*V2)}{\mu}$

specific productivity qP [pg/c/d]: $\frac{titer2*V2-titer1*V1}{\Delta IVCD}$ *1000000

Titer 1= titer at time 1 [mg/L] V1= volume at time 1 [mL]

Titer 2= titer at time 2 [mg/L] V2= Volume at time 2 [mL]

Specific metabolite consumption qM [pg/c/d]: $\frac{M2*V2-M1*V1}{\Delta IVCD}$*1000000*-1

Specific metabolite production qM [pg/c/d]: $\frac{M2*V2-M1*V1}{\Delta IVCD}$*1,000,000

M1 = metabolite concentration at time 1 [mg/L]

M2 = metabolite concentration at time 2 [mg/L]

Adapted oxygen consumption rate

Oxygen consumption [Nmol/c/d]: O_2*F*24/V_m/ΔIVCD*10000000

O_2= oxygen percentage in the gas inlet

F= Gas inlet flow rate [L/h]

V_m= molar gas volume 22.4 [L/mol]

3. Results

3.1 Subcloning

By diluting the cell suspensions with the subcloning medium in 1:5 steps, we approximated the cells per well in the 384 well plates to either 50 cells per well, 10 cells per well and finally 2 cells per well.

The cloning efficiency (number of wells seeded/number of wells with visible growth) shows how successful the cloning process was. A too high cloning efficiency percentage (over around 30%) in the lowest dilution could point to a wrong dilution, as there are more than 1-2 cells per well, and therefore the survivability increased.

The Following percentages were calculated for each clone:

Table 2: Calculated plating efficiencies of different subcloning experiments

	RBD (from parental clone 2P7)	**CSs (from parental clone 131A4)**	**CD19-AD2 (from parental clone D19)**
2 cells / well	15%	15.7%	14.5%
10 cells / well	99%	99%	90%
50 cells / well	100 %	100%	100 %

In the 2 cells/well dilution the cloning efficiencies do not pass the 16% (Table 2), which pointing to a correct dilution.

Clone selection of growing wells

To further sort out high producers and fast growers we performed semi quantitative ELISAs of all growing well cultures after transferring them from 384 to 96 well plates. Due to dilution and cell count variation, a limited number of wells were inoculated with a single cell. These wells were marked during microscopic inspection and preferred for further selection if growth was visible. Figure 5 shows the typical distribution of ELISA read out of individual wells.

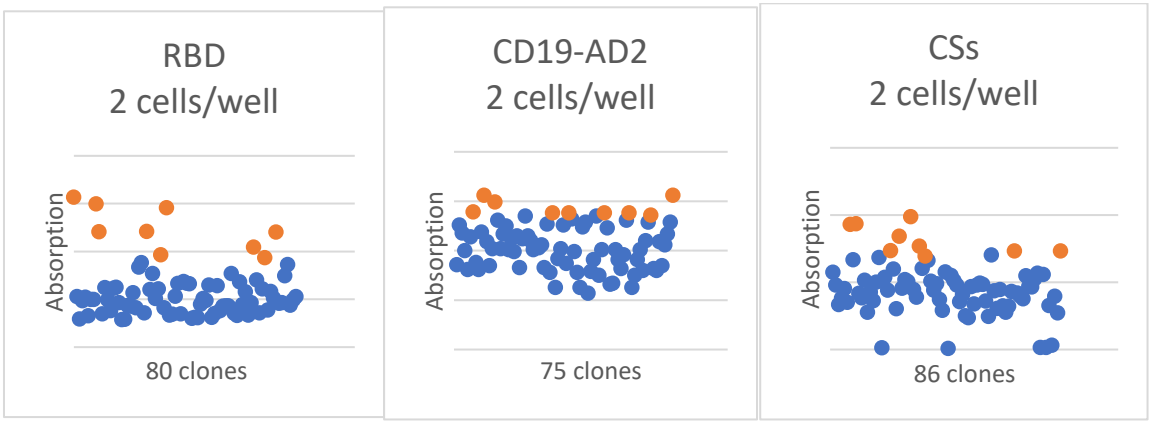

Figure 5: ELISA read out from the diluted supernatant (1:50 for RBD, 1:50 for CSs and 1:20 for CD19-AD2) of the 2-cell derived wells. The orange marked points symbolize wells which were transferred to an expansion plate

At least twenty clones of each recombinant cell line (expressing RBD, CSs and CD19-AD2) with high absorbance in the 96 well plate were transferred to a further expansion plate.

6 clones (featuring the highest titer on the expansion plate) of each parental clone were selected for further analysis and propagated to 50 mL shake tubes. After 3 passages in shake tube cultivation conditions, quantitative ELISAs were performed of each culture, to determine the highest producers. The 3 best performing clones of each cell line were then kept in culture while the others were discarded.

3.1.1 RBD subclones

The 6 subclones selected from the expansion plate were passaged 3 times in routine culture medium and the titer measured by quantitative ELISAs at the 4th or the 3rd day in cultivation. Combined with the cell count data measured by the ViCellXR, the specific productivity and the growth rate µ was calculated for the corresponding timeframe (Figure 6).

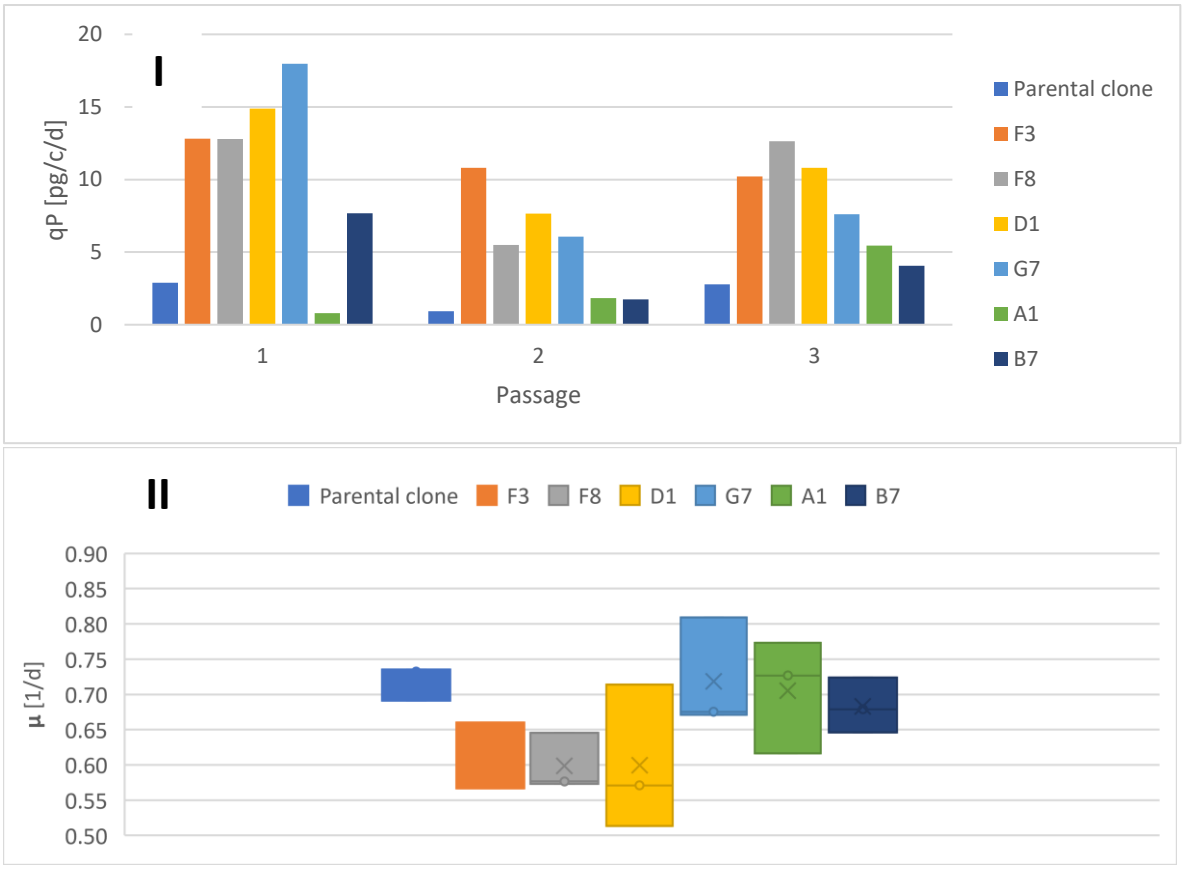

Figure 6: I: specific productivity of the subclones and the parental clones, Titer measured by ELISA, supernatant diluted 1:50; II: μ of the parental clone and subclones

G7 was selected because of its high μ (average over 0.7), consistently high qP between all passages and therefore performing significantly better than the parental clone.

F3 and F8 were chosen because of their high qP between all passages, F3 being the top-producer in passage 2 and F8 being the top-producer in passage 3. Both of them had relatively low average μ (between 0.55 and 0.65) but viability consistently at 99%.

3.1.2 CSs subclones

Seven CSs subclones were selected from the expansion plate and passaged 3 times in ST50 with a working volume of 7 mL. The titer was measured by ELISA at the 4th or the 3rd day in cultivation. Combined with the cell count data measured by the ViCellXR, the specific productivity and the μ were calculated for the corresponding timeframe. Figure 7 shows the qP and the μ for three passages of the expanded clones, in comparison to the parental clone.

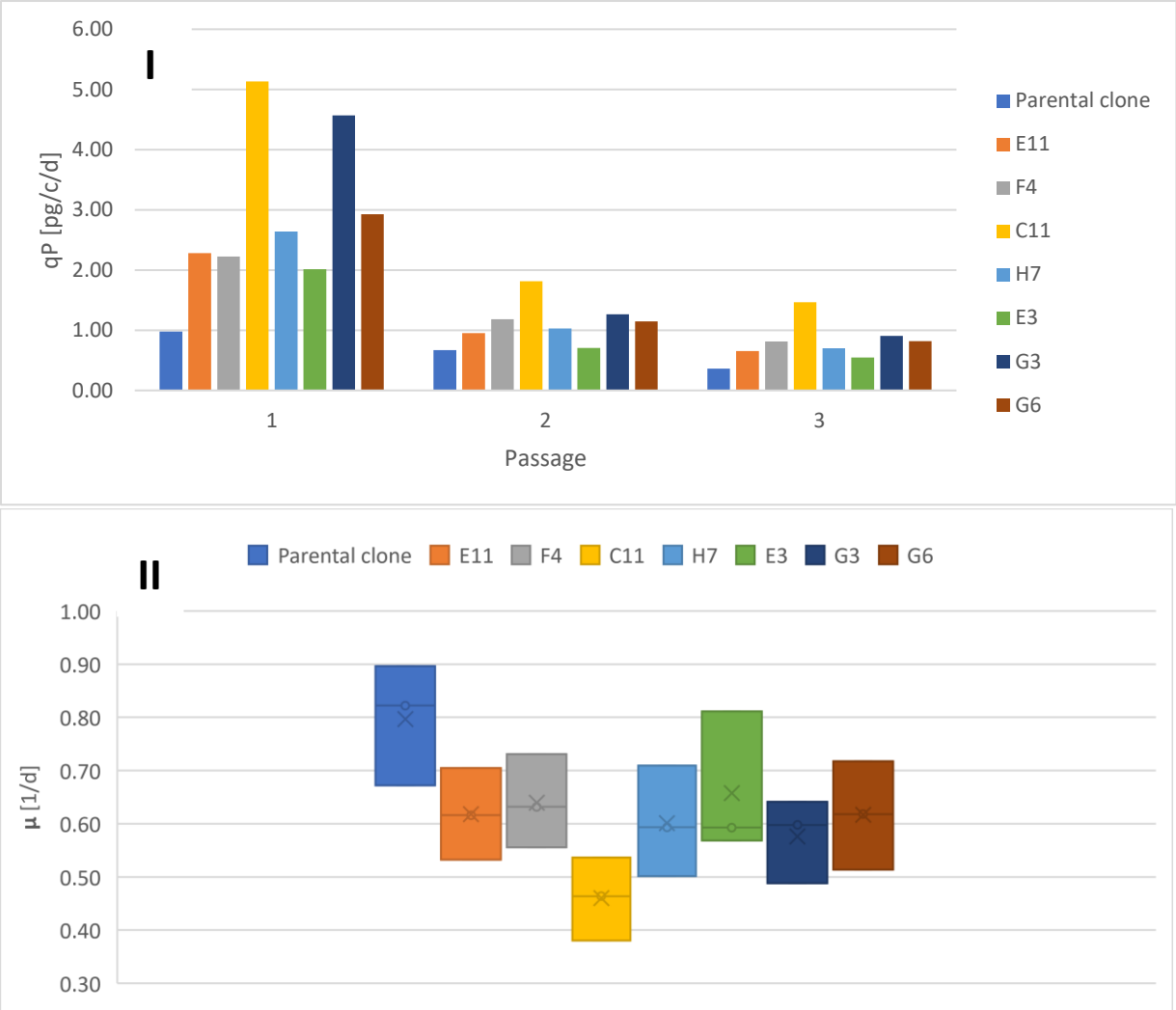

Figure 7: A: specific productivity of the subclones and the parental clones, Titer measured by ELISA (supernatant diluted 1:50) with RBD standard; B: μ of the parental clone and subclones

Of the seven subclones cultivated, C11, F4 and G3 were chosen for further cultivation. C11 was the weakest performer considering growth rate (average μ~0.5), while G3 and F4 both had an average μ of around 0.6 d^{-1}. The parental clone had the highest average μ of 0.8 d^{-1}.

The productivity of all chosen subclones was significantly higher than their parental clone, with C11 reaching 5 pg/c/d in the first passaging cycle, while F4 reached 2.2 pg/c/d and G3 4.6 pg/c/d in the same timeframe. Due to these values being calculated with an RBD standard curve, they are not comparable with the qP values gathered from other experiments calculated with a CSs standard curve.

3.1.3 CD19-AD2 subclones

The six CD19-AD2 subclones selected from the expansion plate were passaged 3 times and the titer measured by Anti-huCD19-AD2-biotin ELISA, coated with Anti-HSA at the 4th or the 3rd day after passaging. Combined with the cell count data measured by the VicellXR, the specific productivity and the μ was calculated for the corresponding timeframe. Figure 8 shows productivity and growth rate of three consecutive passages.

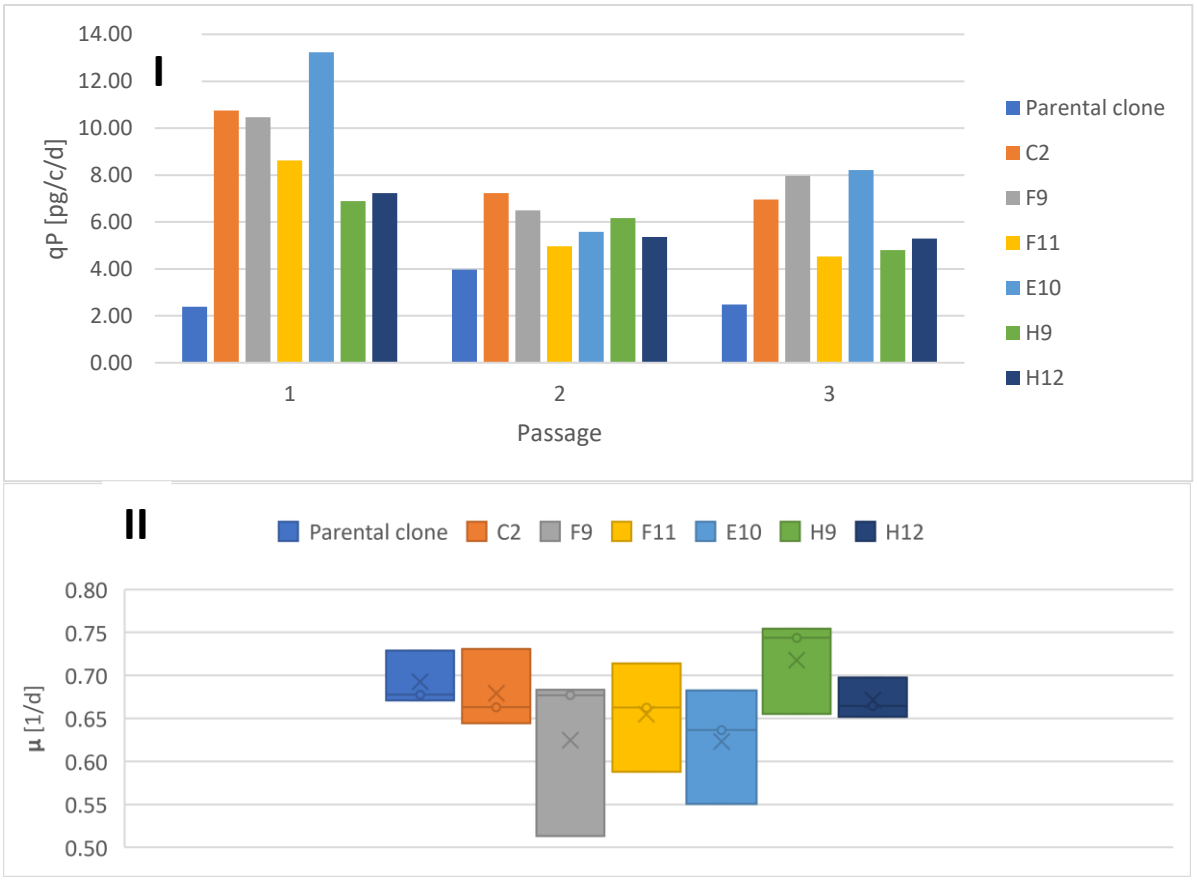

Figure 8: A: specific productivity of the subclones and the parental clones, Titer measured by Anti-huCD19-AD2-biotin ELISA (coated with Anti-HSA, supernatant diluted 1:50); B: μ of the parental clone and subclones

The chosen subclones are C2, F9 and E10. These 3 had the highest productivity over all 3 passage cycles, even though the difference from the parental clone was not as pronounced as with the RBD and CSs subclones (see Figure 6 and Figure 7).

F9 and E10 had slightly lower average μ than the parental clone (~0.6 with F9 and E10 vs 0.7 of the parental clone).

3.2 Semi-perfusion of parental clones

To get an impression of the possible performance of our cell lines in a high cell density setting, we started a semi-perfusion experiment with each of the parental clones. With a complete medium exchange every 24h, high cell densities were achieved. To support this high VCDs we used the DoE medium, which was specifically designed for semi-perfusion settings.

In one ST200, the cultivation medium was supplemented with 1 mM valproic acid starting at day 5 or 6 to see if the chemical chaperone supports recombinant protein production. Valproic acid was determined to be the most efficient chemical chaperone by our group in previous experiments on the difficult to express protein CD19-AD2.

3.2.1 Semi-perfusion of parental RBD clone 2P7 in DoE medium (experiment F198)

The RBD, being a relatively small domain of about 30 kDa is known to be easy to express in HEK cells and comparatively (to the CSs) easy to purify with a HisTrap column. To get a necessary amount of protein for purification experiments and ELISA standards, we started a semi-perfusion. The used working volume was 50 mL in 200 mL shaking tubes, with the lid not containing a sterile filter and therefore being half unscrewed to allow gas exchange. The medium used was our DoE medium (Actipro +12.55% CellBoost3, +0.25% CellBoost7b), with 4mM of stable L-glutamine. To get to high

amount of VCD quickly, the process was seeded with 1.5E6 cells/mL, with a shaking speed of 130 rpm. Figure 9 shows the viable cell density, viability and the specific growth rate of the cells in the semi-perfusion.

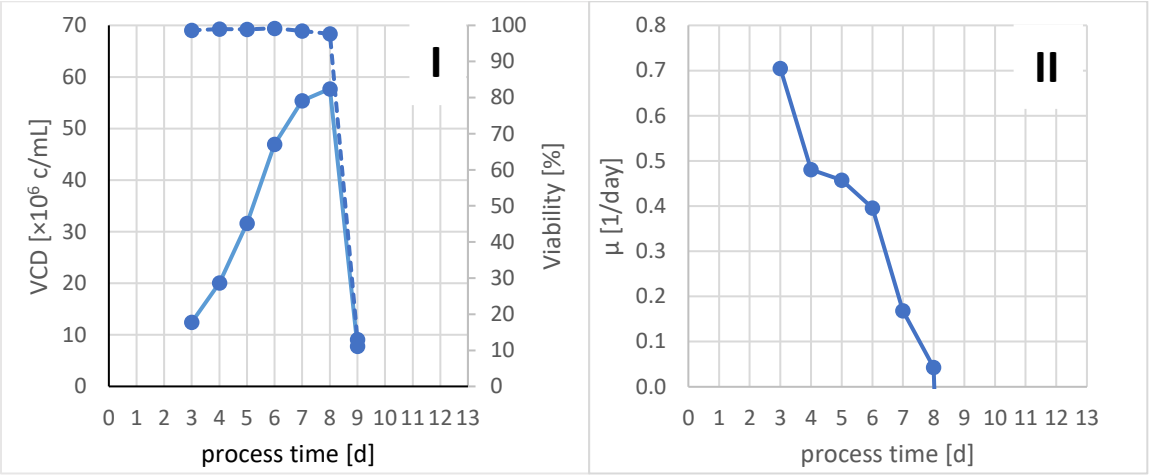

Figure 9: I: Viable cell density and Viability over process time; II: specific growth rate over time

After a rapid growth in the exponential phase until day 6, the growth rate declined in the stationary phase. At day 8, the VCD sank suddenly to 7.7E6 c/mL, and the process was discontinued. The cause for this sudden drop in viability (from 98% to 10%) was probably lack of oxygen, for the unscrewed lid might have been sealed by condensation of water under it.

The titer was measured via anti-His-biotin ELISA, coated with CR3022 (Figure 10). The RBD standard used for the calculations was produced by HEK cells and purified with an HisTrap column.

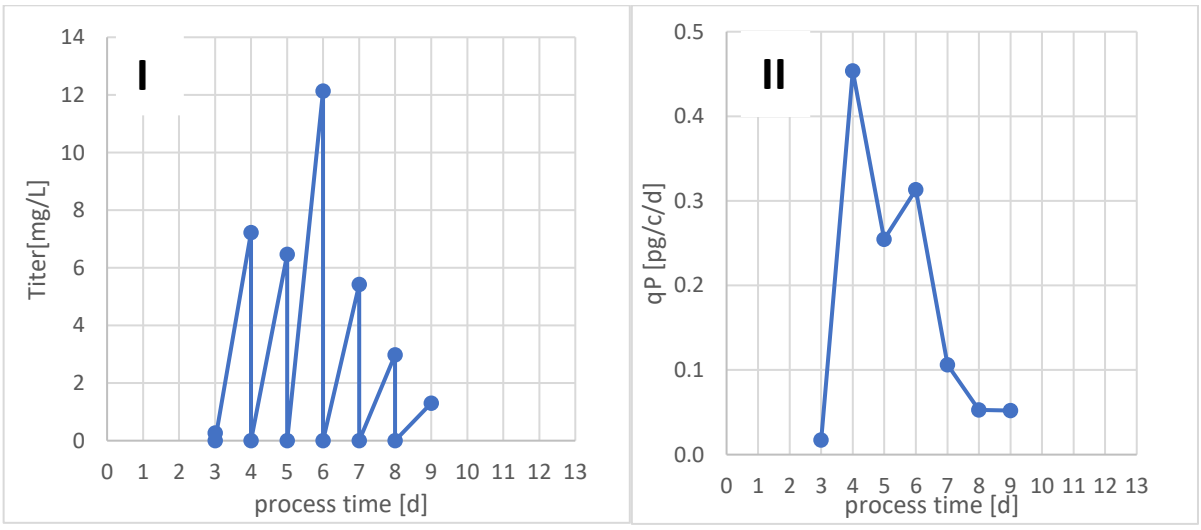

Figure 10: I: RBD titer in the supernatant; II: specific productivity of RBD

In the exponential phase (day 3-6) the specific productivity is the highest with up to 0.45 pg/c/d, and steadily decreases afterwards, with a peak titer on day 6 of 12 mg/L.

Glucose content of the supernatant was measured from the supernatant every 24h and the specific glucose consummation was calculated (Figure 11).

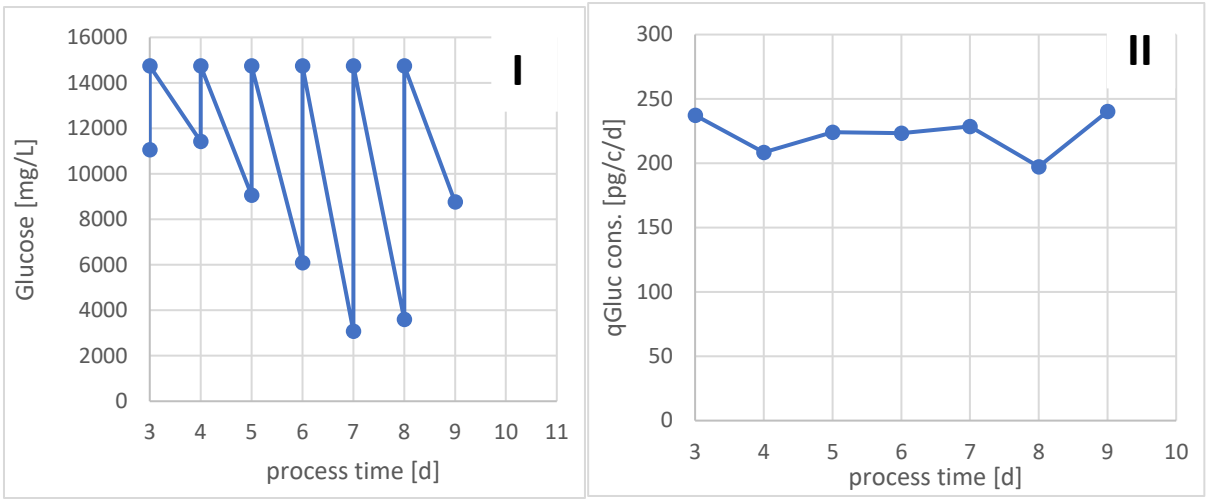

Figure 11: I: Glucose content in the supernatant over process time; II: specific glucose consummation over time

The glucose concentration in the supernatant never went below 3g/L, even though high cell densities with over 50E6 cells/mL were reached. The glucose consumption remained quite steady around 230 pg/c/d.

Lactate concentration in the supernatant was measured every 24h (Figure 12). Due to the semi-perfusion process, the Lactate content was set to zero every 24h.

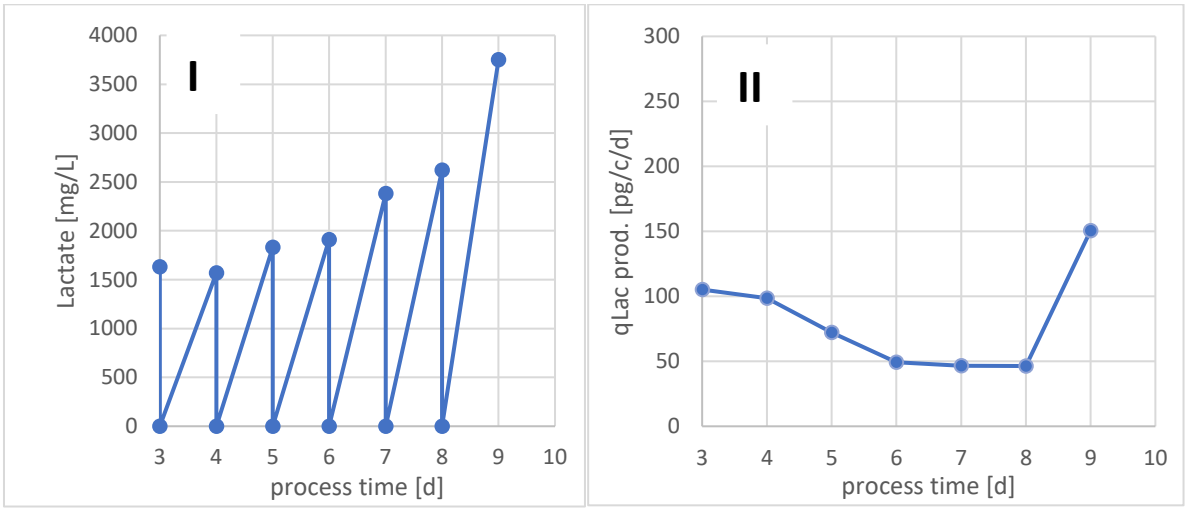

Figure 12: I: Lactate content of the supernatant over time; II: calculated specific lactate production over process time

The overall lactate concentration in the supernatant increases every day, despite specific lactate production decreasing slightly over process time from 100 pg/c/d to 46 pg/c/d. There is a sudden spike in lactate production on process day 9 with 151 pg/c/d (Figure 12, II). Peak lactate concentration was on the last day of the culture, with over 3700 mg/L lactate

Glutamate concentration was measured from the culture supernatant every 24h. Figure 13 shows the glutamate concentration per day and the calculated specific glutamate consumption. In this semi-perfusion setting, the glutamate as well was replenished to 470 mg/L every 24h.

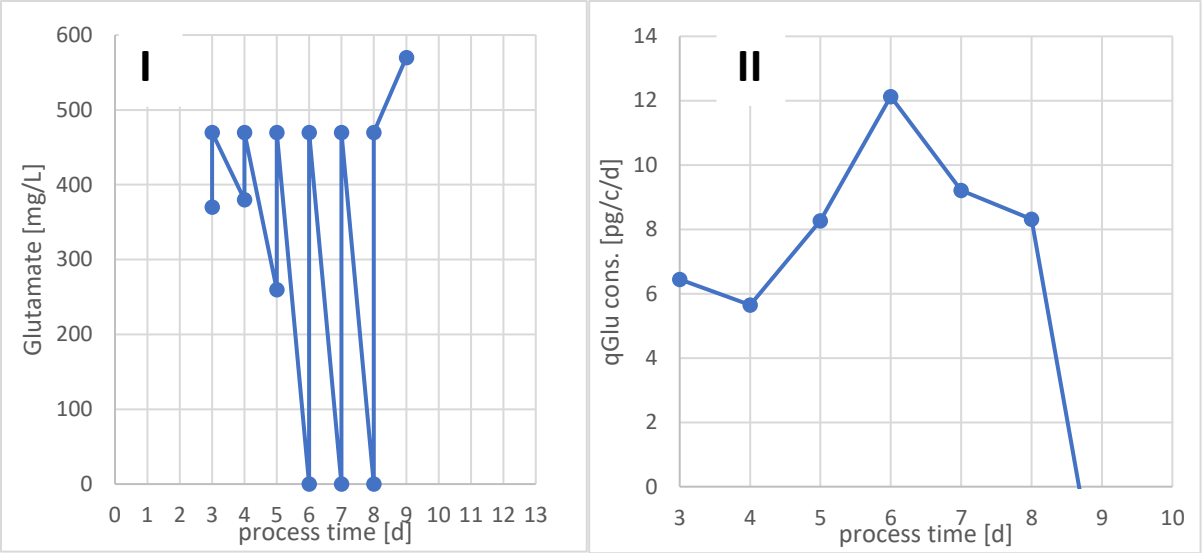

Figure 13: I: Glutamate content in the supernatant over time; II: specific glutamate consummation over process time

Already at day 6, the glutamate concentration dropped to zero before getting replenished, with a peak in glutamate consummation on the same day of 12pg/c/d. Interestingly, on day 9, when the viability dropped to 10%, glutamate seemed to have been produced by the culture.

Figure 14 shows the Ammonia concentration in the supernatant we measured every 24h. The DoE medium contained a small amount of ammonia (39mg/L), to which it was reset after every daily media exchange.

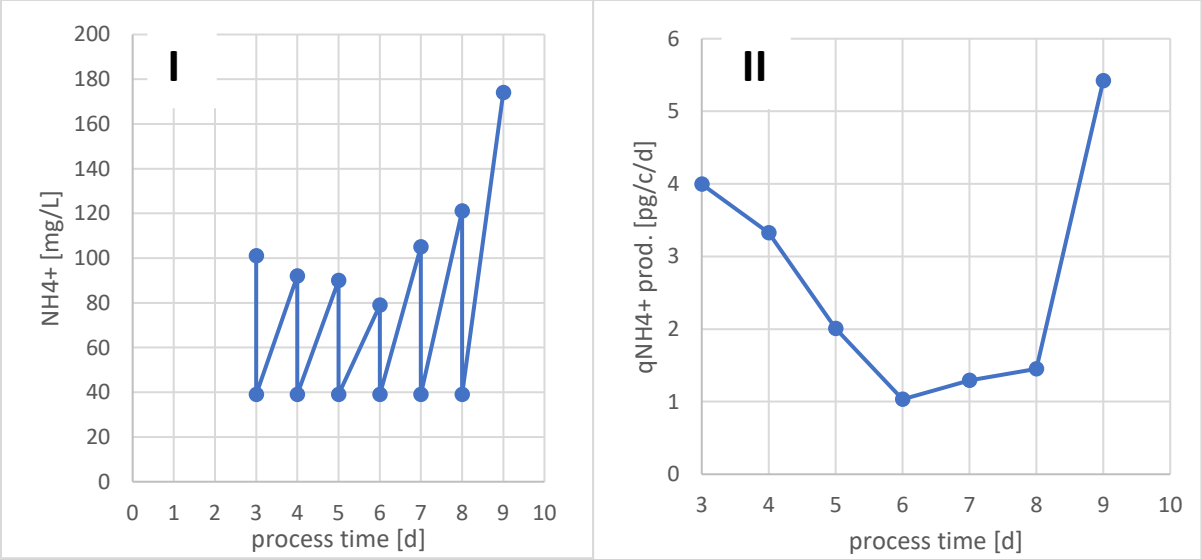

Figure 14: I: Ammonium content in the supernatant over process time; II: specific ammonia production over process time

Specific ammonia production dropped from 4 pg/c/d on day 3 to 1pg/c/d on day 6. Shortly before culture death we see a spike in the ammonia content, increasing from 121 mg/L to 174 mg/L on day 9. The spike in productivity might not be accurate, because of the very low VCD on day 9.

The stable glutamine added to our media was not measurable by the Bioprofiler. The concentration values shown in Figure 15 probably stem from the L-glutamine which was produced by the cells.

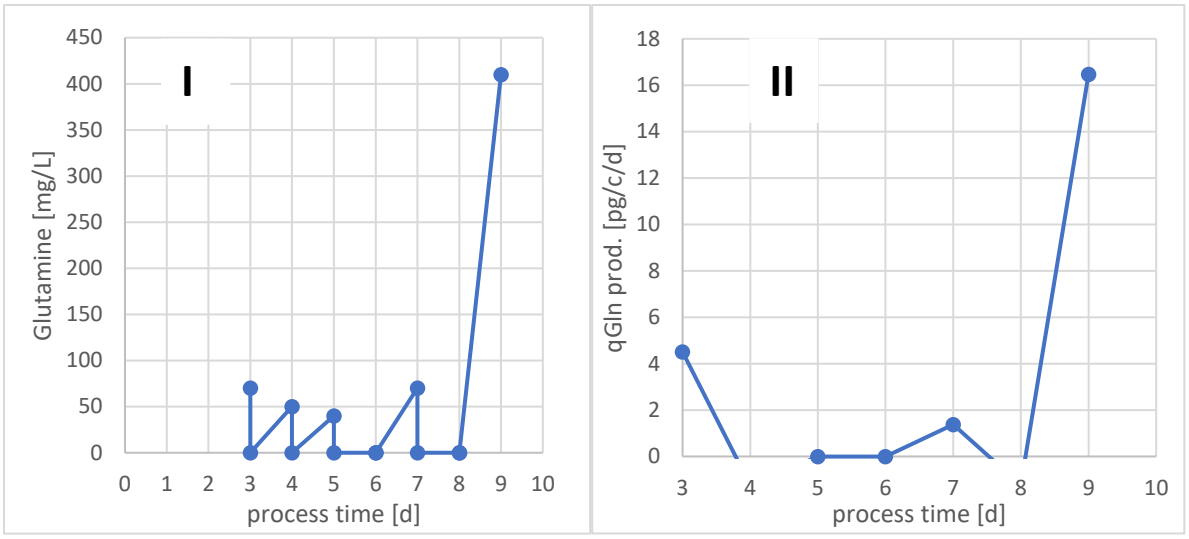

Figure 15: I: L-glutamine concentration measured by Bioprofiler; II: specific glutamine production over process time

Interestingly, we can see a spike in glutamine production between day 8 and 9 (Figure 15, I), reaching over 400mg/L glutamine concentration on day 9.

3.2.2 Semi-perfusion of parental CSs clone 131A4 with and without VPA (experiment F200)

Two semi-perfusions were started, with the same starting conditions. In one culture (named 'A') 1mM of valproic acid was added to the DoE medium starting at day 6. In B the DoE medium was always the same until the culture died. Figure 16 shows the VCD, viability and the calculated growth rate of the process per day.

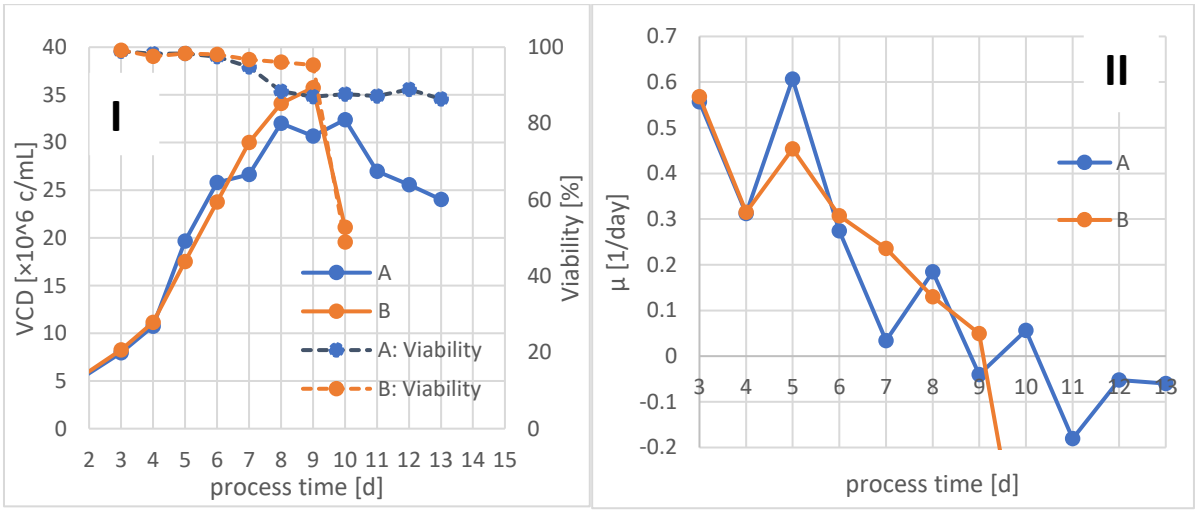

Figure 16: I: Viable cell density and viability of the culture A (+1mM of VPA) and B, measured by VicellXR; II: calculated growth rate of culture A (+1mM of VPA) and B

We can see a decrease in viability in culture A after VPA addition. Culture B grew better until day 9, where we can see a sharp drop in viability. It is difficult to discover why culture B died so early, despite having no limitations in glucose/lactate (see Figure 18, Figure 19) or glutamate (see Figure 20). It is possible that the slightly unscrewed shaking tube lid was not providing enough oxygen in the culture, therefore asphyxiating the culture.

CSs product titer was measured by ELISA (Figure 17). Due to no CSs standard available at this time, RBD standard was used as a substitute. The titer calculated is therefore higher than in reality, as one

of our experiments showed that CSs titer calculated with RBD standard is about the 5-fold lower than with CSs standard.

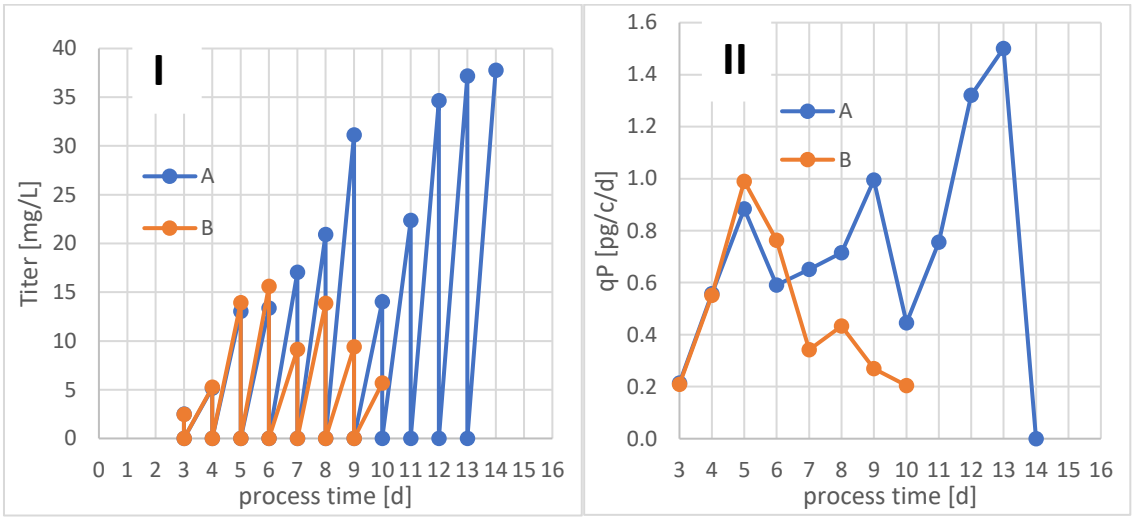

Figure 17: A: Titer of culture A (+1mM VPA) and B over time. ELISA quantified with a RBD standard. B: qP of A (VPA) and B over time

There is an increase of product titer noticeable in culture A after day 5 compared to culture B. The maximum product concentration on day 13 is 38 µg/mL, which was produced by culture A. The qP is highest on the last culture day, namely, 1.5 pg/c/d.

In the semi-perfusion setting, glucose gets replenished every 24h. Already at day 7, culture B used up all the glucose every 24h, while culture A only manages to get to glucose limitations at day 9 (Figure 18).

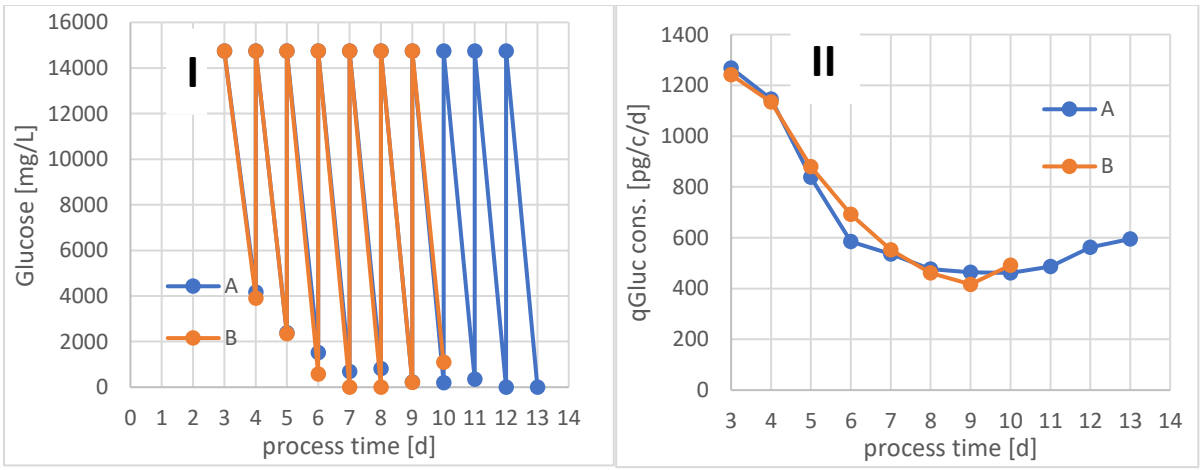

Figure 18: I: Glucose concentration in the supernatant of both cultures. To better illustrate the semi-perfusion condition, the start conc. Of glucose was adjusted every day to the medium swap; II: specific glucose consumption of the cultures over time.

Interestingly, the specific glucose consummation of both cultures is roughly the same over time, and after a decrease in the stationary phase of the cultures, B seems to have a slightly increased consume at the end of the process (Figure 18 II).

After process day 3, lactate content of the culture supernatant was measured daily. Due to the semi-perfusion setting, lactate content was reset to zero every day.

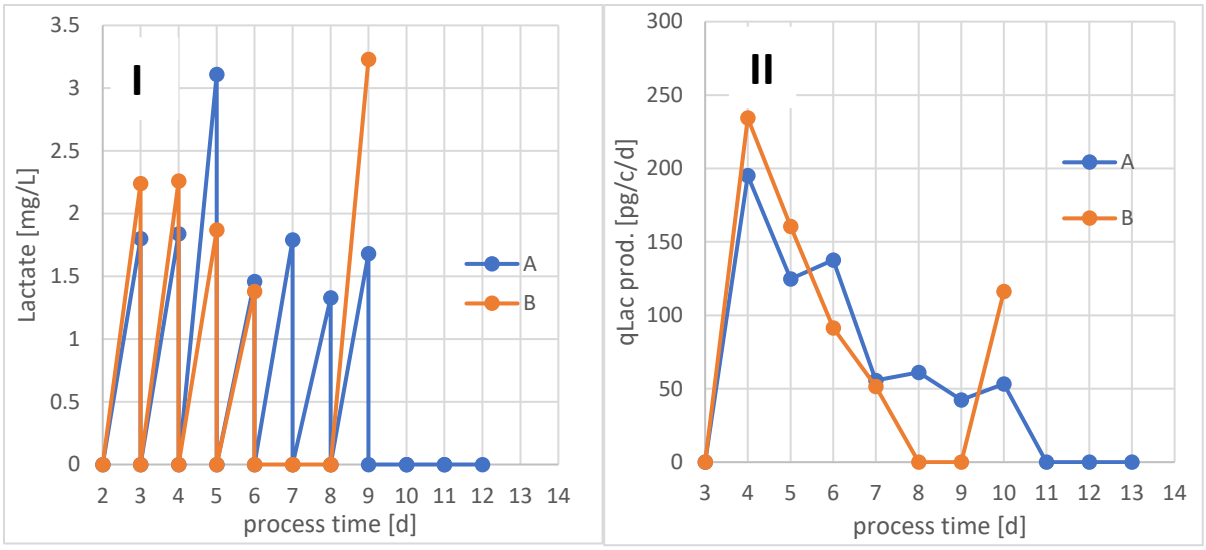

Figure 19: A: Lactate content in the supernatant over process time; II: specific lactate production

Figure 19 shows a high lactate content in the exponential phase (up to 3 g/L in culture A and 2.2 g/L in culture B). Specific Lactate production decreases over process time, and seems to cease completely after day 11 in culture A. This may be the result of glucose limitation, forcing the cells to consume lactate.

In the DOE medium, a substantial amount of glutamate is supplied, namely 470 mg/L. We measured the glutamate content of the supernatant daily (Figure 20).

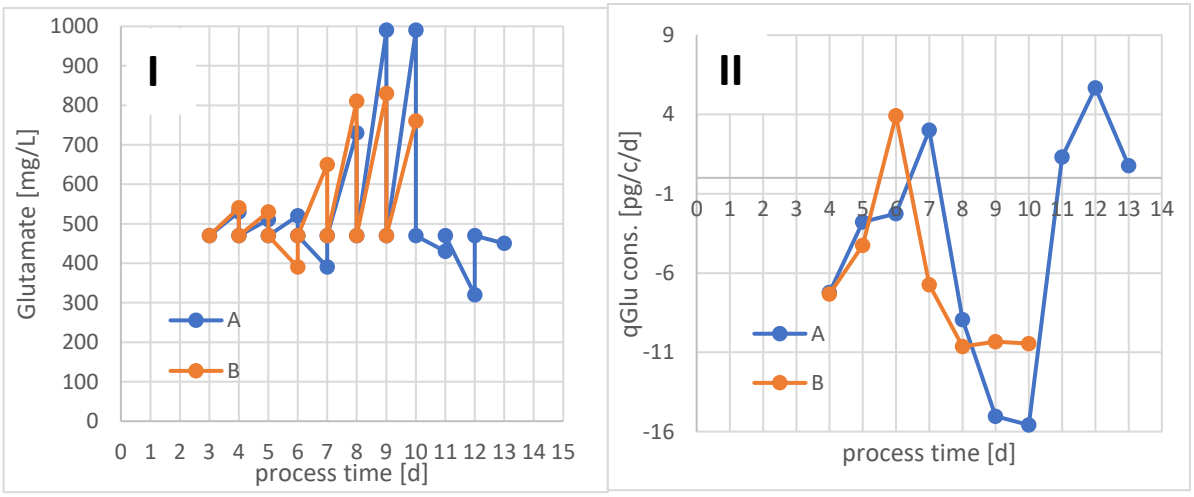

Figure 20: I: Glutamate content of the supernatant over process time; II: specific glutamate consumption of the cultures, negative values signal glutamte production

As we can see in Figure 20, both cultures are producing glutamate in the beginning (except one outlier on day 6 and 7 respectively). On day 11 and forward, glutamate gets consumed.

Ammonia is one of the most important metabolites to be controlled in a fermentation process, due to its negative effect on cell growth and product formation. It is mostly generated by the metabolization of asparagine and glutamine. The ammonia content of the process was measured daily and the ammonia production calculated, as shown in Figure 21.

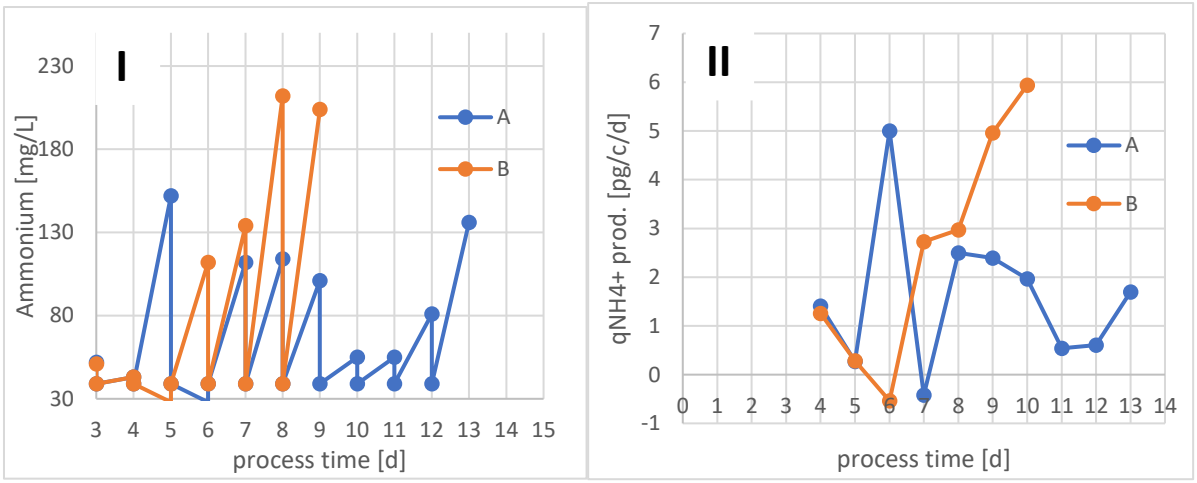

Figure 21: I: Ammonia content of the supernatant over time; II: specific ammonia production over process time

In culture B without VPA, the ammonia concentration as well as production was highly elevated after day 6 in the process and peaked at slightly over 200 mg/L right before the culture viability dropped under 80%. In culture A with VPA, we can discern a nearly steady decrease in specific ammonia production from day 8 until day 12. On day 13, shortly before process end, there was a slight rise in ammonia content and production.

The 4mM of stable L-glutamine in the media was no detectable in our Bioprofiler system. The concentration values in Figure 22 most likely stem from glutamine produced by the cells.

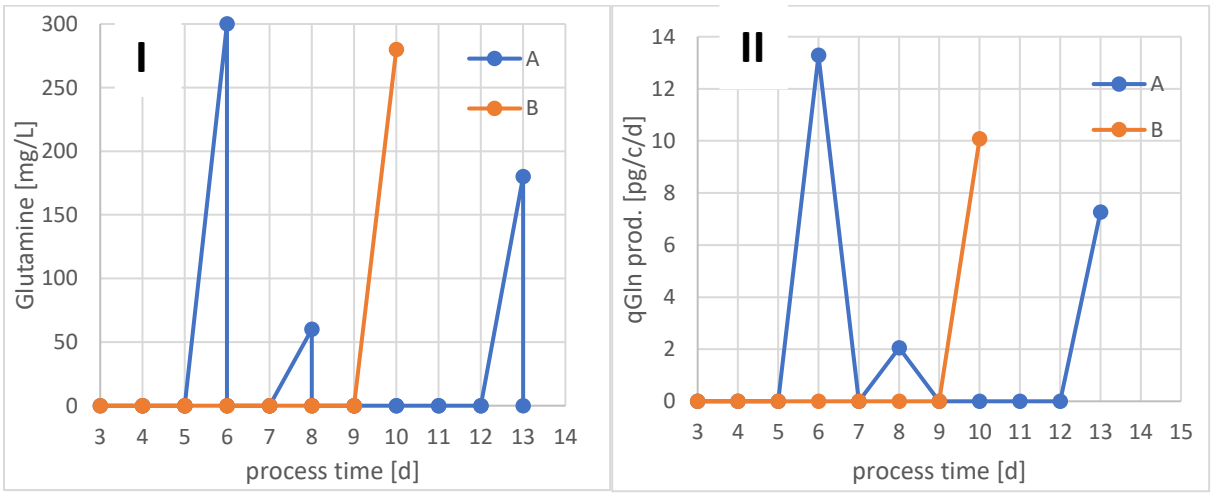

Figure 22: I: L-glutamine concentration measured by Bioprofiler; II: specific glutamine production over process time

Both A and B have a spike in glutamine concentration and production shortly before the process was stopped due to low viability (under (80%). This happened on day 9 for culture B and on day 12 for culture A. A also produced nearly 300mg/L from day 5 to 6.

3.2.3 Semi-perfusion of parental CD19-AD2 clone D19 with and without VPA (experiment F202)

CD19-AD2 is a difficult to express protein, and it was shown in previous experiments by our group that VPA can increase product titer in CHO semi-perfusion culture. We wanted to test the DoE media composition on the CD19-AD2 clone with 0.5mM VPA in higher semi-perfusion volumes, namely 50 mL working volume. VPA was added daily starting at day 5, at the end of the exponential growth phase and beginning of the stationary phase. VPA was added in ST200 “A”. We started with a high seeding intensity of 1.5E6 viable cells/mL (see Figure 23).

At process day 8, the viability of culture B dropped under 10%, with no signs of contamination (Figure 23 I). Due to the nature of the semi-perfusion, we can exclude nutrient limitations (see Figure 26 and Figure 27: no glucose or lactate limitation). The probable cause of the sudden culture death was, as in the semi-perfusion with CSs before, lack of oxygen. The ST200 shaking tubes used for the experiment had no air filter built in the lid, so oxygen influx was managed by unscrewing the lid a few turns. Even though the lid was loosely staying on top of the ST, condensation in the incubator might have caused a small water film to build up under it, and by this sealing the ST200 shut.

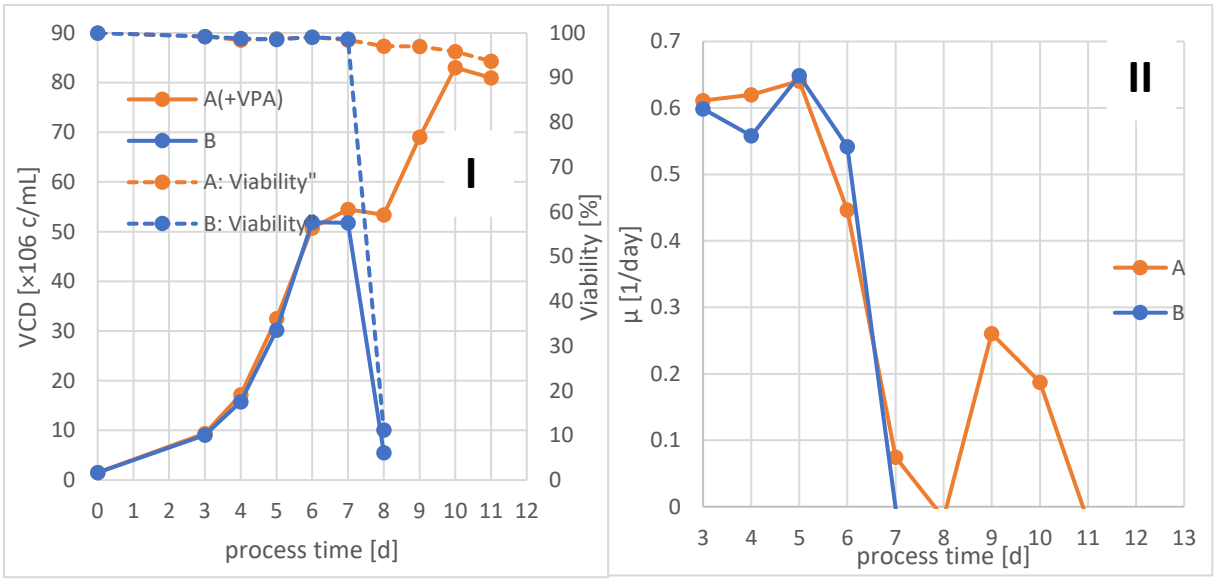

Figure 23: I: Viability and viable cell density over time, of culture A (+0.5 mM VPA) and B (control); II: growth rate over time

The VCD of culture A stagnates after the exponential phase on day 5 and the addition of VPA. After day 8, a spike in growth rate and an increase in VCD is visible. This sudden spike might be explained by a high rate of cell debris in the culture, skewing the VicellXR measurement, as we can see in Figure 24.

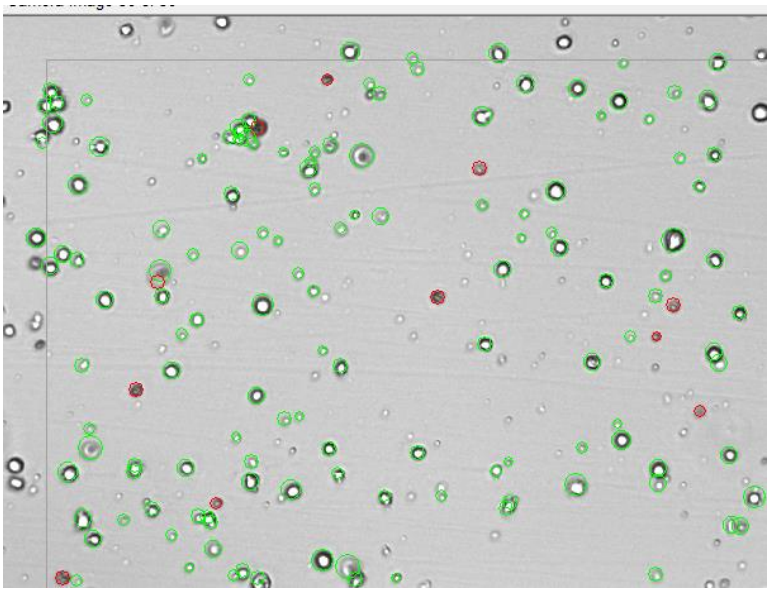

Figure 24: Culture A as seen with VicellXR on process day 9; high amount of cell debris counted as viable cells

Titer of both cultures was measured by AntiHuCD19-AD2-biotin ELISA (plate coated with Anti-HSA) and the specific productivity could be calculated (Figure 25).

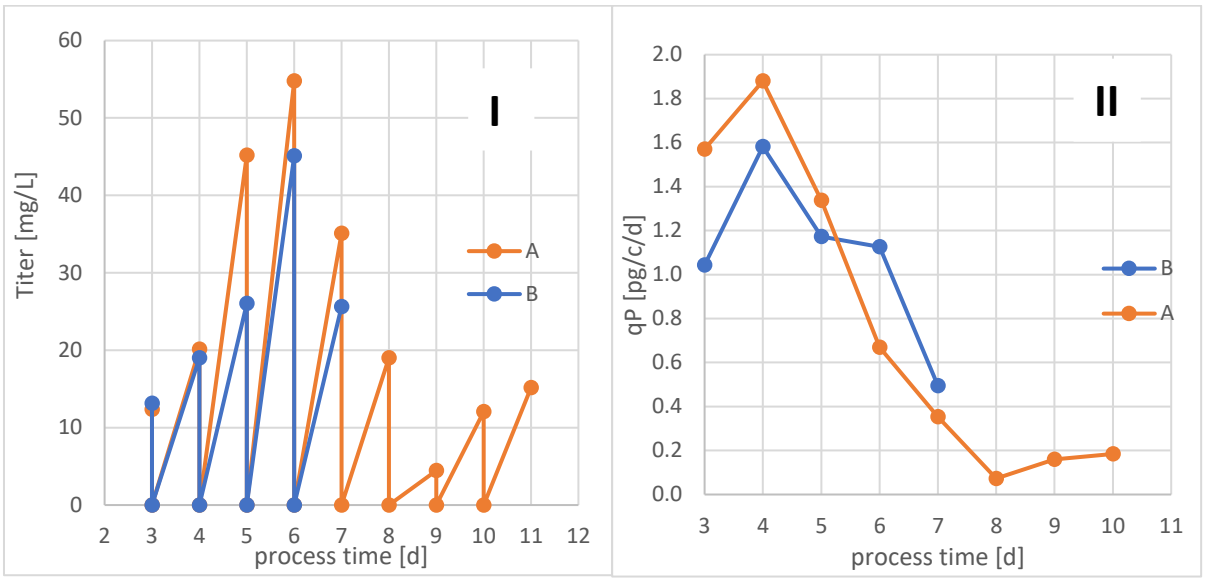

Figure 25: I: CD19-AD2 product titer over time, measured by ELISA; II: specific productivity of the cultures over time

CD19-AD2 Titer and specific productivity was the highest in the exponential phase until process day 5, after which there is a steady decrease visible (Figure 25 II). Highest titer in culture A was on day 6 with 55 mg/L, one day after the VPA addition. Culture B had the highest titer on day 6 as well, with 47 mg/L. Specific productivity peaked at day 4 in culture A with 1.9 pg/c/d, while culture B peaked at day 3 with 1.6 pg/c/d.

Glucose concentration of the centrifuged supernatant was measured by every 24h, and subsequently the specific glucose consumption per day of the cultures was calculated (see Figure 26).

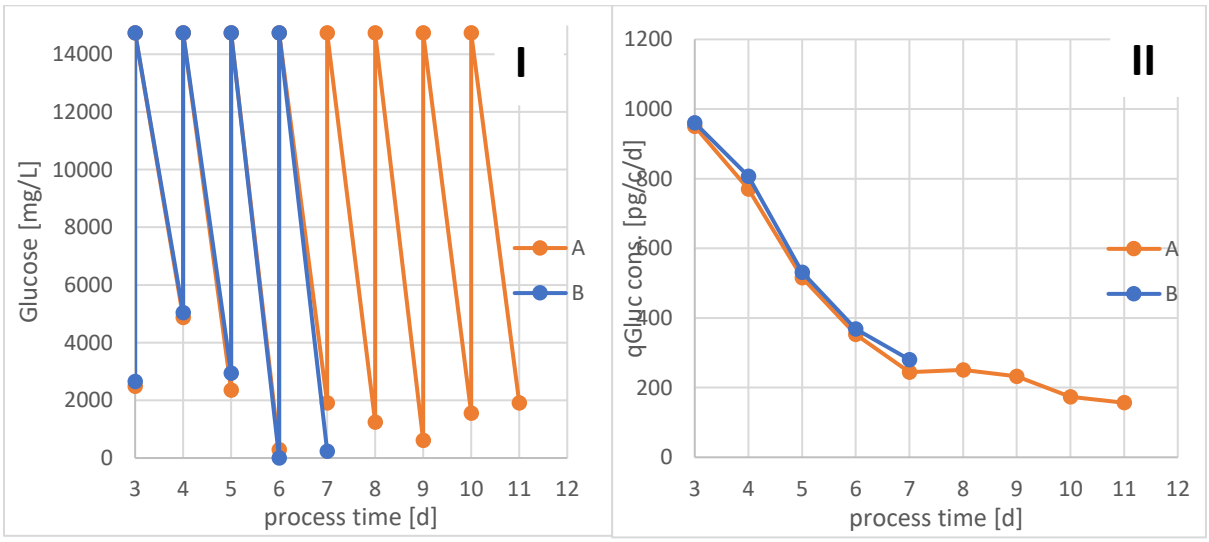

Figure 26: I: Glucose concentration over process time; II: calculated specific glucose consumption over process time

On process day 6, the glucose concentration of culture A in the supernatant was already at zero, as well as on day 7 for both cultures. Due still high amounts of lactate and glutamate present, there was no nutrient energy limitations to cause the sudden culture death in A. Specific glucose consumption decreased until day 7, where it begins to level off.

Lactate concentration of the supernatant was measured daily and the lactate production was calculated (Figure 27). Because the medium was exchanged every 24h, lactate concentration was set to zero every 24h.

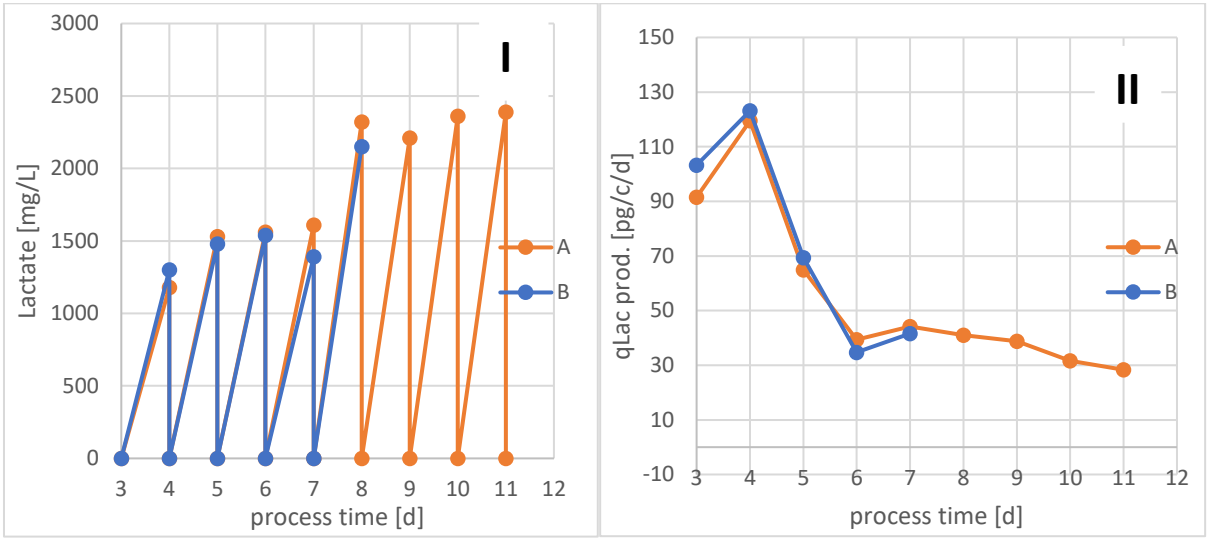

Figure 27: I: Lactate concentration in the supernatant over time; II: Specific lactate production over time

Both cultures behaved very similarly over the process time (up until culture death of A) regarding lactate production (Figure 27, II). After day 7 culture B had very high lactate concentration of over 2000 mg/L, and a quite steady if slightly decreasing lactate production after day 6. Culture A never had depleted its lactate, therefore still having a carbon and energy source despite possible glucose limitations (see Figure 26).

Glutamate concentration was measured every 24 h from the culture supernatant and the glutamate consumption of the culture calculated (Figure 28). In this semi-perfusion setting, the glutamate was replenished to 470 mg/L daily.

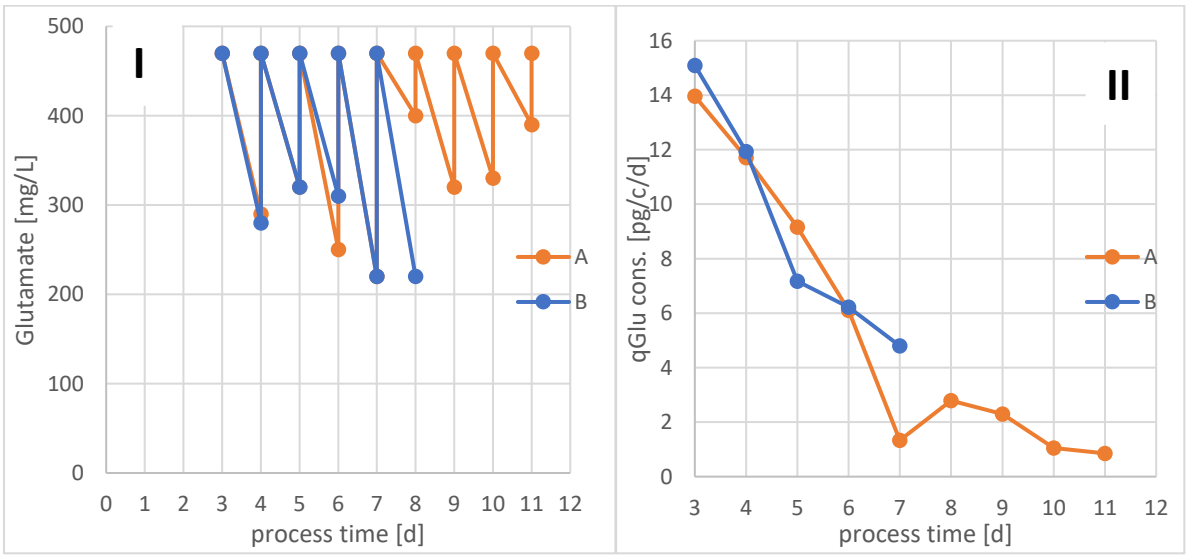

Figure 28 I: Glutamate concentration over time; II: specific glutamate consummation over time

The glutamate concentration in both cultures never decreases below 200 mg/L. The specific glutamate consumption steadily decreases for both cultures until day 7 (Figure 28, II). Culture A seemed to consume less glutamate than culture B, which had a slight increase in Glu consummation at day 8.

In Figure 29 the Ammonia concentration of the centrifuged supernatant and the calculated specific ammonia production are displayed. The DoE medium has a small amount (39 mg/L) of ammonia according to the Bioprofiler measurement.

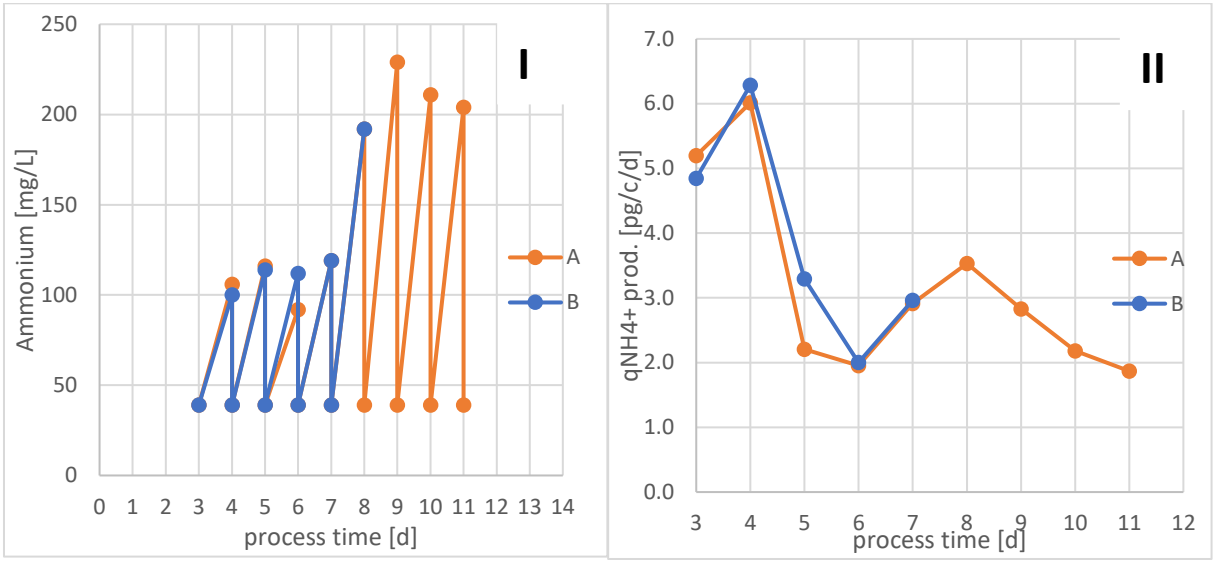

Figure 29: I: Ammonia concentration of the supernatants over time; II: calculated specific ammonia production over process time

Ammonia concentration starts to heavily increase after day 7, until it peaks at 230mg/L (Figure 29, I). Specific ammonia production is high in the first 2 days of measurement, decreases until the end of the exponential phase on day 6 and afterward rises again until day 8 (Figure 29, II). High ammonia concentration and production often go hand in hand with culture death, which is not the case in this culture.

Glutamine concentration of the supernatant was measured daily (Figure 30, I). The 4mM stable L-Glutamine was added every 24h with the medium exchange. The stable L-Glutamine was not measurable in the media via Bioprofiler, therefore any L-Glutamine measured by the Bioprofiler was most likely produced by the cells.

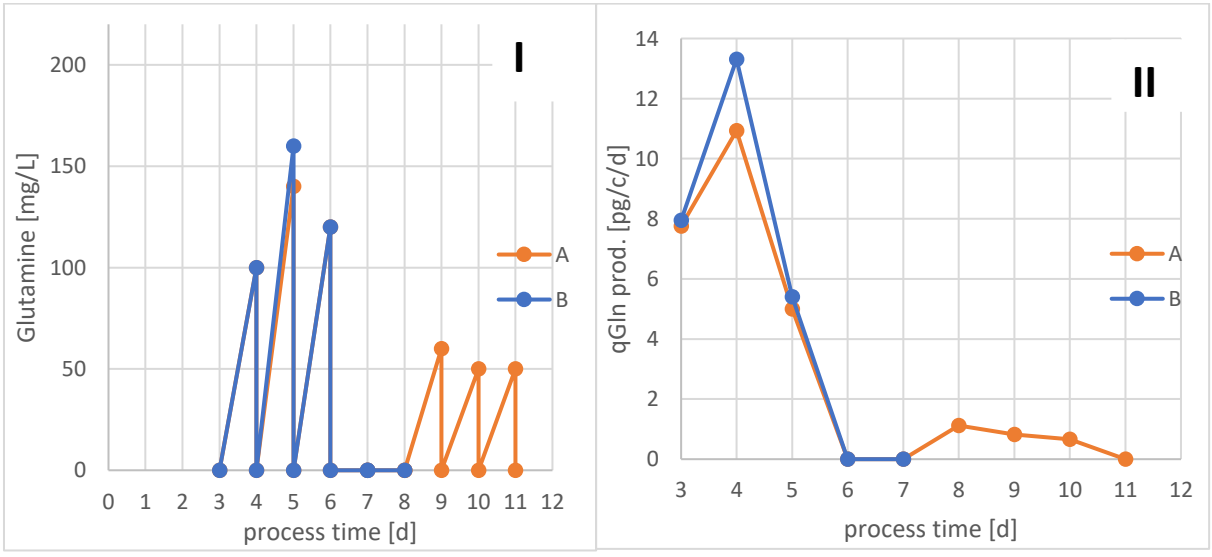

Figure 30: I: L-Glutamine concentration in the supernatants over process time; II: calculated specific glutamine production overprocess time

It seems that culture A and B both produced up to 150 mg/L L-Glutamine on day 5, while also reaching more than 100mg/L on day 4 and day 6 (Figure 30 II). Culture A with VPA produced around 50 mg/L from day 9 to 11. This glutamine in Figure 30 comes from the synthesis from Glutamate via Glutamat-Ammonium-Ligase. We do not know if the dipeptide alanine-glutamine (provided with the medium) was consumed in the metabolism.

3.2.4 RBD purification and LDS Page – Silver staining

We purified the RBD supernatant (d3 to d9 was pooled) from experiment F198 produced by our recombinant CHO-K1 line 2P7 in a semi-perfusion setting. First, we used tangential flow filtration (TFF) to concentrate our supernatant. The retentate was loaded on the HisTrap column, eluted by imidazole buffer and the eluate 1 further purified with a SEC column.

Table 3: Balance of the purification; 100 mL of imidazole running buffer was added to the supernatant before TFF (permeate)

	Volume [mL]	**conc. [mg/L]**	**mass[mg]**	**%**
Supernatant	404.51	4.5	1.82	100.00
Permeate	504.19		0.00	
Load (TFF retentate)	27.78	55	1.53	83.94
flow through	31.27	2.3	0.07	3.95
Wash	20.28	0	0.00	0.00
eluate1	11.97	64	0.77	42.09
eluate2	10.83	61	0.66	36.29
clean	4.44	0	0.00	0.00

It seems that a high amount of RBD got lost in the TFF, around 16 % of the total mass (see Table 3). In the HisTrap, 4 % of the RBD got lost in the flow through, and a further 2% got either lost in the wash or the clean fraction.

To further assess our purification success, we made a LDS PAGE with silver staining of the HisTrap fractions, as well as our RBD product (Figure 31, for sample plan see

Table 4). Furthermore, we dropped similarly processed RBD, produced transiently by HEK, onto the gel. To investigate the possible formation of oligomers, we prepared a reduced and non-reduced part of the gel.

Table 4: Sample plan of the LDS-PAGE; Samples were diluted to reach 500 ng load, 20 µL / well

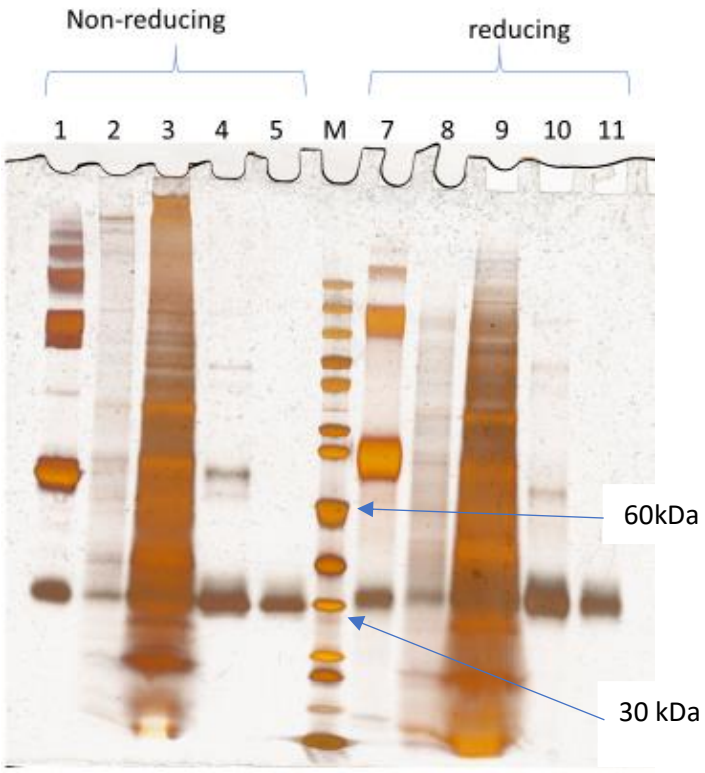

Figure 31: LDS Page with silver staining of the HisTrap factions and SEC final product

Well	load
1	RBD (HEK, HisTrap, SEC)
2	Supernatant
3	Retentate
4	Eluate1
5	RBD (CHO-K1, HisTrap, SEC D1-D8, Monomer)
M	5 µL PageRuler unstained Cat. 26614
7	RBD (HEK, HisTrap, SEC, -20°C storage)
8	Supernatant
9	Retentate
10	Eluate1
11	RBD (CHO-K1, HisTrap, SEC D1-D8, Monomer)

We can see in the non-reduced part that purified HEK-RBD shows several bands over the molecular weight of RBD (~30 kDA; Figure 31, column 1,4 and 5). Most of it seems to be around the projected molecular weight of the dimer, 60 kDa.

The supernatant of our cell suspension (volume reduced via reverse flow and filtered with 20 µm filter) shows a clearly visible band at 30 kDa (Figure 31, column 5). The HisTrap eluate produced by our CHO-K1 cell line shows bands in the 30 kDa range and at 60 kDa (Figure 31, column 4), which confirms a successful purification via Histrap, even though there are still dimers present in the solution. The reduced part shows a slightly weaker band around 60 kDa (Figure 31, column 10), which could mean the dimers split up a bit. A single band at 30 kDa in the slot with our SEC-purified product confirms that only monomers of RBD are present (Figure 31, column 11).

3.3 Batch cultures of top-clones

To differentiate the clones better and get a first impression of productivity and performance, the VCD, viability and titer of every clone was measured every day in the exponential phase, starting with the seeding concentration of 0.3 E6 VCD/mL and measuring daily until day 4. Samples of cells were also taken every day and fixed in ethanol for FACS measurements.

In these experiments the standard routine culture medium was used, namely CD-CHO medium with 4mM L-Gln, 15 mg/L phenol red, 0.5 mg/L G418 and anticlumping agent (1:500). The initial working volume was 15 mL, which decreased over time because of sampling.

3.3.1 Batch cultures of RBD top clones F3, F8, G7

The RBD top clones F3, F8 and G7 were, compared to the CSs and CD19-AD2 clones, the fastest and most vigorous growing in the plate culture setting. The RBD 384 plates were ready to be transferred already 2 weeks after inoculation, compared to the 3 weeks the CSs and the CD19-AD2 subclones needed. In the experiments before we selected subclones F3 and F8 for their high titer concentrations and G7 because it was the fastest growing culture.

Figure 32 shows VCD, viability as well as growth rate of each clone over 4 days in culture.

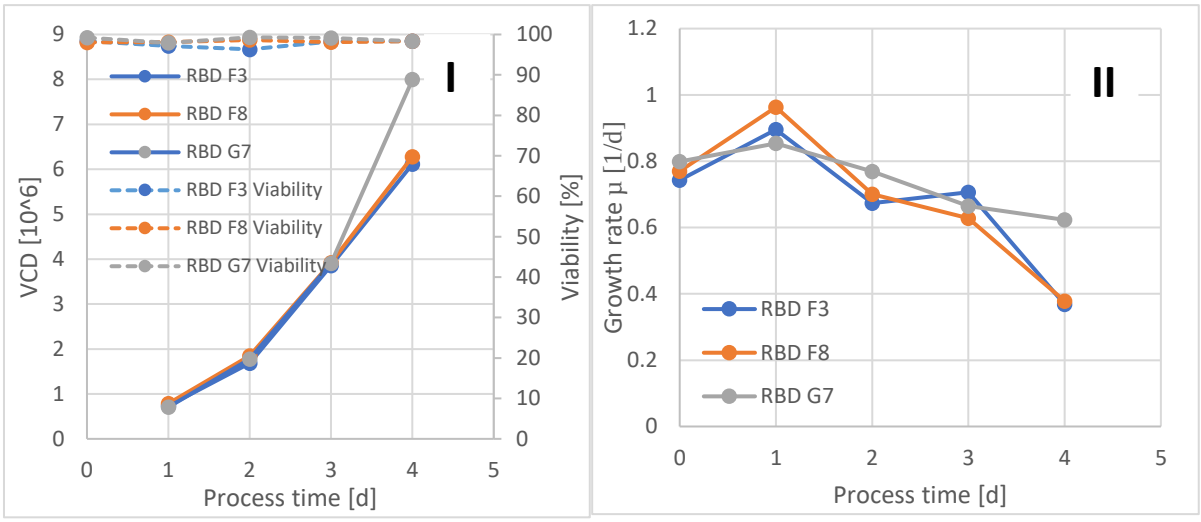

Figure 32: I: Viable cell density and viability of each culture over process time; II: growth rate over process time

Until day 3 the different clones behaved very similarly, having mostly the same VCD and growth rate. On day 4, G7 showed a higher growth rate than the other 2 at around 0.62, while F3 and F8 were under 0.4 (Figure 32, II). G7 also reached 8E6 VCD, while F3 and F8 stayed at 6E6 VCD.

RBD titer was measured by ELISA and subsequently the specific productivity was calculated (see Figure 33).

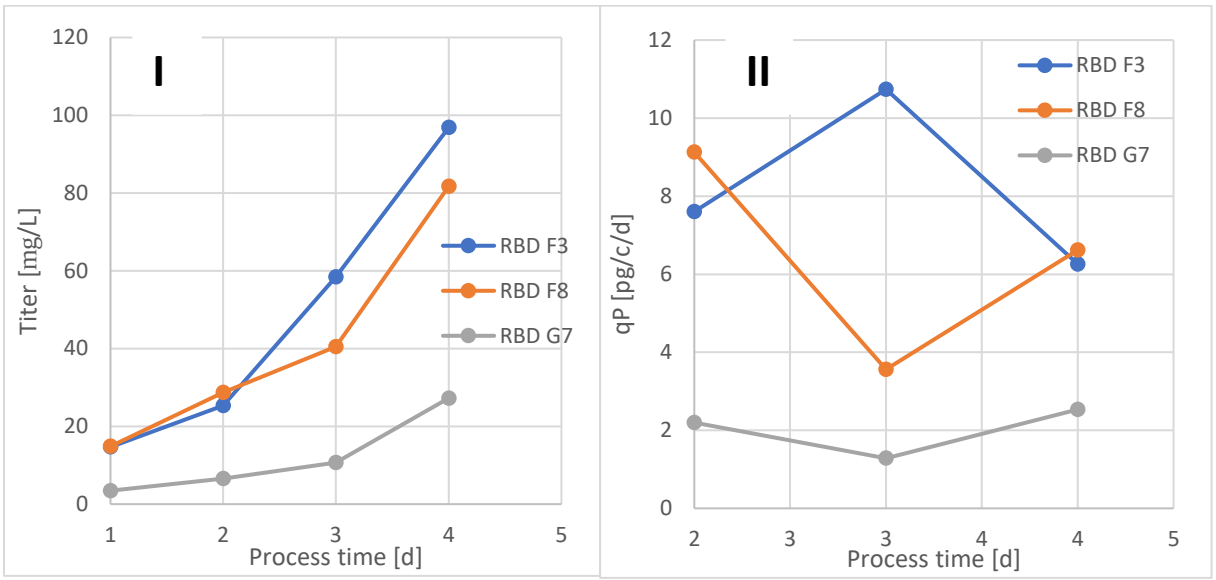

Figure 33: I: RBD titer in the supernatant, measured quantitative ELISA; II: specific productivity qP over process time

Even on this small timeframe we can discern significant differences in RBD titer and productivity between the clones. While G7 might have the highest VCD on day 4, it still has the lowest RBD titer with only 28 µg/mL, compared to F3 (96 µg/mL) and F8 (80 µg/mL) (Figure 33, I). Peak productivity is reached by F3 on day 3 with 11 pg/c/d, while G7 peak was at 2.5 pg/c/d and F8 at 9 pg/c/d.

3.3.2 Batch culture of CSs top clones C11, F4 and G3

The final selection of clones producing CSs were C11, F4 and G3. From experiments before (see Figure 7) it was estimated that C11 is the highest producer, while F4 and G3 behave very similar in growth and productivity.

Figure 34 shows the VCD, viability and the growth rate over the 4-days batch process.

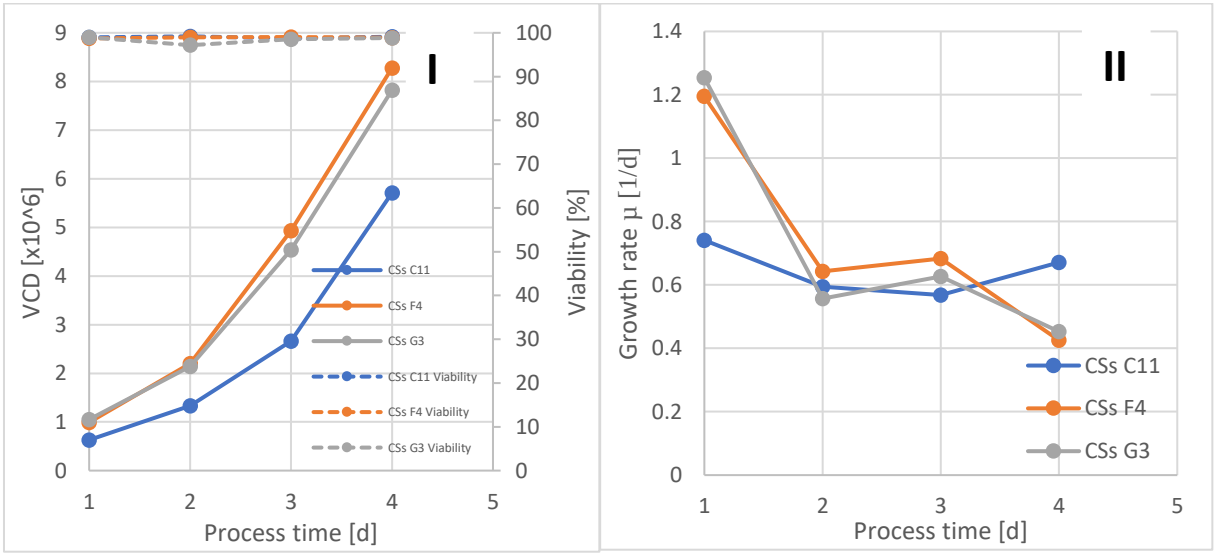

Figure 34: I: VCD and viability over process time; II: Growth rate over process time

Although all 3 clones were seeded with the same VCD of 0.3E6 cells/mL, already on day 1 we can see the difference between C11 and the rest. F4 and G3 started with a very high growth rate of 1.2, while

C11 had a growth rate of 0.7 in the same time (Figure 34, II). F3 and G3 VCD peaked at 8E6 cells/mL, while C11 peaked at 5.7E6 cells/mL (Figure 34, I).

Titer of the cultures was measured and the specific productivity qP calculated, displayed in Figure 35.

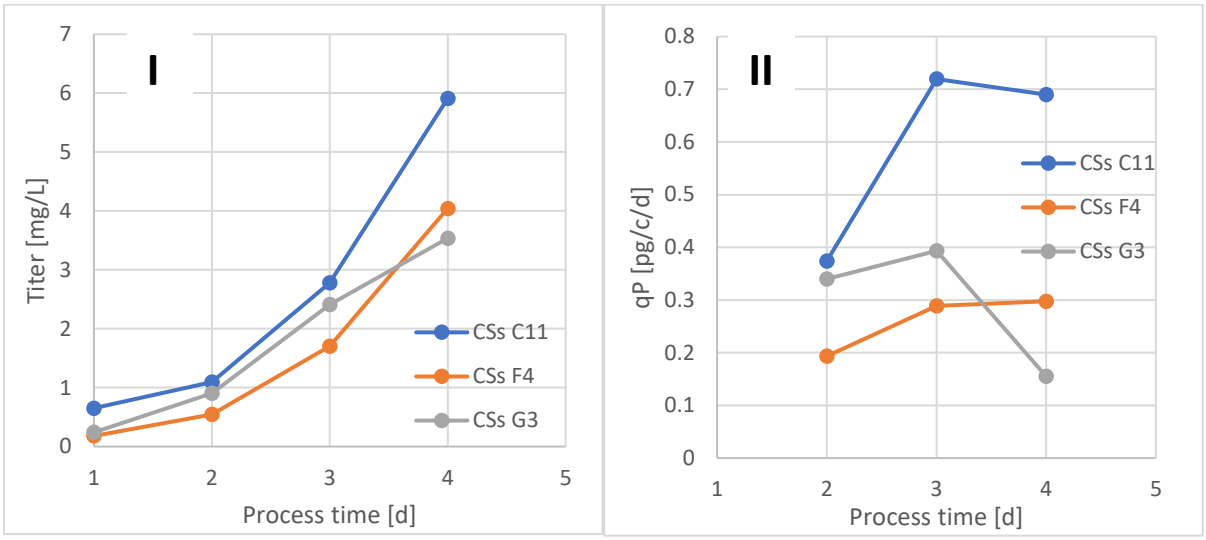

Figure 35: I: Titer over process time, ; II: specific productivity qP over process time

C11 was the highest producer of the three clones, with a peak productivity over 0.7pg/c/d (Figure 35, II). C11 also had the highest titer concentration of 6 mg/L at day 4 (compared to 4mg/L in F4 and 3.5mg/L in G3), while still having 2E6 less viable cells/mL as the rest.

3.3.3 Batch cultures of CD19-AD2 top clones C2, E10 and F9

The three final CD19-AD2 clones were C2, E10 and F9. Previous experiments suggested very similar behavior regarding to growth and productivity in CD CHO medium (see Figure 8).

Figure 36 shows the measured VCD and viability as well as the calculated growth rate.

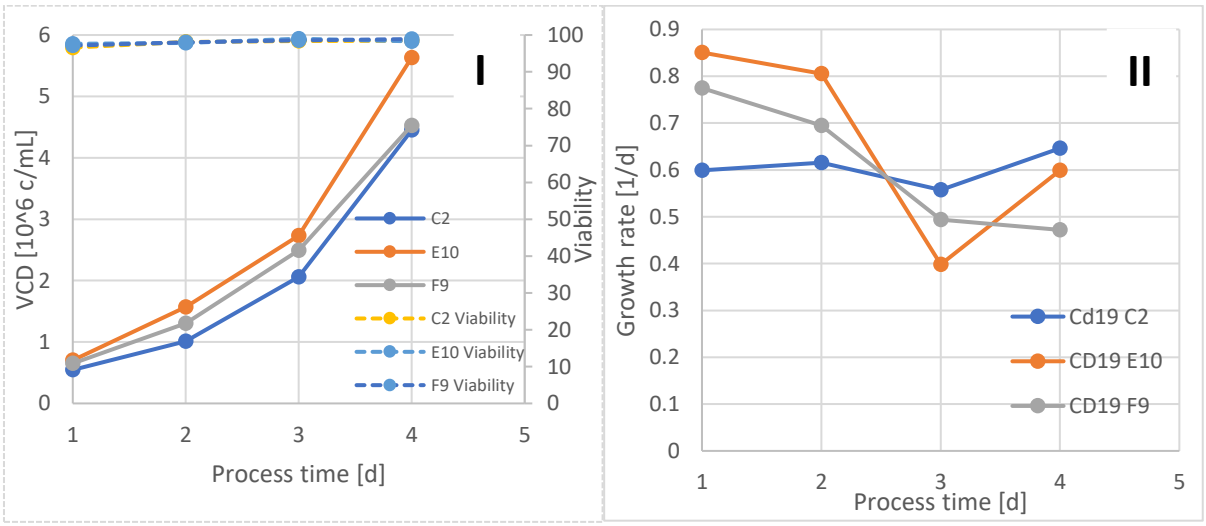

Figure 36: I: VCD and Viability ; II: calculated specific growth rate

On day 4 in culture, at the end of the exponential phase, E10 had the highest VCD with 5.6E6 cells/mL, while C2 and F9 had a VCD of 4.5E6 cells/mL (Figure 36, I). E10 and C2 growth rate slightly

rose on day 4 too (Figure 36, II). E10 and F9 both started with a very high growth rate on the first day, 0.85 and 0.77, respectively.

Titer of the supernatant was measured by ELISA and the specific productivity qP was calculated (Figure 37).

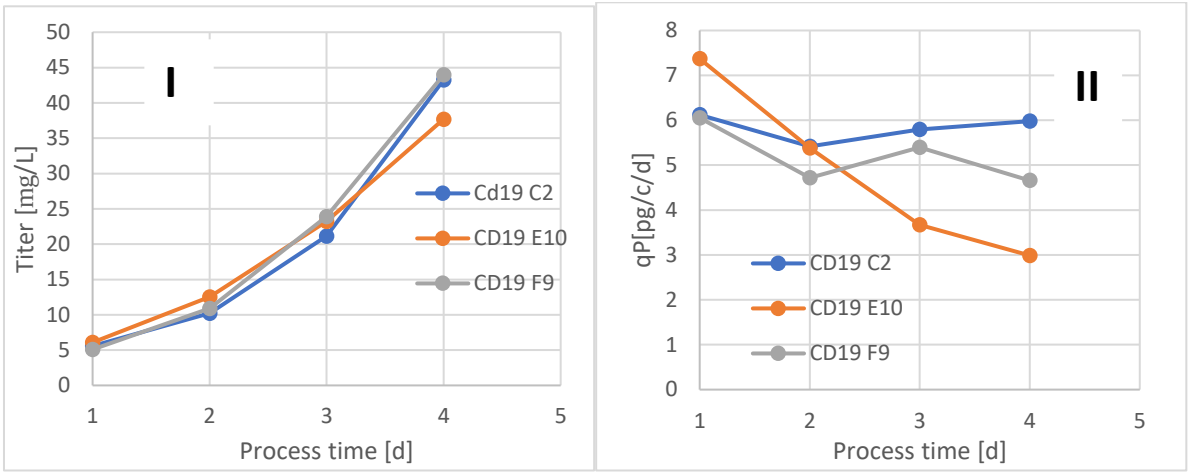

Figure 37: I: CD19-AD2 titer over process time, measured by ELISA; II: calculated specific productivity of the clones over process time

Product titers of the clones were very similar at any point in the exponential phase, with C2 and F9 reaching nearly 45 mg/L (Figure 37, I). C2 has the highest average qP of nearly 6 pg/c/d, while E10 had only 3 pg/c/d on day 4 (Figure 37, II).

3.4 Consecutive passaging of the different cell lines - comparison of clones in routine cultivation

Routine cultivation of all clones was monitored over several weeks, each passaged every 3-4 days. The product titer, cell density and viability were measured at the end of each passaging cycle.

The medium used for all cultures was the CD-CHO medium with 4mM L-Gln, 15mg/L phenol red and 0.5 mg/L G418. Anticlumping agent was added in a dilution of 1:500. The seeding density was always 0.3E6 cells/mL, with a working volume of 10 mL in 50 mL shaking flasks.

It is important to control the titer over longer time periods, as some clones may undergo epigenetic changes which can result in a lower protein expression.

3.4.1 Consecutive passaging of RBD clones 2P7, F3, F8 and G7

The clones expressing the RBD reached high cell densities in 4 days of routine culture, with the parental clone reaching 10.5E6 cells/mL (Figure 38). Subclone G7 reached 9.5E6 cells/mL already 7 passages after transfer from the expansion plate. F8 and F3 reached a maximum VCD of around 7 mio cells/mL. Cryo vials were prepared at passage 8 of the subclones, and all 3 took 2 passages to reach their former VCD.

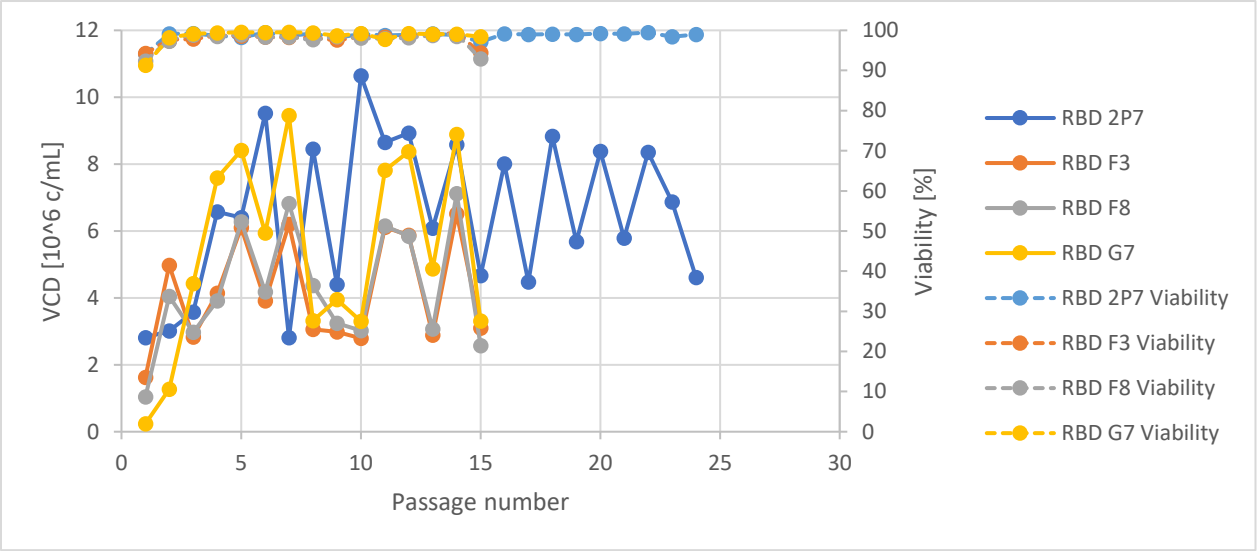

Figure 38: VCD and viability of the RBD clones, measured by ViCellXR

The growth rate of all the RBD clones in routine culture, calculated over the timespan of 3-4 days (see Figure 39), was high, with the parental clone frequently reaching a specific growth rate of over 1. G7 reached similarly high growth rates, while F3 and F8 both peaked at 0.85 at passage number 5.

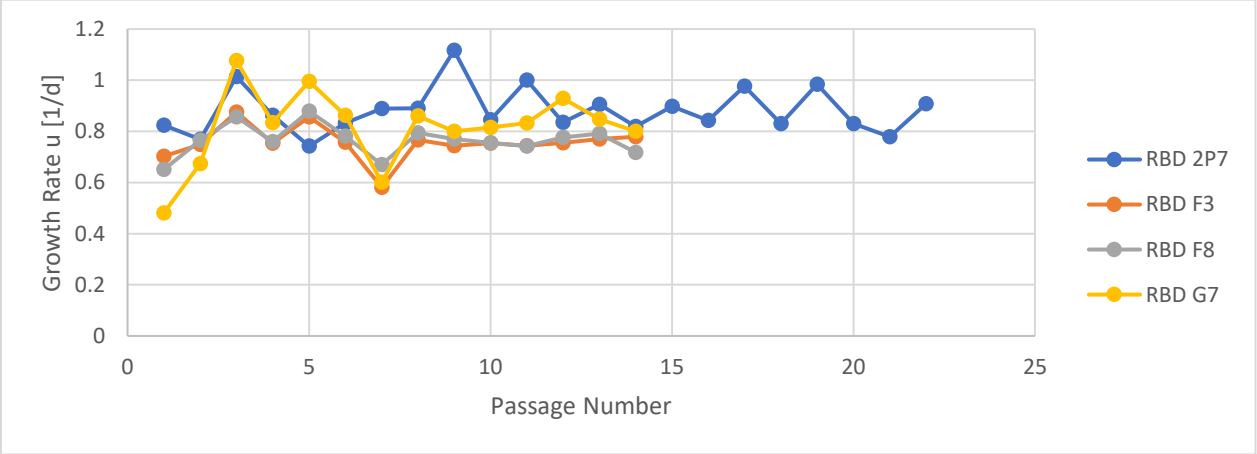

Figure 39: Calculated growth rate over each passage cycle of the RBD clones

RBD titer of the parental clone 2P7 was relatively constant in routine culture, peaking at 22 mg/L (Figure 40). The subclones F3 and F8 showed a capability to reach way higher titers, with up to 96 mg/L by F3 and 81 mg/L by F8 (Figure 40). G7, which displayed the highest VCD and growth rate of the subclones, showed a decreasing trend in titer over passage number, barely surpassing the parental clone at passage 15 (Figure 40).

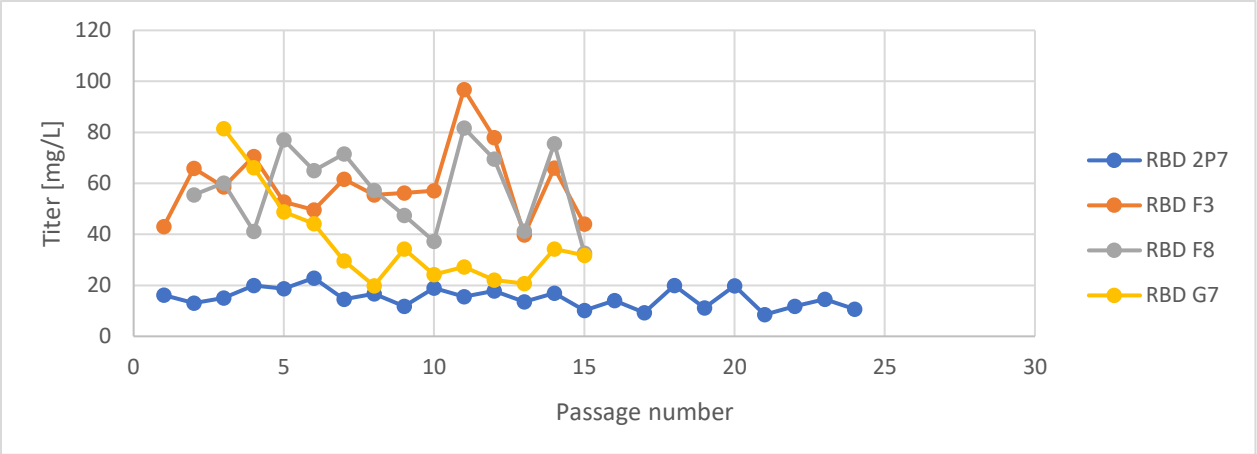

Figure 40: RBD titer of the clones F3, F8, G7 and parental clone 2P7.

The qP of the F3 subclone had its peak at passage 9 with 17 pg/c/d, and F8 at passage 2 with 17.1 pg/c/d, while G7 showing its maximum qP of 13.27 pg/c/d at passage number 1 (Figure 41). F3 was the subclone which showed the least variation of the subclones, as is also shown in the boxplots.

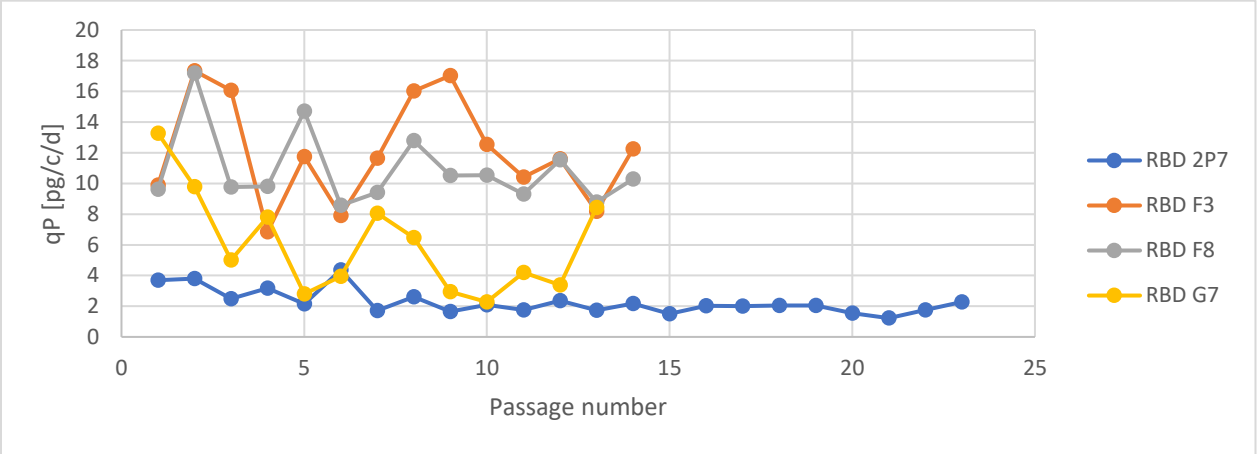

Figure 41: Calculated qp of the RBD subclones and its parental clone 2P7 over passage number

To more easily display the differences between the clones, a boxplot was created of the calculated qP (see Figure 42).

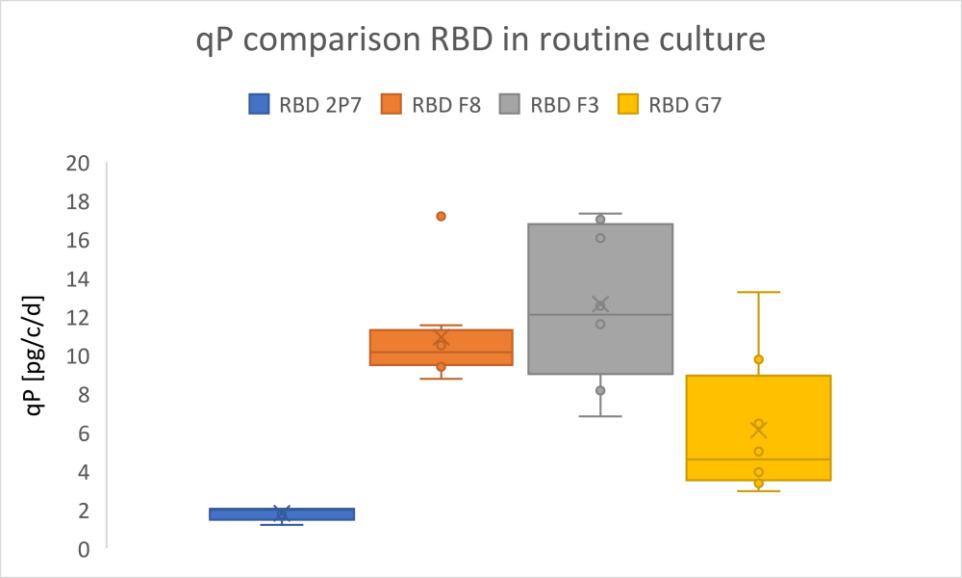

Figure 42: Boxplots of the qP of the RBD subclones and its parental clone

All 3 RBD subclones have significantly higher qP than the parental clone, which has a median of 2 pg/c/d. F3 has the highest median of the subclones with 12 pg/c/d, while also showing the highest variance of all. G7 has the lowest median with 5 pg/c/d. The qP of F8 had the lowest variance, with a median at 11 pg/c/d.

3.4.2 Consecutive passaging of CSs clones C11, 131A4, G3 and F4

The CSs subclones needed 8 passages after the transfer from the expansion plate to the ST50 to reach nearly the same VCD as the parental clone (Figure 43). C11 was the worst performer cell density wise, as it always had 1-2E6 less cells per mL as the parental clone 131A4, while F4 and G3 showed the same or even higher VCD as 131A4 on passage 8 with 7.5E6 cells/mL (Figure 43).

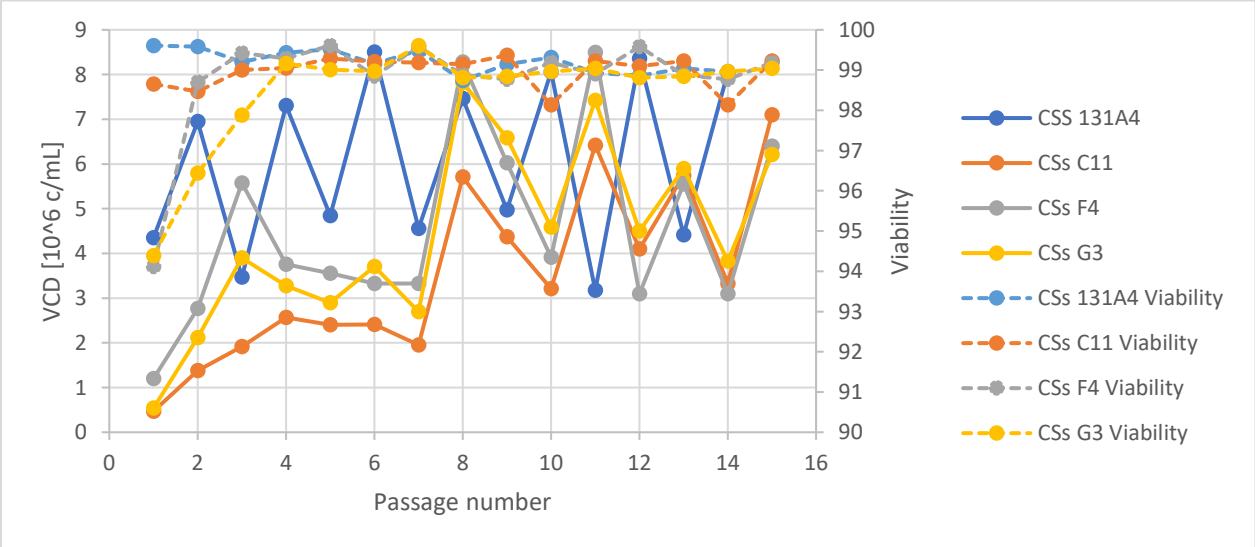

Figure 43: VCD and viability of the CSs clones over passage number

The growth rate of the subclones F4 and G3 was lower than 131A4 until passage 8, while C11 needed 11 passages to reach the same µ of 0.8 as the rest (see Figure 44).

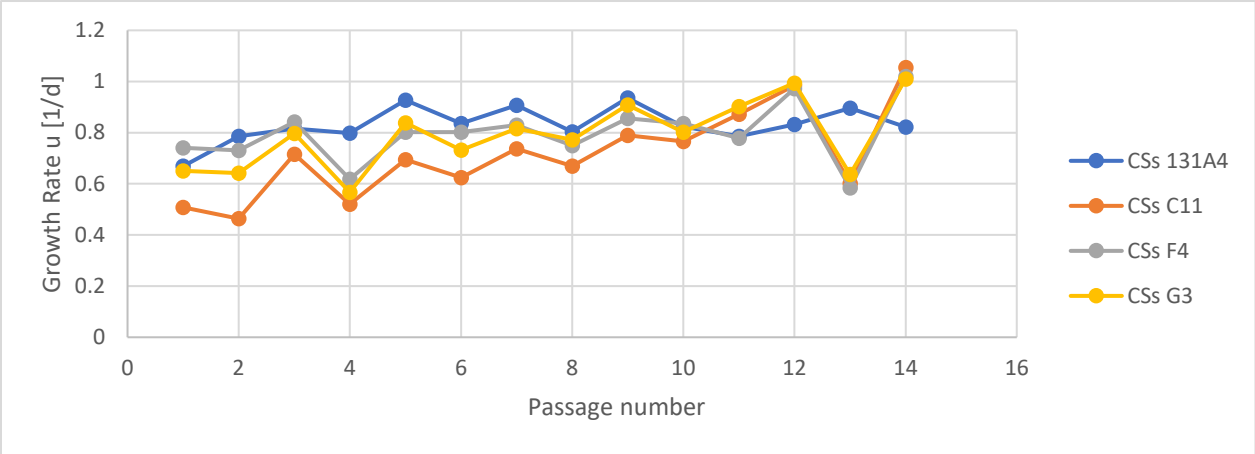

Figure 44: Calculated growth rate for each passage of the CSs clones

The titer of the subclones increased over passage number with C11 peaking at 13.7 mg/L, F4 with 5 mg/L and G3 8 mg/L (see Figure 45). The parental clone 131A4 reached a maximum 2.7 mg/L (see Figure 45).

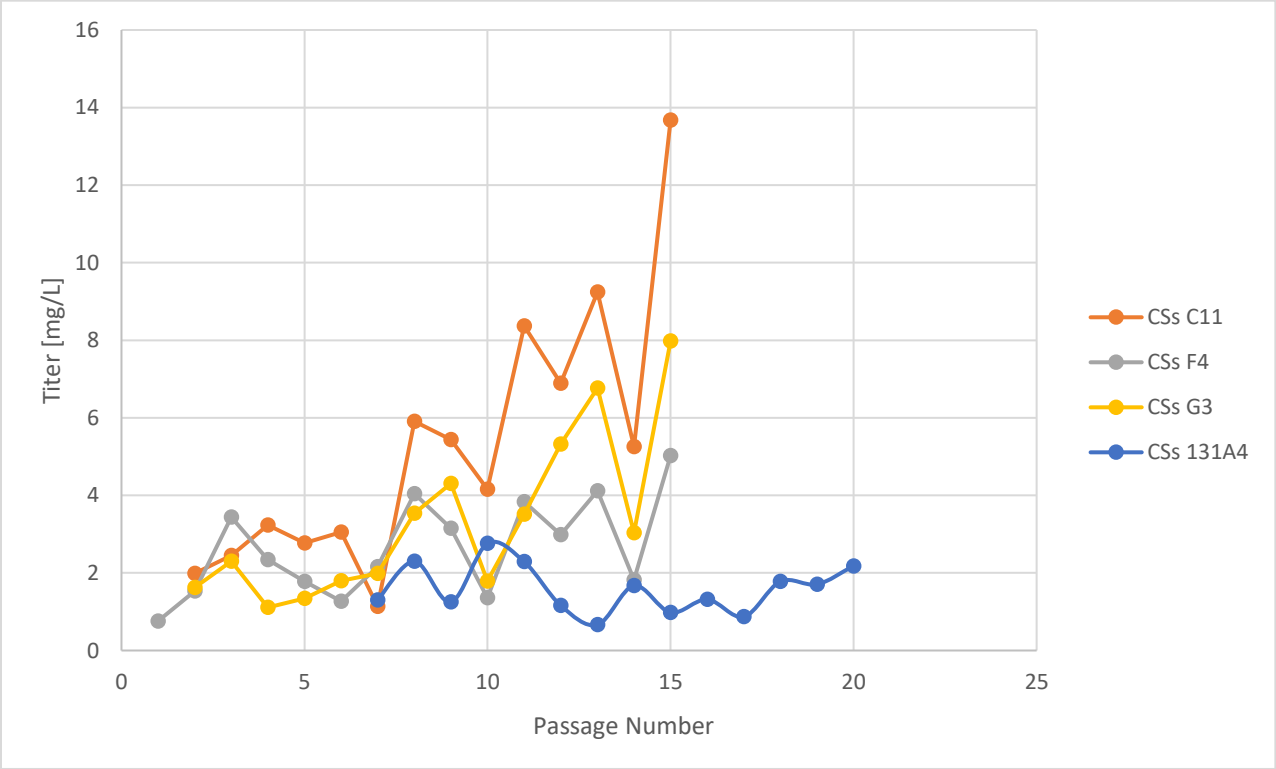

Figure 45: Titer of the CSs clones at the end of a passage cycle, measured by quantitative Anti-His-Biotin ELISA

The qP calculated over a timeframe of 3-4 days, depending on passage, showed a maximum productivity of C11 with 2.3 pg/c/d at passage 14, while F4 and G3 had a peak at passage 6 with 0.6 pg/c/d, only slightly higher than the peak of 1313A4 at passage 11 with 0.5 pg/c/d(see Figure 46).

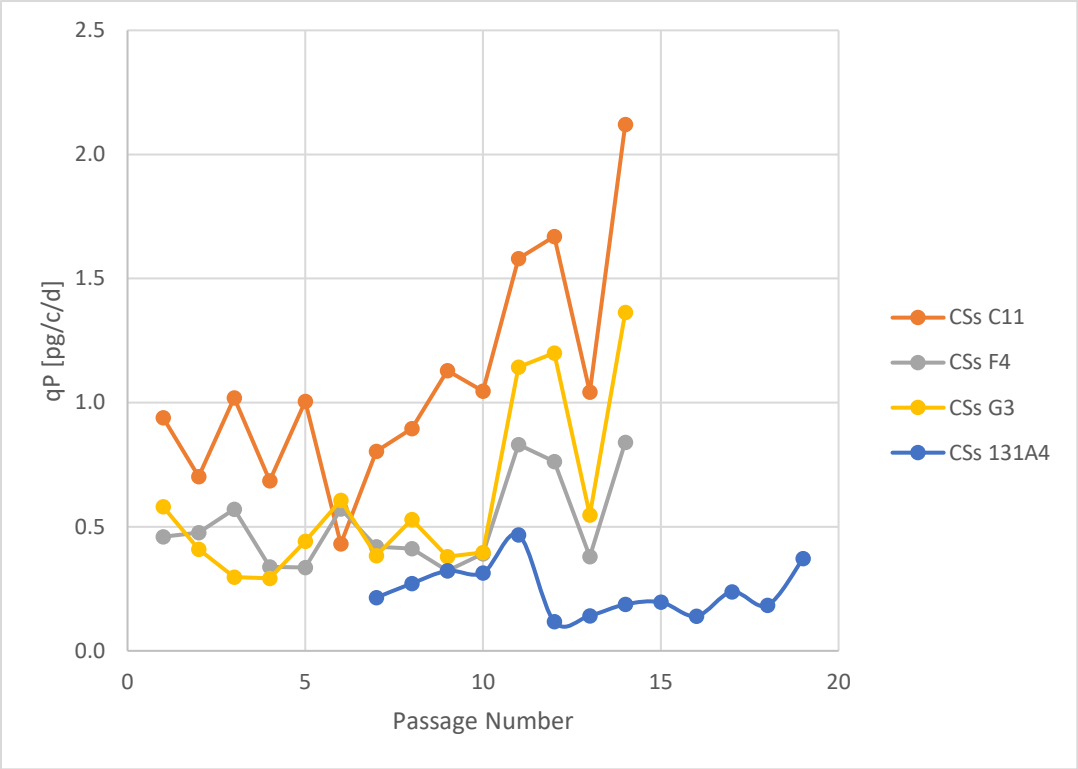

Figure 46: Specific productivity qP over passage number

Figure 47 shows boxplots of the CSs qP to further clarify the differences between the clones.

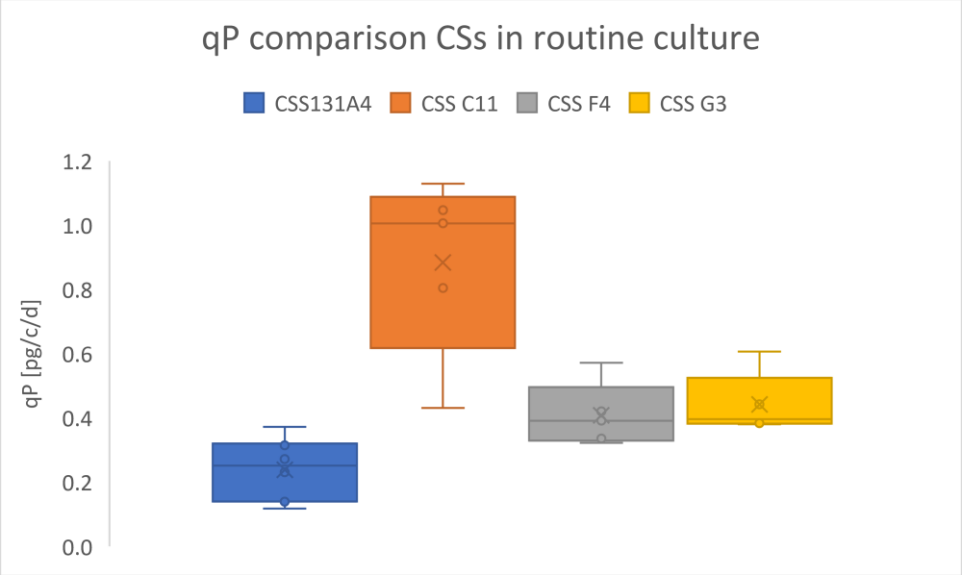

Figure 47: Boxplots of the qP of the CSs subclones and its parental clone in routine culture

We can see that CSs C11 has significantly higher productivity than the parental clone (although also having the highest variance), with a median of 1.01 pg/c/d, 4 times the amount of the parental clone with 0.3 pg/c/d (Figure 47). F4 and G3 both have a median 0.4.

3.4.3 Consecutive passaging of CD19-AD2 clones

The parental clone D19 needed 5 passages after cryo storage to reach a viability over 90% and a VCD of over 2E6 cells/mL in a passage time frame of 3-4 days. After 7 passages, D19 was subcloned, which

resulted in the generation of C2, E10 and F9. From the subclones, cryos were stored at passage number 15. These had a way faster regeneration time compared to the parental clone, reaching a viability of over 90% already after 1 passage. The subclones tended to have slightly higher VCD than the parental clone, with F9 reaching nearly 8E5 cell/mL after 4 days in culture, while D19 reached a maximum of 5.5E6 cells/mL after 4 days (see Figure 48).

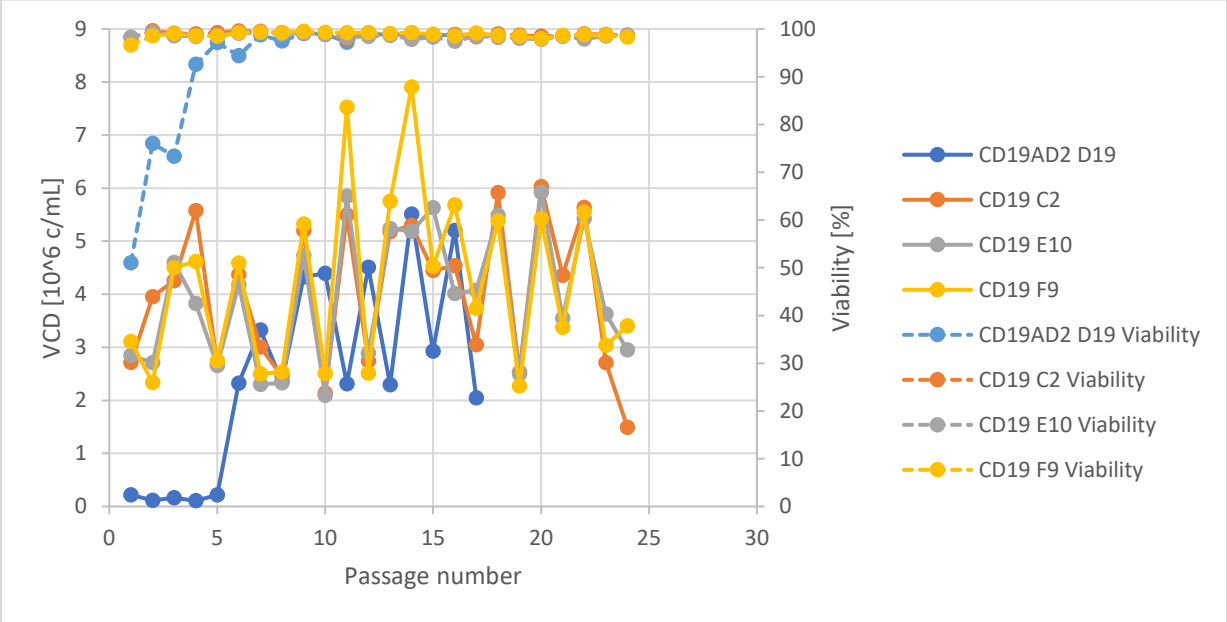

Figure 48: VCD and viability of the CD19-AD2 clones.

The growth rate of the routine culture over 3-4 days was generally in the range of 0.7(see Figure 49). The subclone F9 reached a peak µ of nearly 1, which might be an outlier. Generally, we can observe that all the subclones had the same if not higher growth rate as the parental clone.

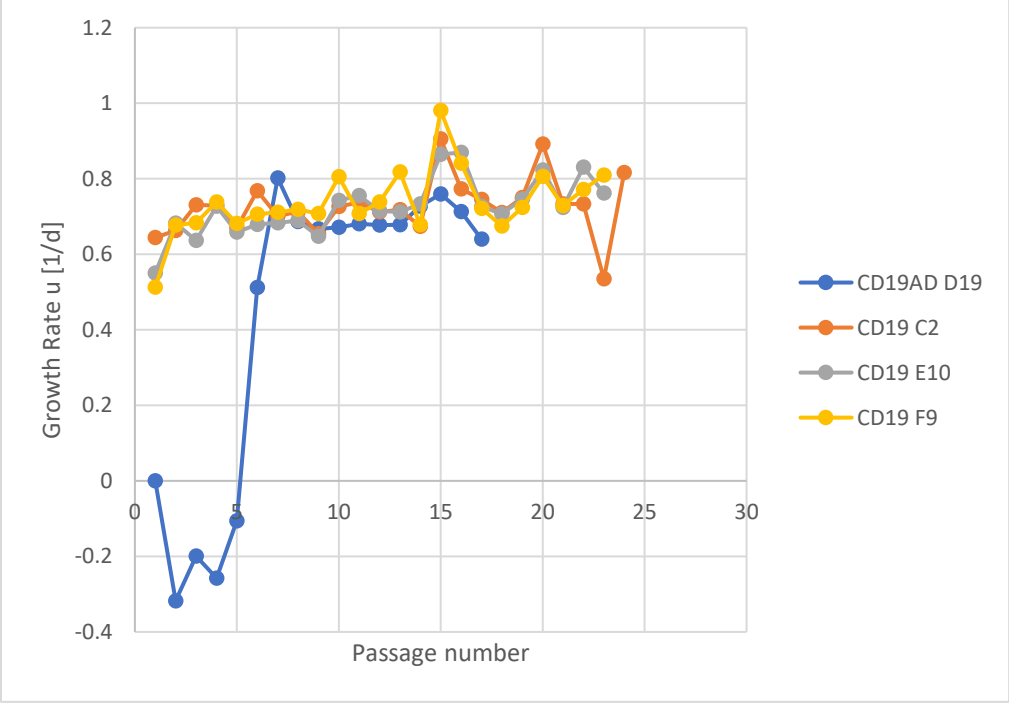

Figure 49: Growth rate calculated over each passage cycle, 3-4 days.

Titer was measured from supernatant sample at the end of each passage cycle. Due to the inconsistent culture duration, a high variance in titer was observed (Figure 50). C2 and E10 reached a maximum titer of 80 mg/L at passage 20 and F9 70 mg/L (Figure 50). The peak titer of the parental clone D19 was 19 mg/L.

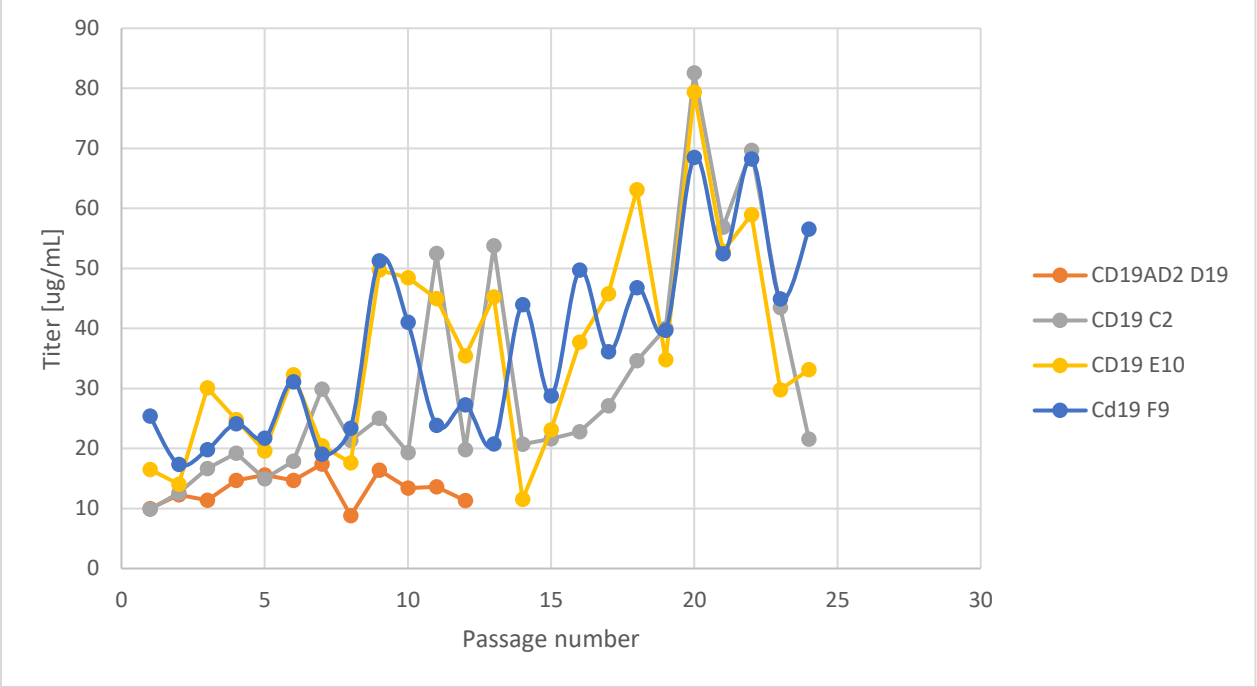

Figure 50: CD19-AD2 titer measured at the end of each passage cycle, measured by quantitative ELISA

We can see in the qP and the titer graphs (Figure 50, Figure 51) that there seems to be a trend in later passages towards higher titers and productivity.

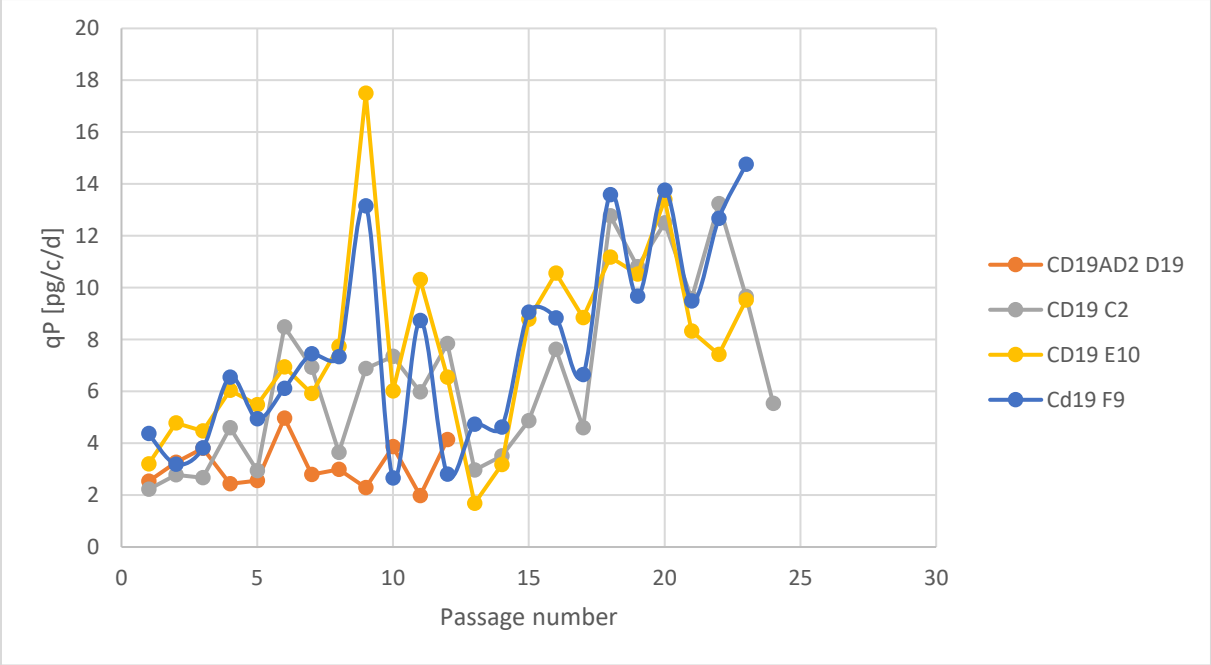

Figure 51: Calculated specific productivity over passage time

To compare the different subclones as well as the parental clone fairly, the specific productivity qP was calculated for each passage. Because the qP and the growth rate were not calculated per day and rather for 3-4 days at once, the average values are not comparable to the batch cultivation.

To further illustrate the differences in specific productivity, boxplots were created (Figure 52).

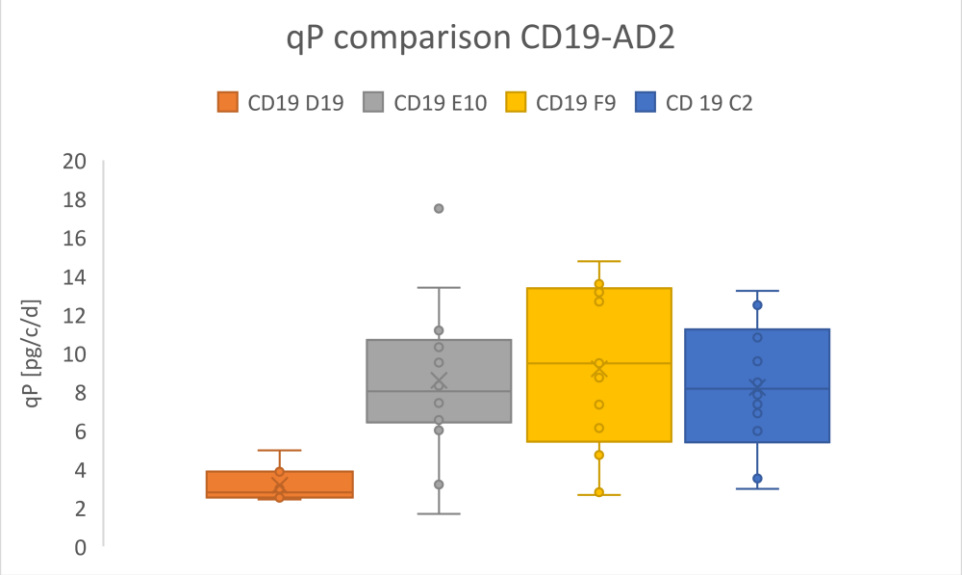

Figure 52: Boxplots of the qP of the CD19-AD2 subclones and its parental clone

The CD19-AD2 subclones differed less than the other protein-clones from the parental clones. The parental cone D19 had a median of 3pg/c/d (Figure 52). The subclones, all showing a high variance in their productivity, had a median of 8pg/c/d (E10 and C2) and 9 pg/c/d (F9). But they sometimes also displayed lower productivity than the parental clone.

3.4.4 Western blot of routine culture supernatants of all three proteins

To determine possible differences in protein size between the clones of one protein or wrong expression, we loaded an SDS-PAGE with the supernatant of each clone 4 days after passage and performed a Western blot (see Figure 53 for the blot, Table 5 for sample data). Anti-His biotin was chosen for detection. In every well the same volume of supernatant was loaded.

Table 5 : Sample plan of Anti-His Biotin Western blot, every well was loaded with 12 µl supernatant; Supernatant of the CSs and RBD subclones was taken from passage number 11 and of the CD19-AD2 from passage number 15

Well Nr:	**1**	**2**	**3**	**4**	**5**	**6**	**7**	**8**	**9**	**10**
Sample	marker 5uL prestained	CSs C11	CSs F4	CSs G3	RBD F3	RBD F8	RBD G7	CD19-AD2 C2	CD19-AD2 E10	CD19-AD2 F9
ELISA [mg/L]		8.4	3.8	3.5	66	75.6	34.2	82.6	79.4	68.5
µg loaded		0.1	0.05	0.04	0.8	0.9	0.4	1	0.9	0.8

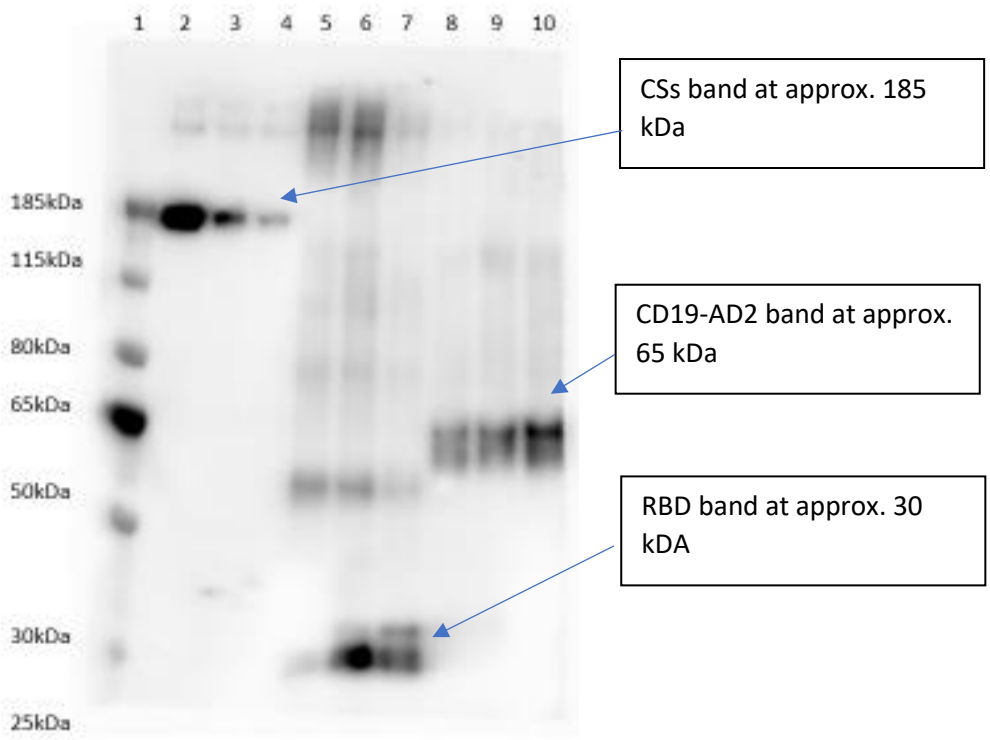

Figure 53: Anti-His Biotin Western blot of routine culture samples

CSs:

We can see in all 3 clones a high intensity band around the 185kDa marker line (Figure 53, column 2,3,4), as well as 2 very weak band in the high molecular weight range, suggesting the aggregation of the monomers and the formation of dimers

RBD:

Interestingly, the clones F8 and G7 show two discernible bands around 30kDa, while F3 does not (Figure 53, column 5,6,7). Between the 50kDa and 65kDa marker lines we can see in all 3 clones a weak band, which indicate the formation of RBD dimers. F3 and F8 show a visible smear over the 185 kDa line, which might point aggregation of RBD into oligomers.

CD19-AD2

We can discern one distinct band slightly below the 65 kDa marker line which corresponds to the fully glycosylated form of CD19-AD2 (Figure 53, columns 8,9,10). The smear below the distinct band, at approximately 60 kDa, could stem from not fully glycosylated protein, or even point to a degradation.

3.4.5 Western blot determination of CSs and RBD with SARS-COV-2 HyperimmuneIgG

We wanted to try out the possibility to make a Western blot with the biotinylated Covid-19 HyperimmuneIgG (Takeda), to see if our recombinant CSs and RBD binds. The blot can be seen in Figure 54, and the sample data is displayed in Table 6.

Table 6: Sample plan of HyperimmuneIgG Western blot; 12 µL of supernatant from passage 11 was loaded

M	1	2	3	4
marker 5uL prestained	CSs C11 0	CSs F4	CSs G3	RBD F3
[mg/L]	8.4	3.8	3.5	66.0
µg loaded	0.1	0.05	0.04	0.8

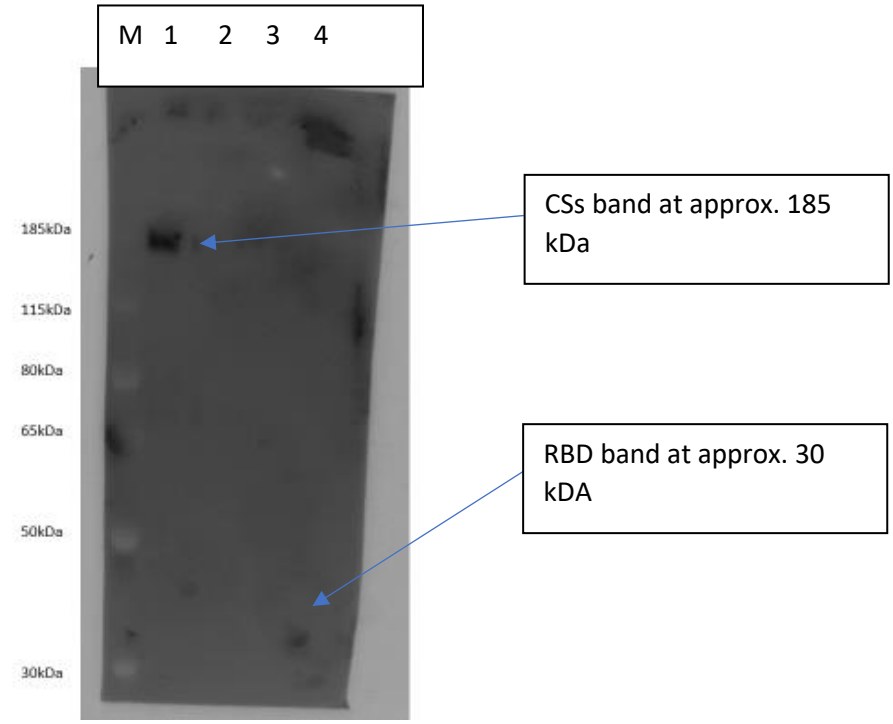

Figure 54: Western blot of the routine culture supernatant with biotinylated HyperimmuneIgG as first conjugate

As we can see in Figure 54, only the CSs C11 clone and the RBD F3 showed a visible, although weak band. The CSs band is, as expected, around the 185 kDa marker line, whereas the RBD band around the 30 kDa marker line. The lack of binding is also seen in the FACS measurements (see Figure 75) where the HyperIgG showed the lowest binding capacities.

3.4.6 Media testing: CDM4HEK vs. CDCHO with CSs clones

In our 4°C cold room, several liters of for 2 years expired CDM4HEK media were stored. To reduce the cost of the planned fed batch, it would be preferred to use this instead of the standard CDCHO medium.

To ensure the medium is still usable, a small 7 day batch with 15 mL culture volume was started. 4mM L-glutamine was added to the media. Sampling was from process day 1 to day 4, with a final sample on process day 7. The VCD, viability and growth rate are shown in Figure 55.

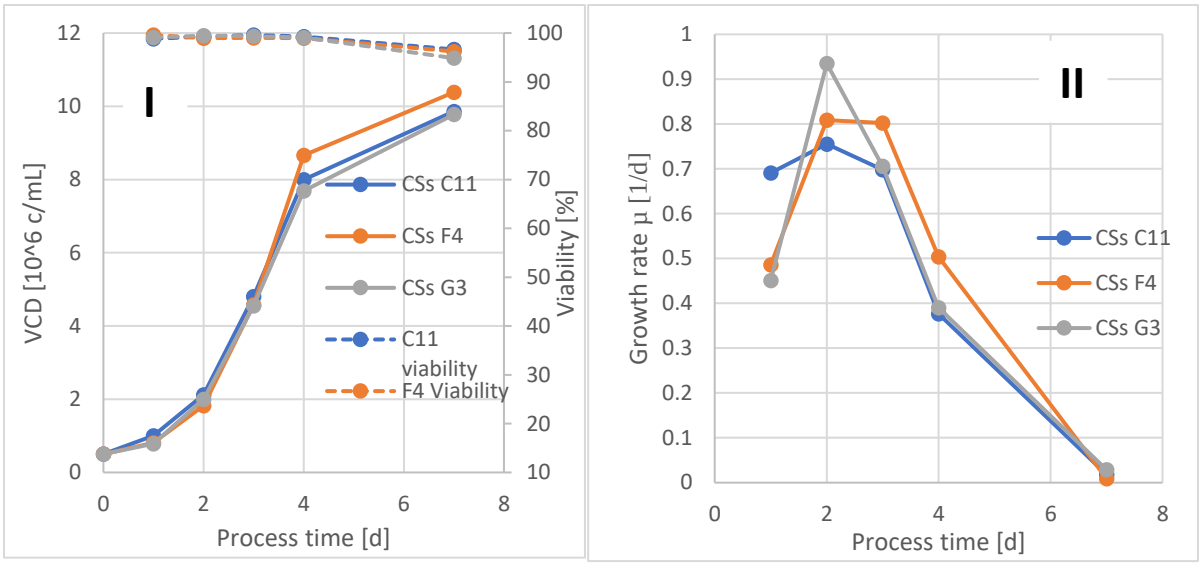

Figure 55: I: VCD and viability of the cultures in CDM4HEK; II: Growth rate over time in CDM4HEK

Regarding growth rate and viable cell density, the expired CDM4HEK medium gives similar results to the CDCHO medium, with no apparent negative differences (compare Figure 55 with Figure 57).

To prove the CDM4HEK media could be used to produce the CSs, the CSs titer was measured from the daily samples by ELISA. Titer and specific productivity are displayed in Figure 56.

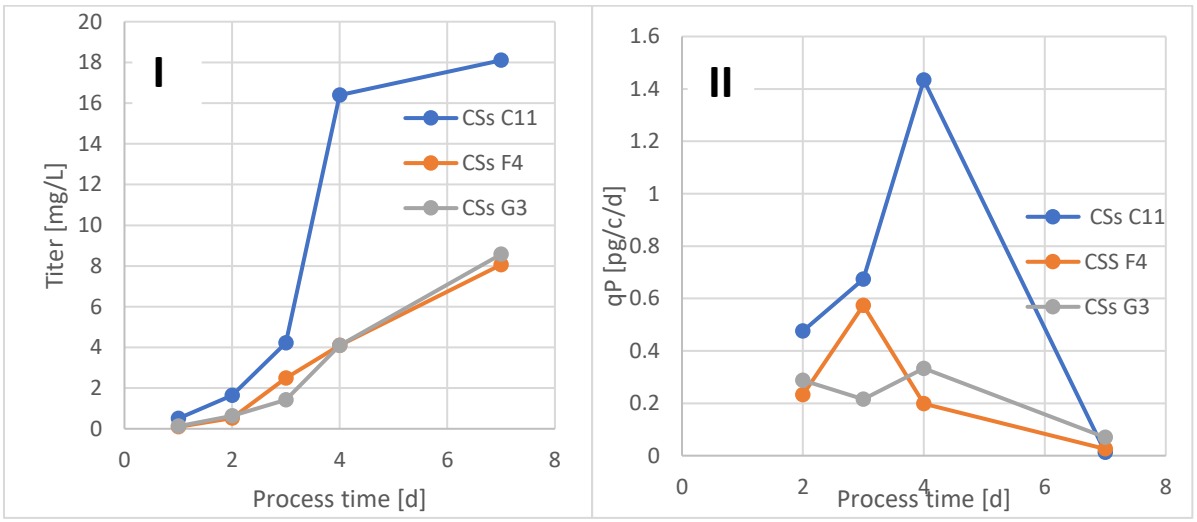

Figure 56: I: Titer in CDM4HEK over process time, measured by ELISA; II: specific productivity qP over process time

In the routine culture, in the same timeframe (day 7 was not measured), the cultures were grown and sampled in the standard CDCHO medium (Figure 57). Interestingly, C11 was the only clone which grew better in CDM4HEK medium, being able to keep up with F4 and G3 in terms of VCD and growth

rate, all of them reaching 8E6 cells/mL (Figure 56). In CDCHO medium, C11 reached only 5.8E6 cells/mL.

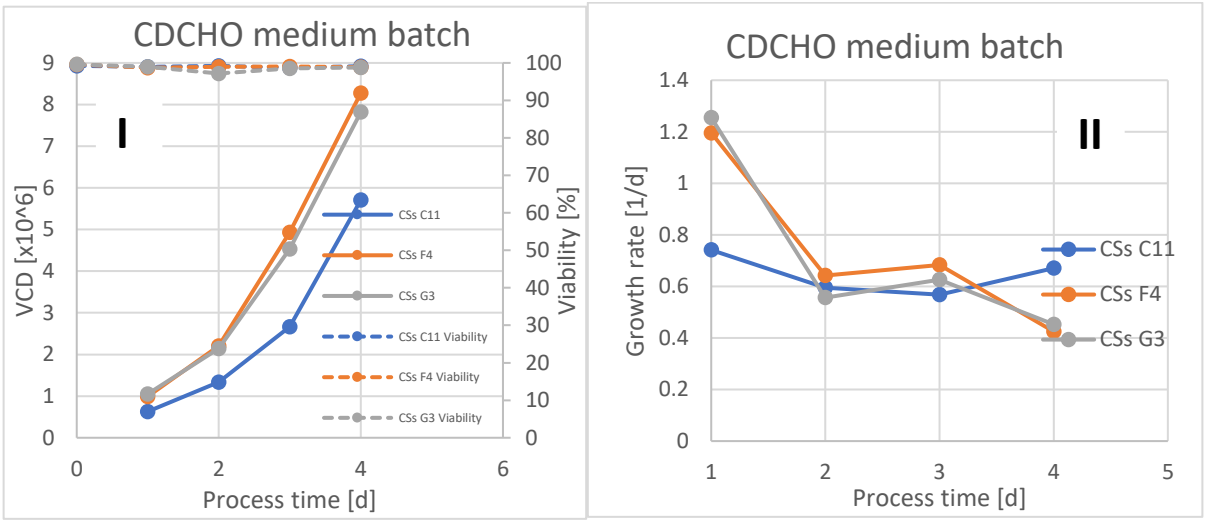

Figure 57: I: VCD and viability of the CSs subclones in CDCHO medium; II: growth rate of the CSs subclones in CDCHO medium

In Figure 58 the titer and specific productivity in our standard routine medium are displayed. Compared to the values in Figure 56, we can see that the CDM4HEK medium has to detrimental effect on titer or productivity of the CSs clones.

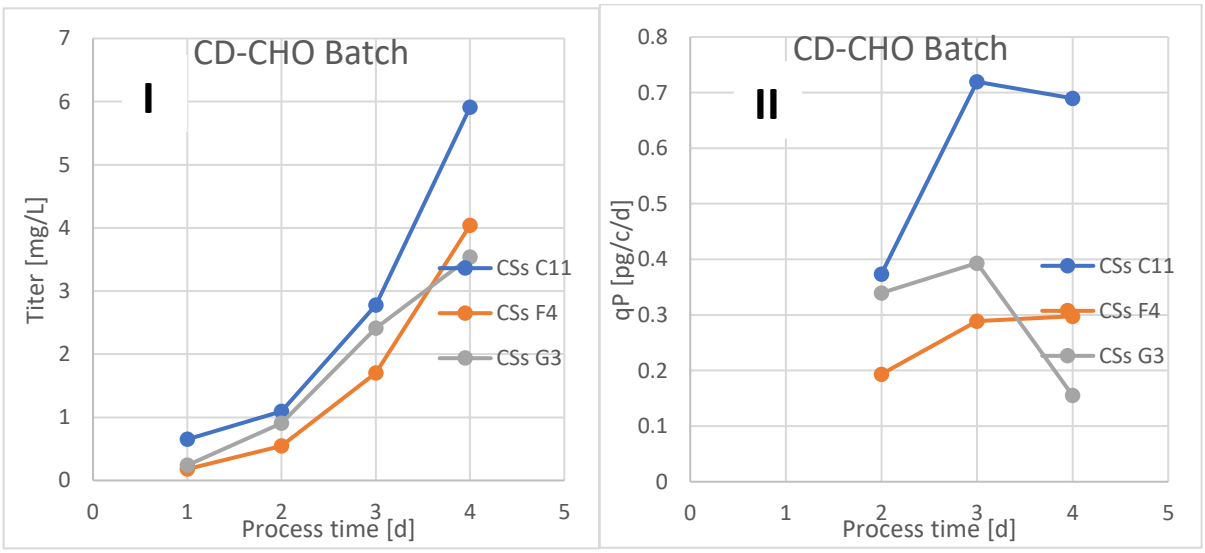

Figure 58: I: Titer in CDCHO over process time, measured ELISA); II: specific productivity qP over process time

It seems that the CDM4HEK medium, even though expired, has no negative effect on cell growth and productivity. Subclone C11 even produced significantly more (more than 2fold titer increase) CSs in the CDM4HEK medium compared to CDCHO (Figure 56).

3.5 Multiple reactor Fed-Batch with CSs C11 (experiment F206)

To test our top clone at different conditions which may influence the cell growth, production and metabolite consumption, we started a 4-reactor fed batch fermentation with the DASGIP system. The four DASGIP reactors have each a volume of 2 L, and we used a working volume of 500 mL. The

expired CDM4HEK medium was used as a medium basis, with an addition of 6 mM L-Gln. 6mM L-Gln addition was chosen to not limit cell growth in the exponential phase caused by L-Gln limitation. More than 6 mM would result in a higher ammonia production, which has detrimental effects on cell growth and productivity.

A biphasic process (two temperatures, with and without VPA) to reach a maximum of CSs production was planned: After inoculation (0.3 E6 VCD/mL) the first 6 process days (most of the exponential phase), all reactors operated under the same standard conditions, 37°C; pH 6.8; stirrer 80 rpm; DO over 30%; O_2 content in gas flow 21%; feeding with Fed A and Feed B combo at day 3 and 6. Due to a malfunction in the pH electrode, one reactor could not adjust the pH to the setpoint of 6.8 and had to be discarded. On process day 6, after a high amount of biomass was already produced, the culture conditions of reactor 1 (T1) and 4 (T4) were changed.

Reactor T1 was adjusted to 1mM of VPA.

Reactor T2 was kept under standard conditions at 37°C as control.

Reactor T4 was subjected to mild hypothermia (reactor temperature to 32°C)

From day 7 on feeding was adjusted according to metabolite content and osmolarity. As a feeding strategy, Feed A was added in volumes of 3% of the reactor working volume, in combination with Feed B in volumes of 10% the added volume of Feed A. This feeding regiment was used when both the glucose and L-glutamate concentration in the media were decreasing and/or low. If only the glucose concentration was low and the osmolarity increased, the pure glucose solution (250 g/L) was added. Depending on lactate and glucose concentrations, glucose was fed, ranging from 0.3-1.5g per reactor (see Table 7, Figure 59), even though no specific setpoint in metabolite concentrations was defined. To curb down lactate production, feeding was reduced or even suspended if the lactate concentration was high (over 1g/L)

Day	**total glucose** added [mg]			**total glutamate added [mg]**			**Feed A fed [mL]**			**Glucose solution fed [mL]**		
	T1	**T2**	**T4**	**T1**	**T2**	**T4**	**T1**	**T2**	**T4**	**T1**	**T2**	**T4**
3	907	917	911	113	114	114	13.2	13.4	13.3			
6	843	850	839	106	106	100	12.2	12.3	12.2			
7	852	853	858	106	106	102	12.4	12.4	12.5			
8	1098	1427	1168							4.2	5.5	4.5
9	909	909	623							3.5	3.5	2.4
10	858	1684	856		101			11.6		3.3	3.3	3.2
11	911	936	833							3.5	3.6	3.2
12	746		760	94		91	10.8		11			
13			443									1.7
14	261		418							1		1.6
15			366									1.4
16			734									2.8

Table 7: amount of glucose and l-glutamate fed to the reactors; l-glutamate is a component of the feed A+B combination

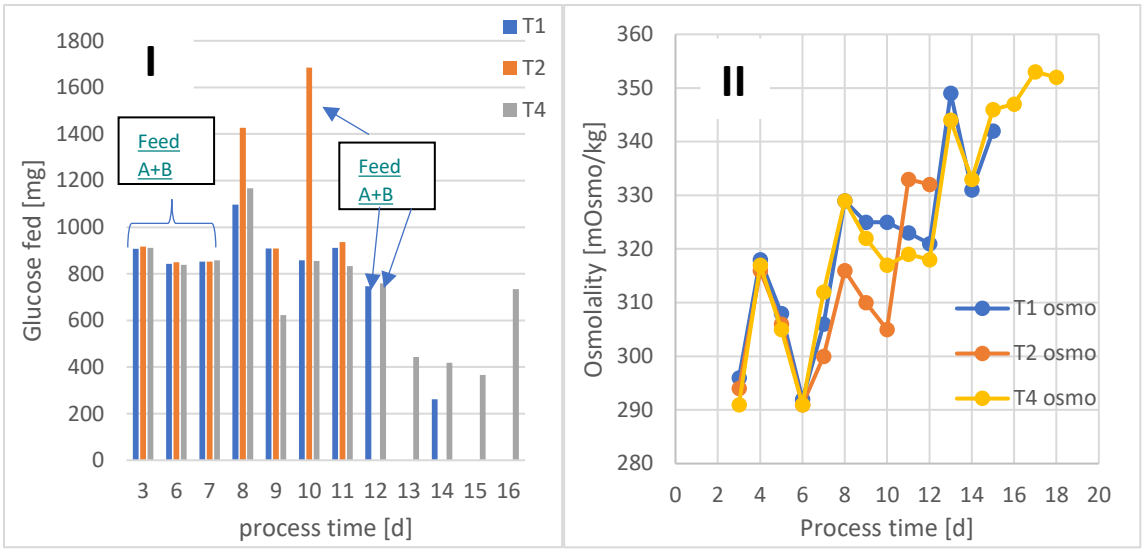

Figure 59: Glucose fed per day per reactor; if the feed A+B combination was not used, only glucose solution was fed; II: Osmolality of the ractors T1(+1mM VPA on day 6), T2 (control) and T4 (32°C after day 6) over process time; sharp increases were caused by the Feed-combination

High osmolality in the cell suspension can severely diminish cell performance and in some cases influence product quality, so it was an important parameter to control. Feed A +B combination would significantly increase the osmolality, so to keep it in check, glucose solution was used when we saw a steep rise in osmolarity. Osmolality increased slower in the control reactor T2 compared to T1 and T4, only reaching higher osmolality after process day 10 (Figure 59, II)

In Figure 60 I the VCD and viability of the reactors are shown, measured every 24h. Figure 60 II displays the calculated growth rates per day.

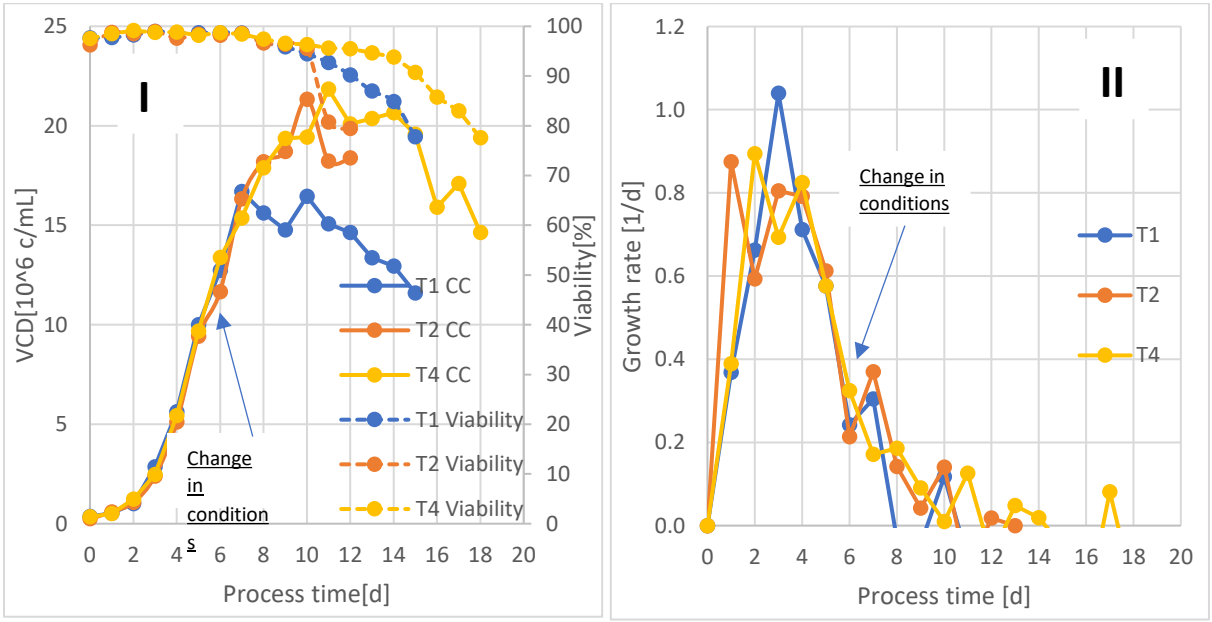

Figure 60: I: Viable cell density (CC for cell count in the diagram) and viability of the reactors T1(+1mM VPA on day 6), T2 (control) and T4 (32°C after day 6); II: Growth rate over time of the different reactors, T1(+1mM VPA on day 6), T2 (control) and T4 (32°C after day 6)

In T1 (1mM of VPA) the viability and VCD decreased steadily after VPA addition on day 6, but kept viability over 80% until day 15.

In T2, the control operating under standard conditions, the viability dropped at day 11, , decreased to 80% and was therefore discontinued.

T4 (hypothermic conditions from day 5 on) showed no decrease in VCD compared to T2 and continued to have viability above 80% until day 18.

After initially high µ around 0.8 (T1 even reaching above 1), we could observe a fast decline in the stationary phase of the culture (Figure 60 II).

Due to the unexpected high product concentration of T4 (up to 0.55 mg/L), the ELISAs were redone 2 times, resulting in the same outcome. The titers of each reactor and the specific growth rate are shown in Figure 61.

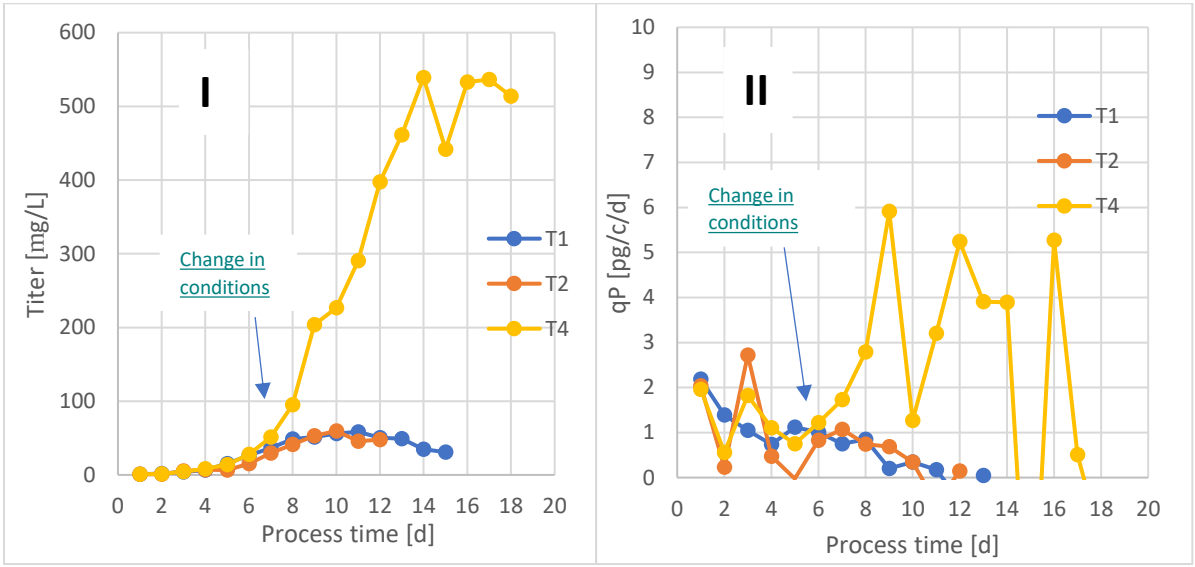

Figure 61: I: Product concentration in the reactors T1 (+1mM VPA on day 6), T2 (control) and T4 (32°C after day 6) over time, measured by ELISA; II: Specific CSs productivity over process time of the reactors T1(+1mM VPA on day 6),T2 (control) and T4 (32°C after day 6)

T4 with lower reactor temperature had a nearly 10fold higher product titer compared to T1 and T2, from a peak titer of 58 mg/L in T1 and T2 to 550 mg/L in T4 (Figure 61 I). The reactor with VPA addition had roughly the same titer concentration over process time as our control reactor with standard conditions. The drop in product concentration on d15 in T4 should be considered as an outlier.

Although the specific productivity is not well suited to compare these reactors with a long-time frame and high cell number[32], it gives a good general view on the performance of the reactor. T4 outperforms the other 2 reactors after day 6 by a huge margin, peaking at 6pg/c/d on day 9 (Figure 61). The qP of both T1 and T2 slowly decline after day 6, and T1 reaches the zero-point on day 11.

Glucose concentration was measured daily. Either by the Feed A and B combination or with glucose/H_2O solution the glucose content in the reactor was influenced, visible by the sudden upward spikes in Figure 62, I.

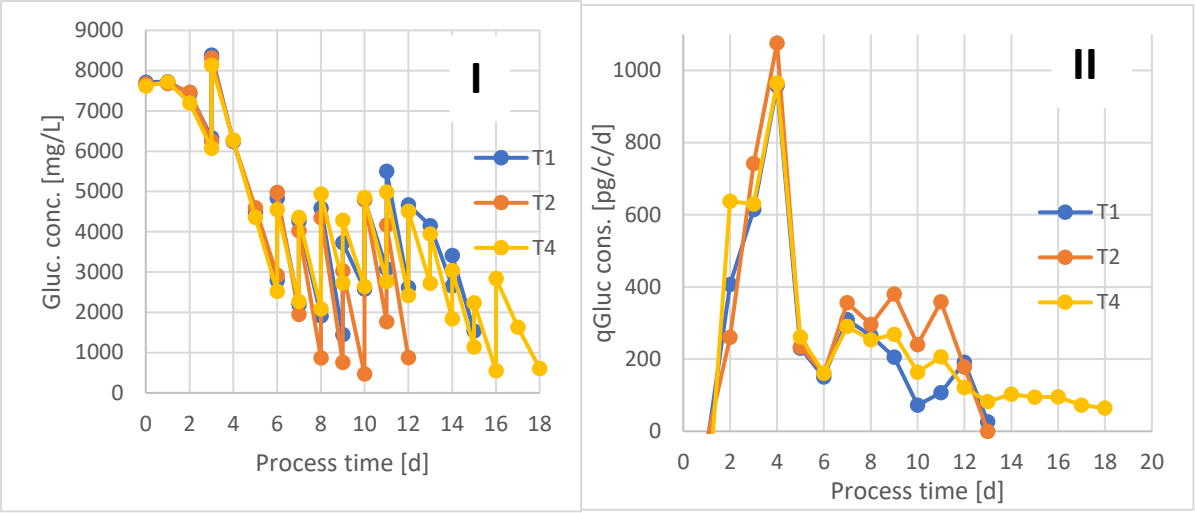

Figure 62: I: Glucose concentration over the reactos T1(+1mM VPA on day 6), T2 (control) and T4 (32°C after day 6) process time, measured by Bioprofiler; II: calculated specific glucose consumption

In the stationary phase T2 had the highest glucose consumption and the reactor was fed every day (Figure 62 II). T4 as well as T1 had slightly lower glucose consumption, and glucose feeding was not done continuously, to curb lactate production. Figure 62 III shows the amount of glucose in mg fed per day.

Lactate was measured approximately every 24h. It is one of the most important metabolites to control in a process, as it gets abundantly produced by glycolysis. It has negative impact on the cell growth and can influence product quality. There are several ways to induce lactate metabolic shift, like limiting glucose and glutamine availability[33,34].

Lactate was produced in high amounts in the exponential phase, with all reactors peaking at day 7, T4 reaching 1.7 g/L, T1 and T2 reaching 1.6 g/L (see Figure 63 I). Lactate concentration of T1 and T2 dropped rapidly after day 7 to zero on day 10, while lactate production was constantly low and in the negative (see Figure 63 II), which means lactate was consumed. The lactate concentration of T1 stayed at 0 with an outlier at day 14, despite glucose feed. In T4 lactate dropped to its lowest point of 450 mg/L on day 12, and afterwards raising again until process stop at day 18, where lactate concentration peaked at 1.84 g/L.

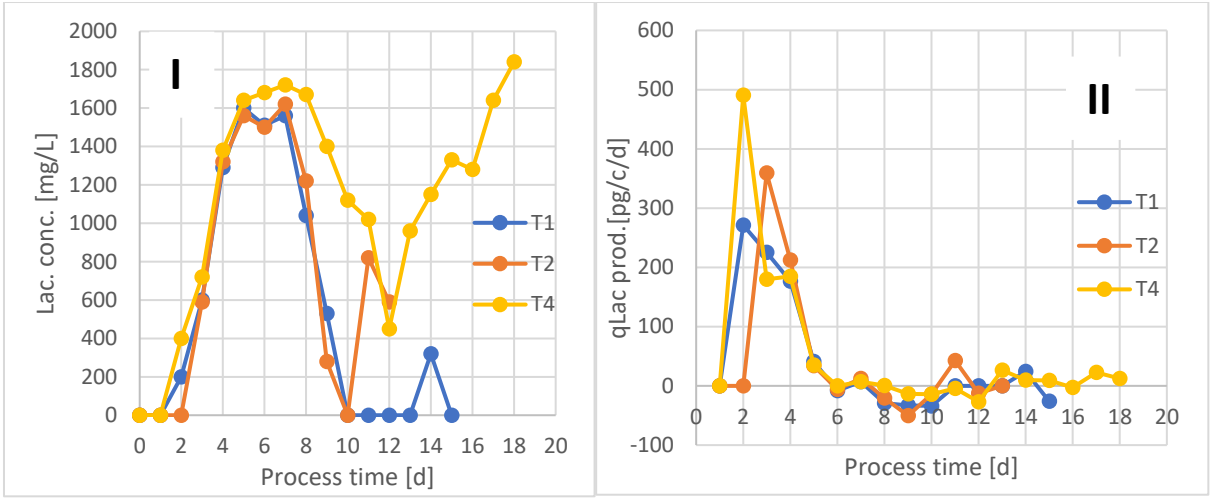

Figure 63: I: Lactate concentration of the reactors T1(+1mM VPA on day 6), T2 (control) and T4 (32°C after day 6) over process time, measured by Bioprofiler; II: Specific lactate productivity over time

The medium of the reactor was supplemented initially with 6mM L-Glutamine, and the remaining concentration measured every day (Figure 64). By process day 6, every reactor had its L-glutamine reserve depleted, as the feed combination did not contain glutamine. T2's L-Gln concentration already reached zero at process day 5.

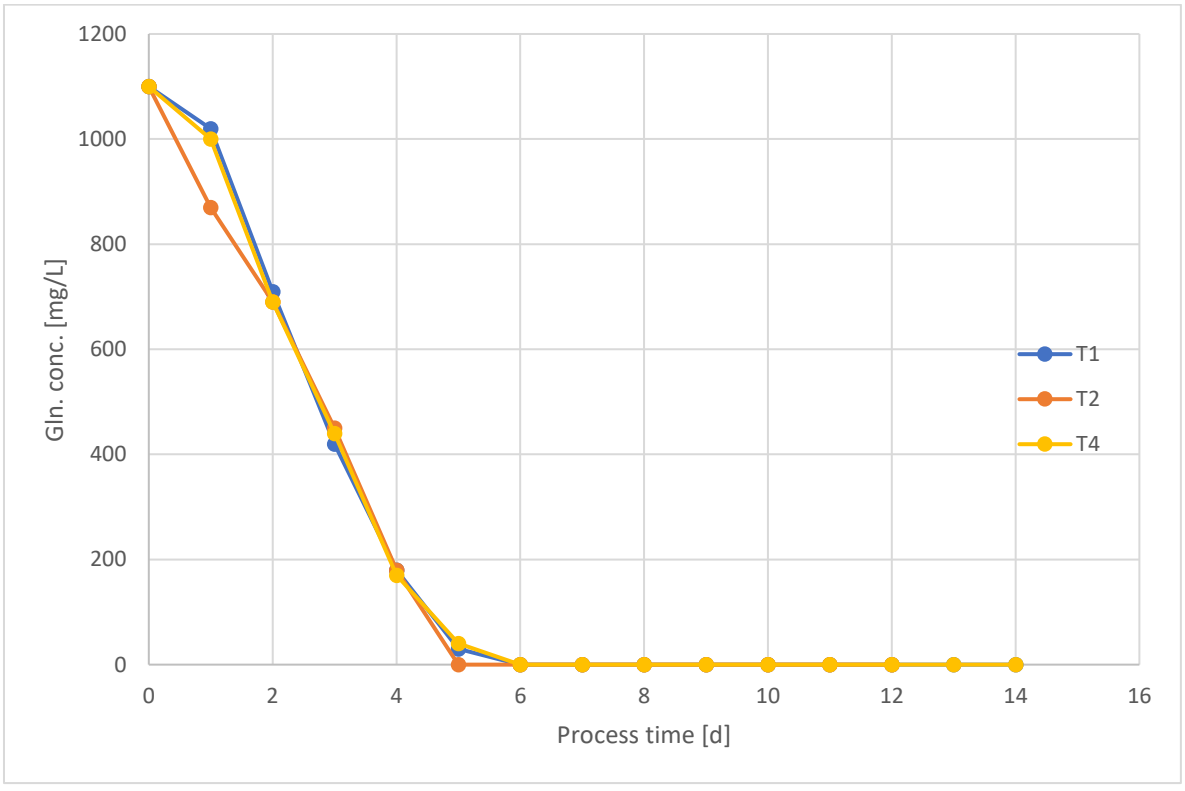

Figure 64: L-Glutamine of the reactors T1(+1mM VPA on day 6), T2 (control) and T4 (32°C after day 6) concentration over process time, measured by Bioprofiler

L-glutamate concentration was measured every 24 h. It serves as an energy source and can be metabolized to L-glutamine via the glutamine synthetase. The Feed combination contained L-glutamate, so after every feeding of Feed A+B there is a sudden increase in concentration (see Figure

65). T2 had the most feeding per timeframe until process stop at day 12 and reached concentration up to nearly 900 mg/L L-glutamate (see Table 7, Figure 65 I).

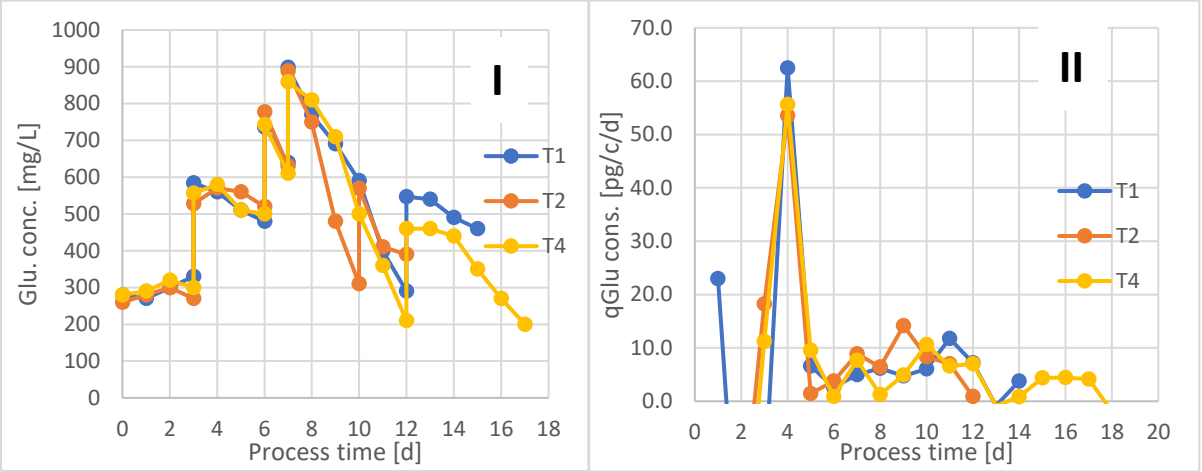

Figure 65: I: L-Glutamate concentration of the reactors T1(+1mM VPA on day 6), T2 (control) and T4 (32°C after day 6) over process time measured by bioprofiler; II: calculated specific L-glutamate consumption over process time

After an initial spike of glutamate consumption at day 4 in all reactors, the specific consumption decreased to under 10 pg/c/d (see Figure 65 II), with a small outlier on day 9 with reactor T2.

Ammonia is a byproduct of normal cell metabolism, produced in high amounts by metabolization of L-glutamine and L-asparagine. High ammonia levels in the supernatant decrease growth rate, cell viability and can influence product quality. Ammonia is necessary for the last step of the conversion of L-glutamate to L-glutamine via the glutamine synthetase. So, to curb the ammonia levels, we supplemented the medium initially with 6mM L-glutamine, which is higher than our standard 4mM in routine culture, but we did not feed any additional L-glutamine. Ammonia concentration and consumption are displayed in Figure 66.

In the exponential phase there is a steep rise of NH_4^+ concentration up to 140 mg/L in all reactors, coinciding with the consumption of all the L-glutamine in this timeframe (see Figure 64). Specific productivity of NH_4^+ has a peak on process day 1 and 2 with up to 30 pg/c/d and decreases rapidly to zero at day 6 (Figure 66 II). After the change in environmental condition (VPA addition in T1 and temperature decrease in T4) we can see a fast rise of NH_4^+ concentration in T2 up to 200 mg/L by day 12, were the viability in the reactor dropped to under 80% (see Figure 60). T1 and T4 reached the same concentration 2 days later. The ammonia levels of T4 only began to rise after day 10, 2 days later than the other 2 reactors. T4 reached 250 mg/L on day 18, were the viability dropped to 80%. Interestingly, specific ammonia production followed in T1 and T4 was very similar.

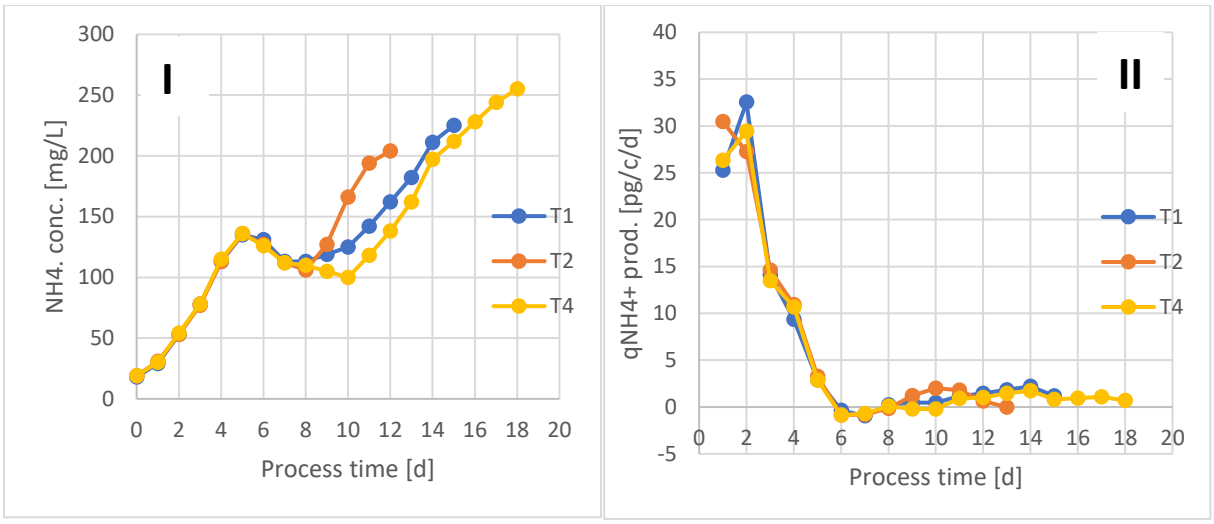

Figure 66: I: Ammonium concentration of the reactors T1(+1mM VPA on day 6), T2 (control) and T4 (32°C after day 6) over process time; II: calcuated specific ammonia production pg/cell/day

The DO in all the bioreactors was set to 30%. To supply enough oxygen without increasing stirrer speed (set to 80rpm), pure oxygen had to be added to the gas flow after day 4. Gas inlet flow was set to 3 L/h. Oxygen percentages and a modified oxygen consumption of the reactors are shown in Figure 67.

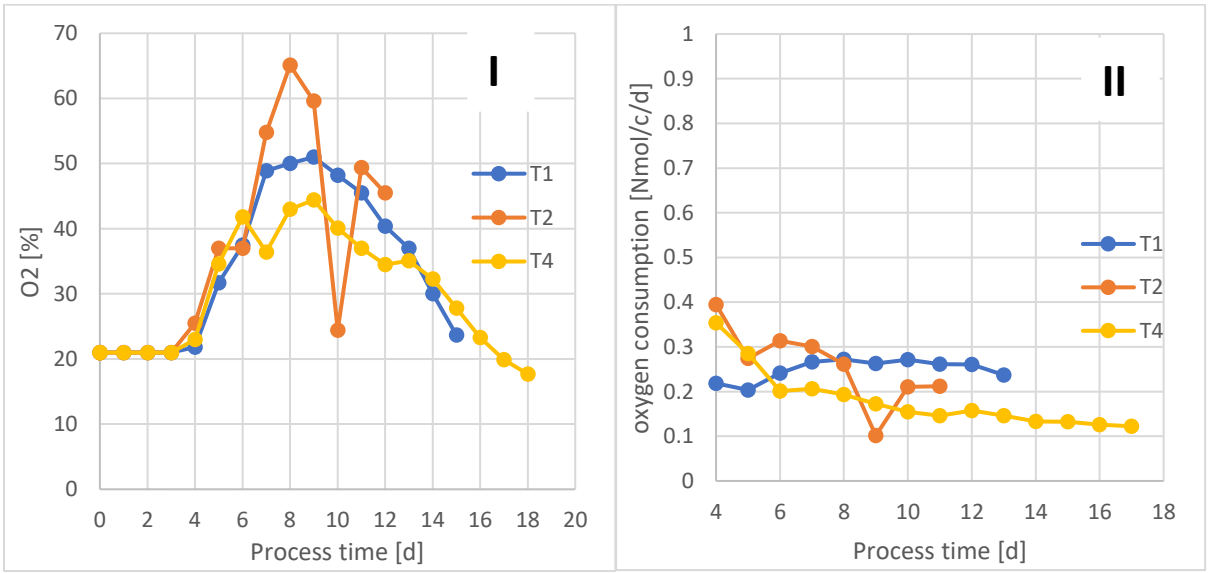

Figure 67: I: Oxygen percentage of the reactors T1 (+1mM VPA on day 6), T2 (control) and T4 (32°C after day 6) in the gas inlet flow; II: calculated oxygen consumption per day.

Until process day 8, T2 under standard conditions had the highest oxygen consumption of all the reactors. T4 under mild hypothermia conditions had a constantly lower oxygen consumption than both T1 and T2, while T1 had the highest oxygen consumption after process day 8.

CO_2 was supplied in the gas inflow and the percentage was adjusted automatically by the DASGIP system to control the pH (setpoint to 6.8) in combination with the base. But because the pH never dropped lower than 6.8, no base addition was necessary. The CO_2 percentages in the gas inlet are shown in Figure 68.

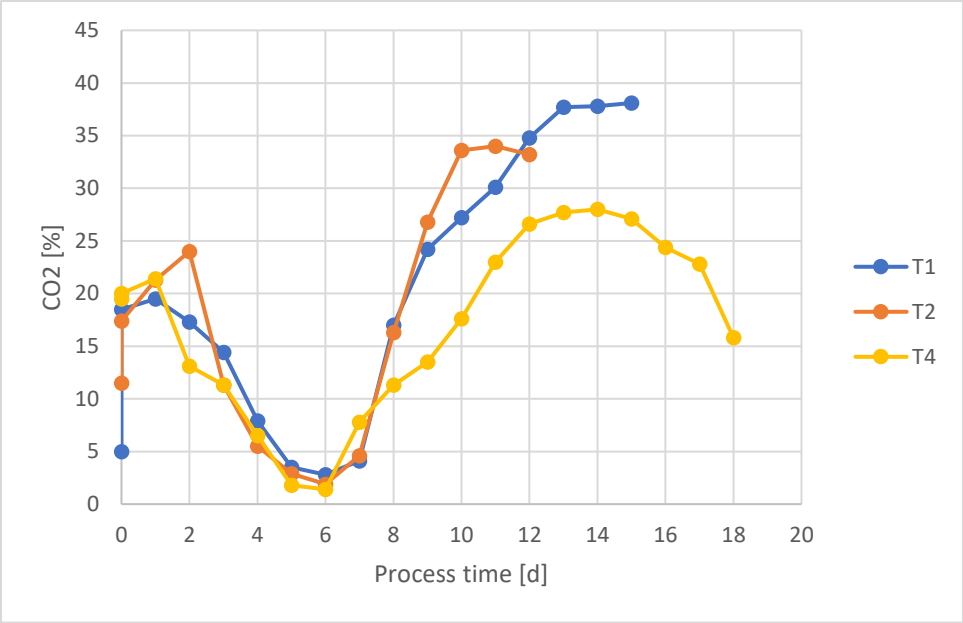

Figure 68: CO_2 percentage in the gas inlet flow of the reactors T1(+1mM VPA on day 6), T2 (control) and T4 (32°C after day 6)

The CO_2 supply decrease from the first day until day 6 coincides with the consumption and the concentration of L-glutamine as well as the high lactate production which decreases the pH. Reactor T4 used less CO2 after the mild temperature decrease on day 6. Increasing ammonia concentration and therefore an increase in pH was countered by an increase in CO2 inflow after day 6.

3.5.1 LDS-PAGE of the unprocessed reactor supernatant

LDS-PAGE of the unprocessed reactor supernatant (stored at -20°C) was performed to further prove our estimated high titers in reactor T4 at d9. To accomplish this, we loaded the gel with the reactor supernatant of d3 to d17 always with 13µL. Supernatant T4 of d9 was additionally applied in a 1:4 dilution to reach the same concentration range as the other supernatants to verify the data from the ELISA. In the reduced part of the gel as well the columns 11 (T1, d9) and 14 (d9, T4) were loaded with the same amount of CSs (Figure 69). Should supernatant of T4 at d9 have a significantly lower CSS product titer than anticipated, the bands should be significantly weaker compared to the bands of T1 and T2 at d9. The sample data is shown in

Table 8 and Figure 69 shows the silver-stained gel.

Table 8: Sample plan of the LDS-PAGE of the reactors T1(+1mM VPA on day 6),T2 (control) and T4 (32°C after day 6); d3 stands for process day 3, d9 stands for process day 9 and d17 for process day 17

	Lane	**samples:**	**conc. [mg/L]**	CSs amount in 13 µL [ng]
non-reducing:	1	F206 d3 T1	4	52
	2	F206 d3 T2	5	65
	3	F206 d3 T4	4.5	58.5
	4	F206 d9 T1	50	650
	5	F206 d9 T2	50	650
	6	F206 d9 T4	200	2600
	7	F206 d17 T4	500	6500

	8	F206 d9 T4, 1:4	200	650
	M	5 µL PageRuler unstained Cat. 26614		
reducing:	9	F206 d3 T1	4	52
	10	F206 d3 T4	4.5	58.5
	11	F206 d9 T1	50	650
	12	F206 d9 T4	200	2600
	13	F206 d17 T4	500	6500
	14	F206 d9 T4 1:4	200	650

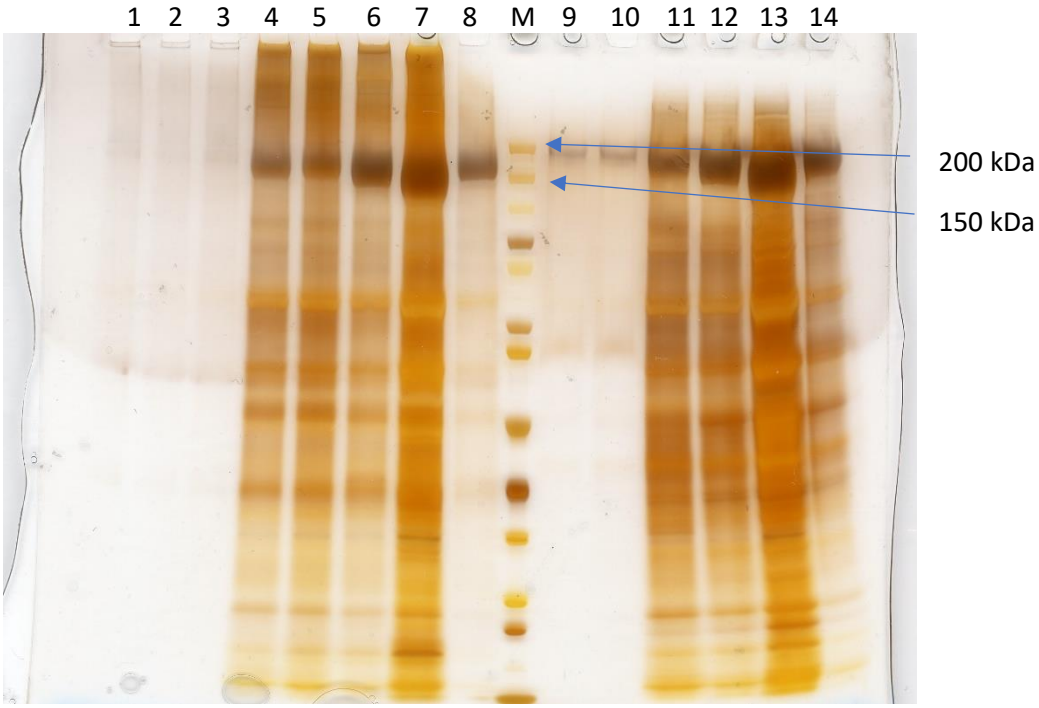

Figure 69: Silver staining of SDS-PAGE; unprocessed Reactor supernatant

The dark, easily discernible band between 150 kDa and 200 lies in the molecular weight range of the CSs protein (174-200 kDa[15]). Given the high concentration measured in the ELISA, it is assumed that this band roughly represents the CSs in the supernatant. Column 8 with supernatant of T4 at day 9 was diluted to match the concentration of the supernatant from T1 and T2 at column 4 and 5(Figure 69). We can presume that the supernatant of T4 on d9 really has the measured concentrations, as the diluted silver staining band assumed to be CSs has next to the same intensities as the undiluted wells loaded with the same concentration. In the reduced site, we can even see bands at d3 of the reactors T1 and T4.

3.5.2 Total protein content- BCA assay

Cell samples of the fed batch were analyzed for total protein content by the BCA assay. The BCA assay was performed on the cell lysates of every reactor, from 2.5E6 cells of process day 3 and process day 9. Figure 70 shows the results of the assay.

On process day 3, all reactors had slightly more than 80 pg total protein per cell, while on process day 9 T1 and T4 had slightly less (77 pg in T1 and 71 pg in T4). Cells of T2 had only 61 pg total protein per

cell, significantly less than the rest. It was mentioned in literature that the total protein content in the cells is reduced in the stationary phase compared to the exponential phase, which aligns with our results. Although it is important to note that the BCA assay is not very accurate on determining the protein content and these results should be viewed with caution.

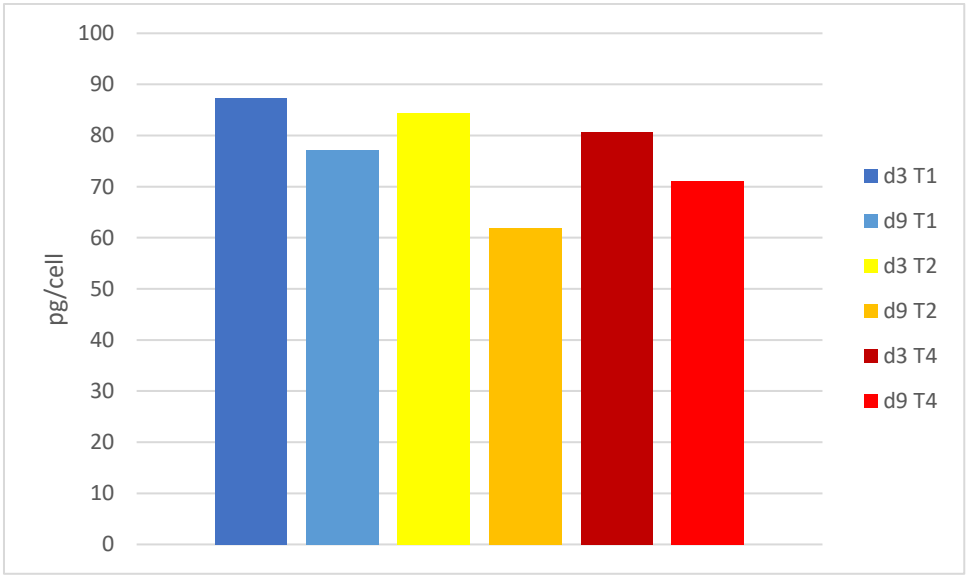

Figure 70: BCA assay with cell lysates of the of the reactors T1(+1mM VPA on day 6), T2 (control) and T4 (32°C after day 6); d3 stands for process day 3, d9 stands for process day 9;

3.5.3 Size exclusion chromatography (SEC) with Multi Angle Light Scattering (MALS) of purified CSs product

An analytical SEC-MALS was performed on the HisTrap purified reactor supernatant to determine possible differences in oligomer content of the different reactors. Different reactor conditions can result in changed proportions of the oligomers to each other, which is an important quality attribute. With the MALS detector we can determine the molar masses of our CSs product from the purified harvest and conclude on the different quantities of oligomers of our product. Put simply, it measures the light scattered from a multiple of angles of a molecule, the intensity of which is dependent on the molecular weight of the analyte. For the SEC a high-pressure liquid chromatography (HPLC) system was used with the Superose 6 increase 10/300 GL column (Cytiva). This prepacked column with a cross-linked agarose matrix allows for a fast separation of high molecular weight proteins due to its relatively high flow rate.

The monomeric CSs has 138 kDa with 22 N-glycolysations sites [35] resulting in a total molecular weight of about 180-200 [14] kDa, and the trimer has therefore about 540-600 kDa.

The harvested supernatant of the CSs fed batch was concentrated by TFF and let run through a HisTrap column. T1 resulted in 1.26 mg/mL, T2 3mg/mL and T4 2.1 mg/mL of product. 50 µg of purified product was loaded onto the SEC column for each.

In T2, the reactor which ran under standard conditions, the plot of UV signal over retention time features one predominant peak between minute 17 and 19 (see Figure 71). This main faction features molecular mass from 475 kDa to 650 kDa, resulting in an average of 591 kDa and the peak topping at 607 kDa. Molar mass faction 2, which can distinguish between run time minute 13 and 16 contains tetramers and aggregates with a molecular mass over 700 kDa up until 1400 kDa.

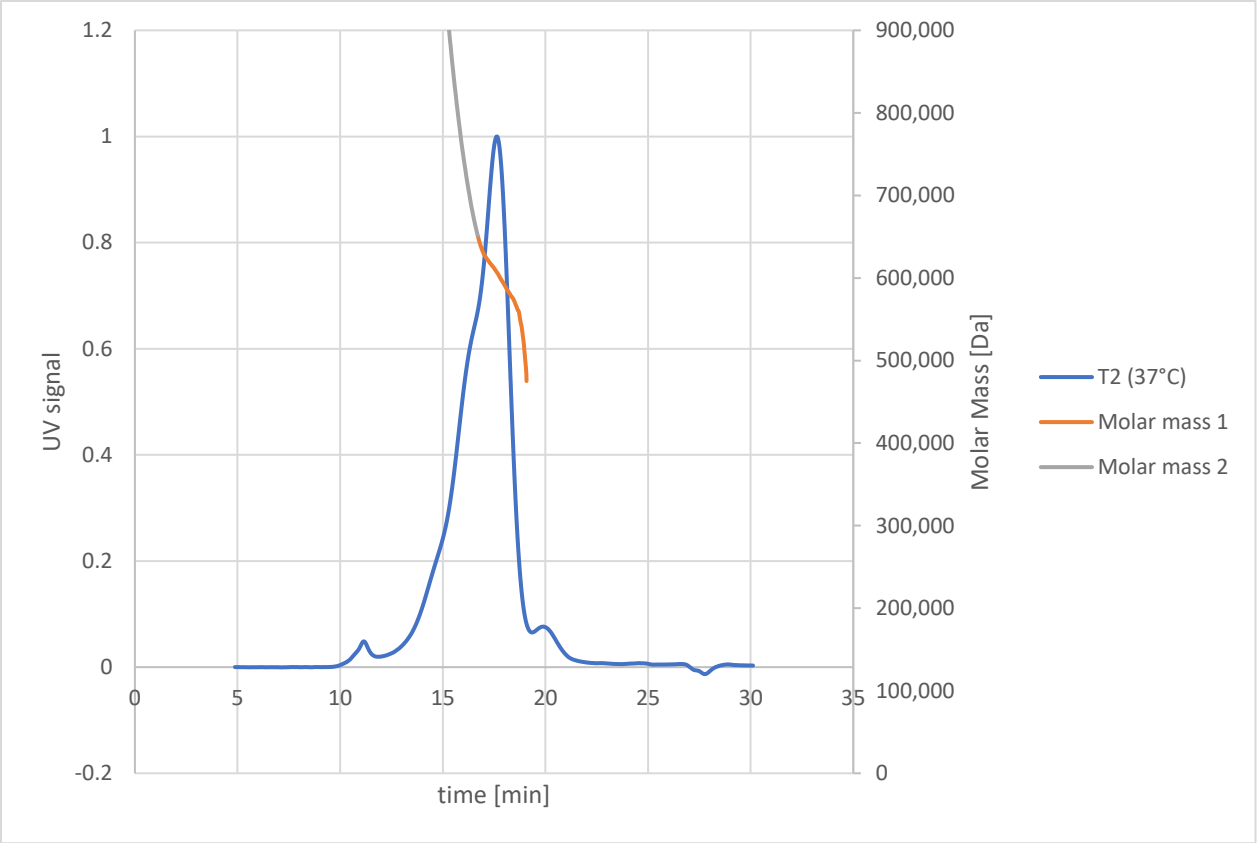

Figure 71: UV signal over run time in the column; CSs product of reactor T2; the main doublepeak contains two molar masses of CSs. Molar mass 1 ranging from 475 kDa to 650 kdA and molar mass 2 ranging from 650 kDa to 1558 kDa

The UV signal over run time plot of T4 (Figure 72), the reactor run at 32°C, showed a very sharp peak topping at minute 18 featuring Molar mass 1. It contains the trimers with a molecular mass of 572 to 616 kDa, the average being 589 kDa and its peak at 588 kDa. There is a small peak visible at minute 15, containing molar mass fraction 2 with aggregates over 800 kDa up to 1560 kDa. The peak top around minute 15 contains proteins with molecular mass of around 1094 kDa, pointing to an aggregation of 2 homotrimers together, next to a small amount of oligomers with a molecular mass up to 1560 kDa

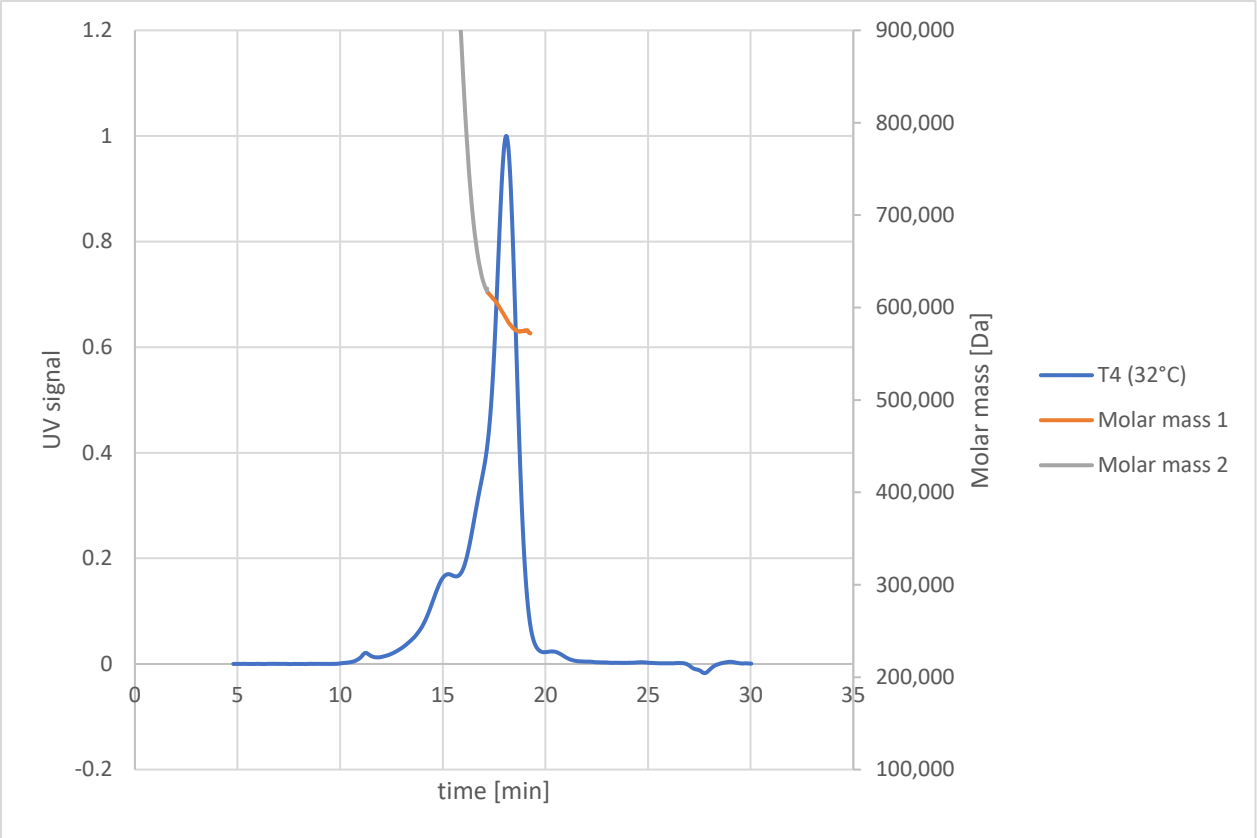

Figure 72: UV signal over run time in the column; CSs produced by reactor T4; A sharp main peak is visible with the molar masses ranging from 572 kDa to 616 kDa; a small peak before features the molar masses ranging from 620 kDa to 1546 kDa

The UV signal over run time plot of reactor T1 (Figure 73), were 1mM of VPA was added, features a broader main peak than the plots of T2 and T4. The main peak peaks at minute 17 with at a molecular mass of 610 kDa. Molar mass 1, which reaches from minute 16 to 19, already contains tetramers with over 800 kDa and molar mass 2 contains aggregates with a molecular mass of over 1560 kDa. Due to the steep slope of molar mass 1 and 2 in the plot (Figure 73), we can assume a wide range of differently weighting CSs oligomers, and the average molar mass of 1 is also higher than T2 and T4 with 640 kDa.

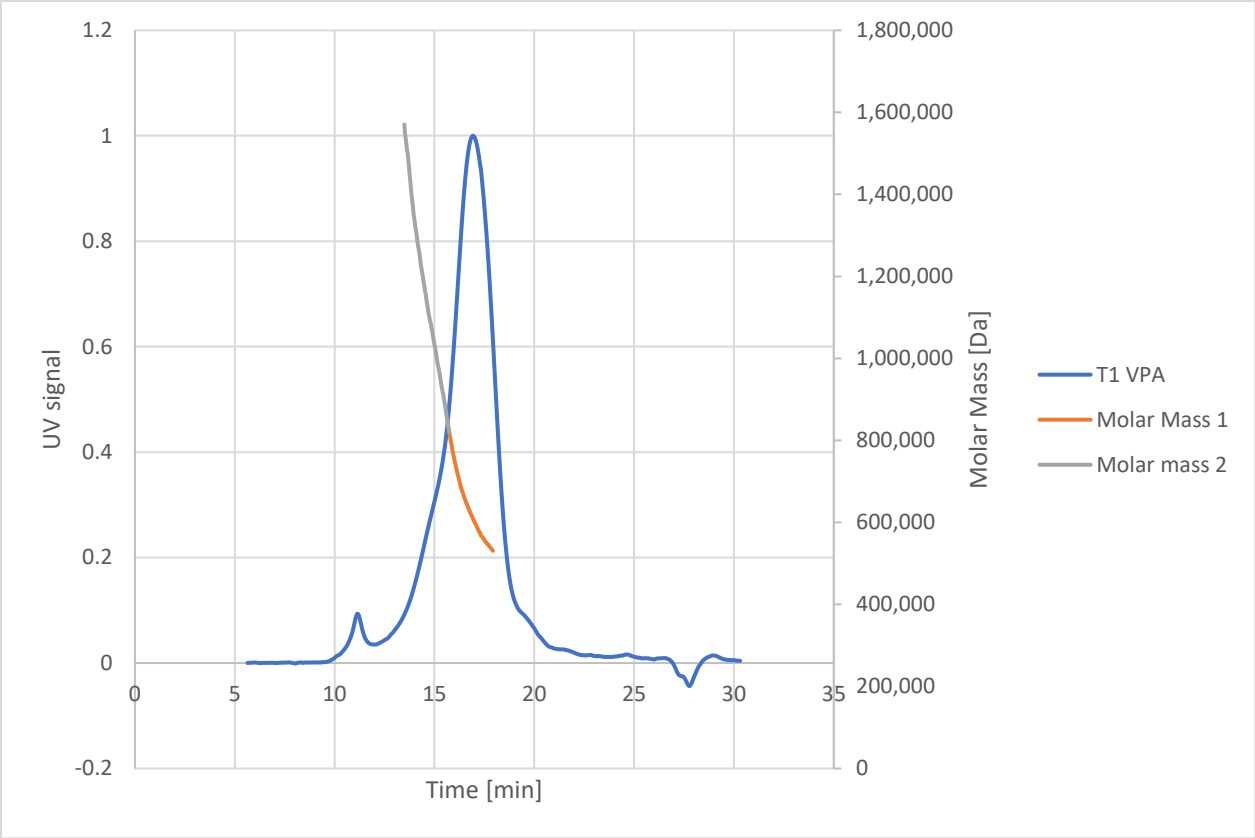

Figure 73: UV signal over run time in the column; CSs produced by reactor T1; One main peak containing 2 molar mass factions,Molar mass 1 ranging from 550 kDa to 850 kDa and Molar mass 2 ranging from 852 kDa to 1560 kDa

3.5.4 Western blot of reactor supernatants

To assess the formation of oligomers in the reactors and any changes thereof because of different reactor conditions we loaded the 4-12% bis-tris NuPAGE LDS-PAGE gel with the supernatants of d3 and d9 from the reactors(Western blot see Figure 74, data set see Table 9). As a comparison the supernatant of the routine culture from the F4 and G3 strain was added too. The Western blot was detected with HyperIgG-biotin in a dilution of 1:100.

Table 9: sample plan of western blot from the reactor supernatant (lane 1-6) and the routine culture supernatant of F4, G3 (lane 7 and 8)

Lane	**M**	**1**	**2**	**3**	**4**	**5**	**6**	**7**	**8**
	Marker	F206 d3 T1	F206 d3 T2	F206 d3 T4	F206 d9 T1	F206 d9 T2	F206 d9 T4	CSs RC F4 0828	CSs RC G3 0828
Medium/conditions	5 µL pre-stained	fed batch CDM4HEk VPA	fed batch CDM4HEK	fed batch CDM4HEk 32°C	fed batch CDM4HEk VPA	fed batch CDM4HEK	fed batch CDM4HEk 32°C	CDCHO RC	CDCHO RC
Conc.[mg/L]		4	5	4.5	51	54	200	4	3.5
Amount [ng]		48	60	54	612	648	2400	48	42

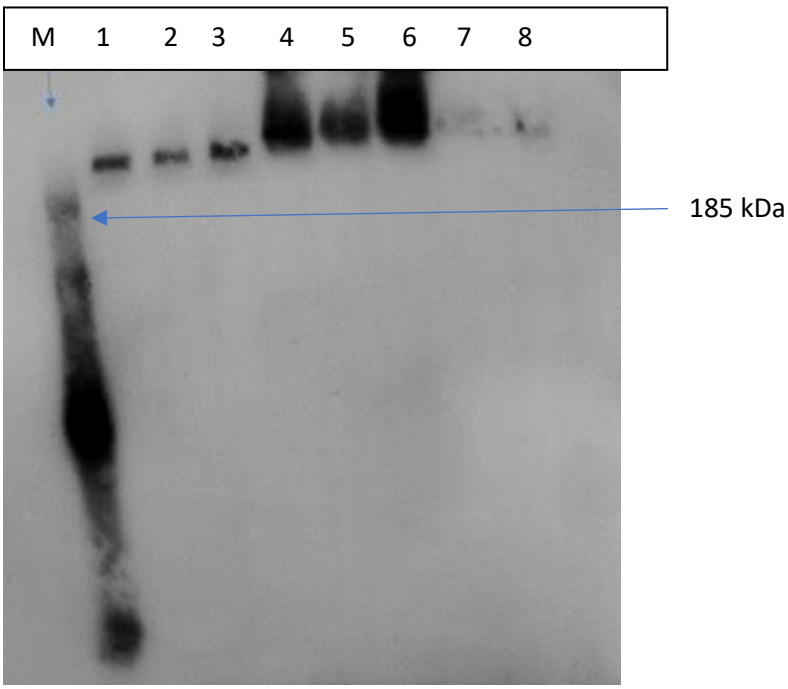

Figure 74: Western blot of reactor supernatants d3 and d9 (1-6) and routine culture supernatant of F4 (7) and G3 (8) detected with HyperIgG-biotin 1:100

On process day 3 (Figure 74, column 1-3) we can see in all reactors a single band around 200 kDa, as the marker bands start at 185 kDa. This band is in the kDa range of the CSs monomeric form, confirming correct CSs expression with no aggregation or fragmentation in the early stages. At process day 9 (Figure 74, column 4-6), it looks different: we can see bands over the 200kDa marker line, which could point to an aggregation of the CSs after a certain time in culture. The wells loaded with routine culture of the other cell lines F4 and G3 displayed only a weak signal band, although it contains nearly the same concentration of CSs as the wells on reactor d3.

3.6 Flow Cytometry

We used flow cytometry to test our subclones for homogeneity of intracellular product content, as well as binding to the CR3022, anti-His and Hyperimmune IgG (Takeda). By making the cell membrane permeable with detergent Triton X-100, biotinylated antibodies to our products and the Streptavidin-Alexa 647 fluorescent conjugate could enter the cells and mark them.

Cell population of at least one million cells were fixed at specific time points in cultivation (mostly on the end of the exponential phase) with cooled ethanol and stored at +4°C.

The bars named #1, #2 or #3 in the FACS histograms (called marker in the sample data tables) mark the zero point of fluorescence intensity regarding the corresponding negative control (#1-> negative 1, #2 negative 2, #3 negative 3). All cells within the markers display a higher fluorescence than the negative control.

We tested the binding of CR3022, anti-His and Hyperimmune IgG to one subclone of our RBD and CSs lines (see Figure 75, sample data Table 10). As negative control a population of CSs F4 was used and

the sample prepared without the first antibody.

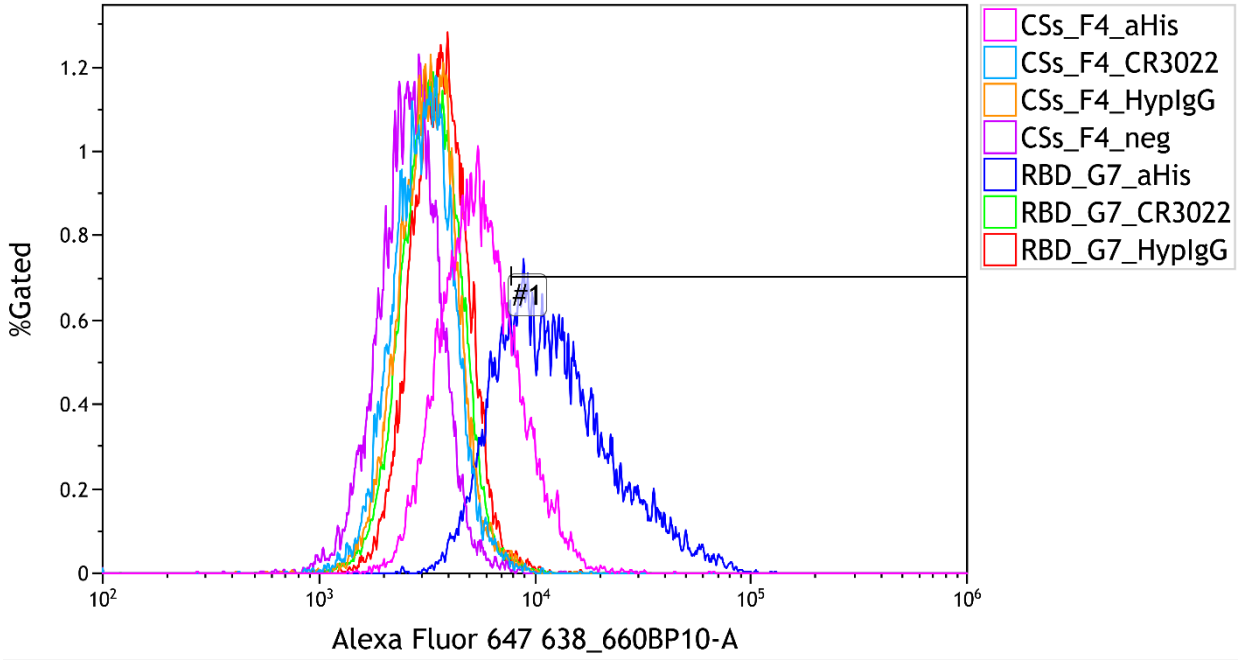

Figure 75: Gated FACS histogram of CSs F4 and RBD G7 with different antibody conjugates: CR3022-biotin (1:100), anti-His-biotin (1:100) and Hyperimmune IgG (1:20)

Table 10: Sample data of Figure 75; Total %: percentage of cells gated; X-Gmean: geometric mean of the fluorescence intensity; Median: Median of fluorescence intensity; Marker #1 %: percentage of cells with a higher fluorescence intensity than the marker setpoint at the negative control; Marker #1 gmean: geometric mean of the fluorescence intensity of the cells within Marker #1; Marker #1 Median: Median of the fluorescence intensity of the cells within Marker #1

Data Set	Total [%]	X-GMean	Median	Marker #1 [%]	Marker #1 gmean	Marker #1 Median
CSs F4 His	88.5	5503	5432	17.95	9945	9463
CSs F4 CR3022	88.5	3028	3080	0.37	9049	8642
CSs F4 HyperIgG	88.67	3185	3234	0.53	8513	8374
CSs F4 negative	76.96	2600	2650	0.12	10276	8661
RBD G7 His	88.14	12158	11295	66.68	15280	13725
RBD G7 CR3022	88.76	3301	3332	0.59	9109	8590
RBD G7 HyperIgG	88.9	3601	3632	0.83	9230	8652

The anti-His antibodies seemed to be the best choice for the assay, as they gave the only significant difference to the negative in both RBD and CSs. The median and the gmean show very similar values (Table 10), pointing to uniformal peaks.

3.6.1 Comparison of subclones with flow cytometry

If we assume the intracellularly detected product content gives an indication of the titer in the supernatant, we can make a comparison in productivity of the subclones via the fluorescence intensity of the ethanol fixated cell populations.

Two negative control preparations were studied, by either skipping the first antibody conjugate in the sample preparation or by skipping both.

Of each subclone, samples from day 1 and from day 4 in culture were taken, to detect different intracellular product concentration at the beginning and the end of the exponential phase.

CD19-AD2

The CD19-AD2 subclones showed a remarkable high mean fluorescence (Figure 76 and Table 11) marked with anti-His-biotin<->Streptavidin Alexa fluor 647. This could indicate to a high intracellular product concentration in the cells.

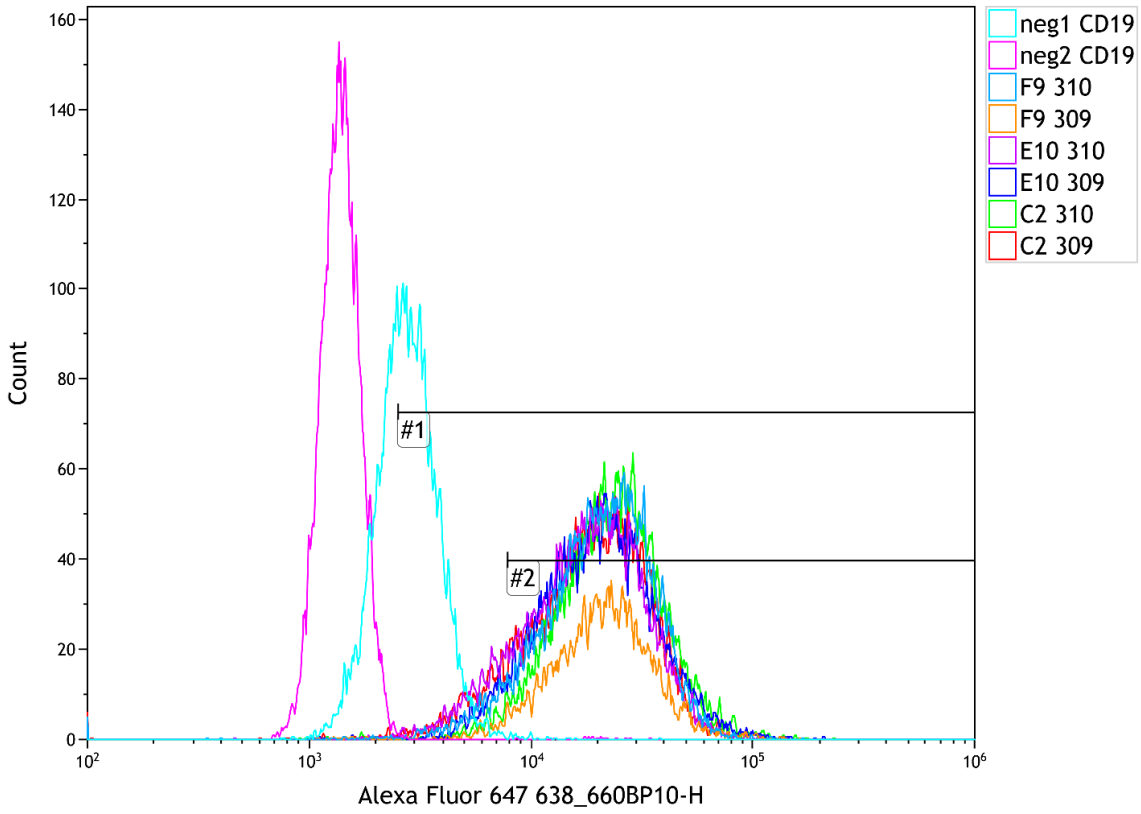

Figure 76: Histogram of fluorescence intensity to cell count; anti-His-biotin (1:50) conjugated to streptavidin-Alexa 647 (1:100); Subclones F9, E10, and C2 expressing CD19-AD2; 309 stands for routine culture day 1, 310 for routine culture day 4

Table 11: Sample data of Figure 76; Total %: percentage of cells gated; X-Gmean: geometric mean of the fluorescence intensity; Median: Median of fluorescence intensity; Marker #1 %: percentage of cells with a higher fluorescence intensity than the marker setpoint at the negative control; Marker #1 gmean: geometric mean of the fluorescence intensity of the cells within Marker #1; Marker #1 Median: Median of the fluorescence intensity of the cells within Marker #1; the same applies for the columns of Marker #2.

Data Set	Total [%]	X-GMean	Median	Marker #1 [%]	Marker #1 gmean	Marker #1 Median	Marker #2 [%]	Marker #2 [%]	Marker #2 Median
neg1 CD19	80	2736	2738	50	3311	3193	0	10392	9780
neg2 CD19	79	1382	1384	0	9730	17948	0	19554	19859
F9 310	81	19362	20860	80	19629	20932	75	21501	22000

F9 309	41	20451	21255	41	20703	21320	39	21595	21743
E10 310	81	16805	18068	81	16918	18116	71	19767	19935
E10 309	77	19413	19986	77	19511	20013	72	21169	21057
C2 310	78	22305	23123	78	22476	23163	76	23413	23675
C2 309	81	17394	18960	80	17726	19060	71	20428	20616

There isn't any difference in the histogram visible between the subclones in intracellular product content. In terms of geometric mean, C2 had the highest fluorescence with 22305 on day 4, and 17394 on day 1. In F9 there is only a slight difference in G-Mean between day 1 and 4, from 19362 to 20451. The highest difference in G-mean is seen with C2, from 17393 to 22305. E10 shows the lowest overall fluorescence on day 4 with only 19986. There is a significant distortion between negativ2 (neg2; both conjugates not added to sample) and negative 1 (neg1; conjugate 1 skipped in sample preparation). This 'space' in between negatives points to either an unspecific binding of the Alexa fluor 647 or just a retention of the conjugate in the cell, despite several washing steps.

CSs

The CSs samples were prepared with a higher concentration of biotin-CR3022 (1:50) compared to our first FACS binding experiment, to offset the relatively low binding. The biotinylated CR3022 was chosen because of the better availability and reduced cost, which was substantial, compared to the anti-His-biotin that we couldn't produce by ourselves. The corresponding FACS histogram is shown in Figure 77 and Table 12 displays the collected data of the samples.

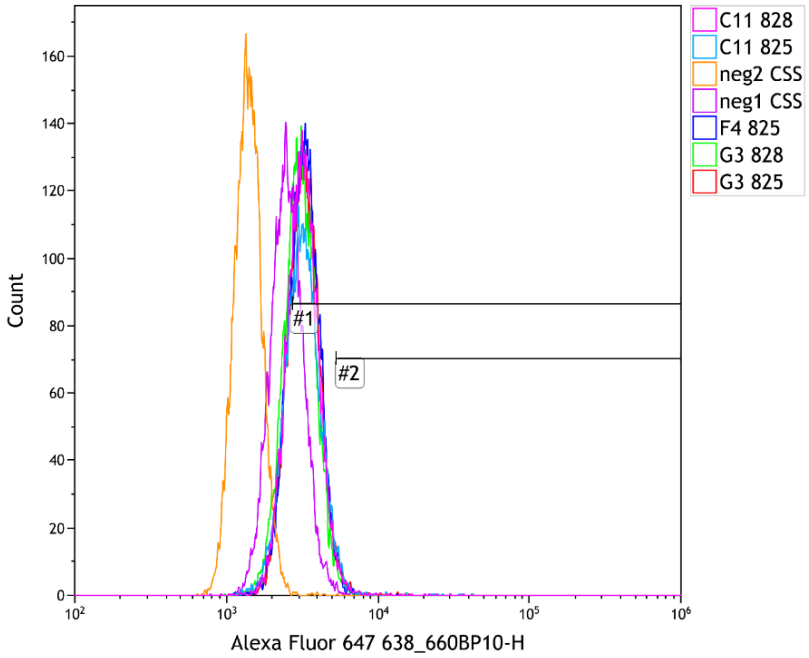

Figure 77: Histogram of fluorescence intensity to cell count; CR3022-biotin (1:50) conjugated to streptavidin-Alexa 647 (1:100); Subclones C11, F4, and G3 expressing CSs; neg1: CR3022-biotin skipped; neg2: both conjugates skipped

Table 12: Sample data of Figure 77; Total %: percentage of cells gated; X-Gmean: geometric mean of the fluorescence intensity; Median: Median of fluorescence intensity; Marker #1 %: percentage of cells with a higher fluorescence intensity

than the marker setpoint at the negative control; Marker #1 gmean: geometric mean of the fluorescence intensity of the cells within Marker #1; Marker #1 Median: Median of the fluorescence intensity of the cells within Marker #1; the same applies for the columns of Marker #2.

Data Set	Total [%]	X-GMean	Median	Marker #1 [%]	Marker #1 X-gmean	Marker #1 Median	Marker #2 [%]	Marker #2 [%]	Marker #2 Median
C11 828	84	3164	3178	63	3498	3416	2	6334	5772
C11 825	77	3152	3163	55	3562	3465	2	6405	5721
neg2 CSS	88	1382	1389	0	3963	3677	0	8262	9266
neg1 CSS	86	2496	2503	32	3205	3117	0	5968	5460
F4 825	86	3206	3242	66	3524	3469	1	5866	5603
G3 828	86	3020	3049	59	3423	3352	1	5793	5679
G3 825	83	3214	3236	64	3537	3466	2	6239	5733

In the histogram we can't discern a significant difference between the each subclones or their intracellular product content in the first days (day1 and day 4) of cultivation. Only minor deviations are seen in the fluorescence geometric mean between the subclones and cultivation days. This is interesting, as the product titer in the supernatant showed that C11 produced considerably more CSs than the other two subclones.

RBD

To offset the relatively low binding in the first FACS experiment (Figure 75) with biotinylated CR3022, the concentration was adjusted to 1:50 in the sample preparation. The subclones were sampled at day 1 and day 4 of the routine cultivation, except for G7, were the samples of day 4 were already used in the previous experiment. Histogram and corresponding data are shown in Figure 78 and Table 13.

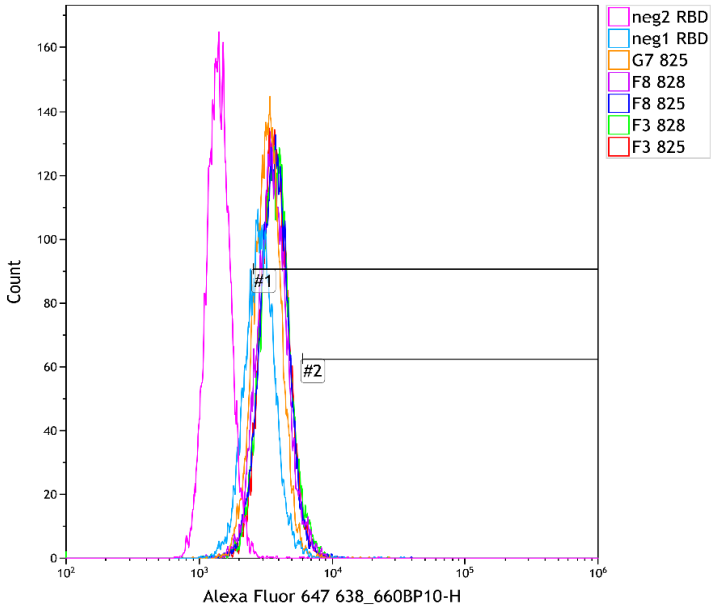

Figure 78: Histogram of fluorescence intensity to cell count; CR3022-biotin (1:50) conjugated to streptavidin-Alexa 647 (1:100); Subclones F3, F8, and G7 expressing RBD; neg1: CR3022-biotin skipped; neg2: both conjugates skipped

Table 13: Sample data of Figure 78; Total %: percentage of cells gated; X-Gmean: geometric mean of the fluorescence intensity; Median: Median of fluorescence intensity; Marker #1 %: percentage of cells with a higher fluorescence intensity than the marker setpoint at the negative control; Marker #1 gmean: geometric mean of the fluorescence intensity of the cells within Marker #1; Marker #1 Median: Median of the fluorescence intensity of the cells within Marker #1; the same applies for the columns of Marker #2.

Data Set	Total [%]	X-GMean	Median	Marker #1 [%]	Marker #1 X-gmean	Marker #1 Median	Marker #2 [%]	Marker #2 [%]	Marker #2 Median
neg2 RBD	87	1389	1395	0	3660	3024	0	10357	12984
neg1 RBD	71	2853	2871	48	3272	3182	0	7869	6536
G7 825	87	3252	3288	74	3468	3429	1	7493	6703
F8 828	85	3519	3531	77	3702	3642	2	6764	6616
F8 825	84	3637	3678	78	3784	3761	2	6893	6560
F3 828	86	3701	3716	80	3840	3802	3	6840	6699
F3 825	85	3665	3682	80	3782	3745	2	6720	6489

In the corresponding histogram we cannot discern any significant differences in intracellular product content between the subclones graphically, although there is a slightly increased fluorescent mean of F3 compared to G7, with 3251 to 3665 on the same cultivation day. There seems to be only a small increase in G-mean fluorescence between day 1 and day 4 of cultivation on every clone.

3.6.2 Flow cytometry of the CSs produced by C11 in Fed-batch

Every 24h of the fed batch, samples with at least 3mio. cells were fixated in ethanol from each reactor to measure the intracellular product content with flow cytometry. The process days 3, 9 and 15 were actually measured to get a better understanding of the possible intracellular CSs fluctuations

between exponential phase (day3), stationary phase (day9) and decline phase (day 15). Furthermore, the binding of the different antibodies anti-His-biotin, CR3022-biotin and HyperimmuneIgG-biotin was tested for each.

In the negative control the 1st antibody conjugate was omitted in the sample preparations.

On the process day 3 there cannot be made a graphical distinction between the reactors, as was expected(see Figure 79, Figure 80, Figure 81 and Table 14, Table 15, Table 16).

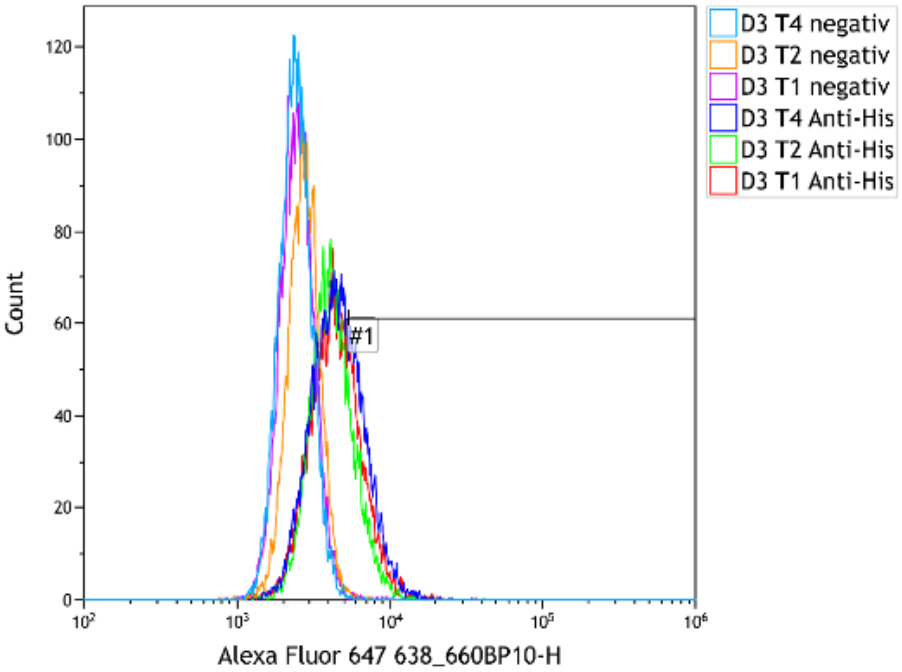

Figure 79: Histogram of fluorescence intensity to cell count on process day 3; Anti-His-Biotin (1:100) conjugated to Streptavidin-Alexa 647 (1:100)

Table 14 Sample data of Figure 79; Total %: percentage of cells gated; X-Gmean: geometric mean of the fluorescence intensity; Marker #1 %: percentage of cells with a higher fluorescence intensity than the marker setpoint at the negative control; Marker #1 gmean: geometric mean of the fluorescence intensity of the cells within Marker #1;

Data set	Total [%]	X-GMean	Marker #1 [%]	Marker #1 X-Gmean
D3 T4 negativ	76	2406	0	7713
D3 T2 negativ	61	2723	0	6099
D3 T1 negativ	72	2471	0	6987
D3 T4 Anti-His	73	4514	24	6980
D3 T2 Anti-His	60	4158	12	6673
D3 T1 Anti-His	64	4363	18	6840

The Anti-His binding on the cell samples of day 3 worked well. All reactors have similar gmean and were well discernable from the control, as seen in Figure 79.

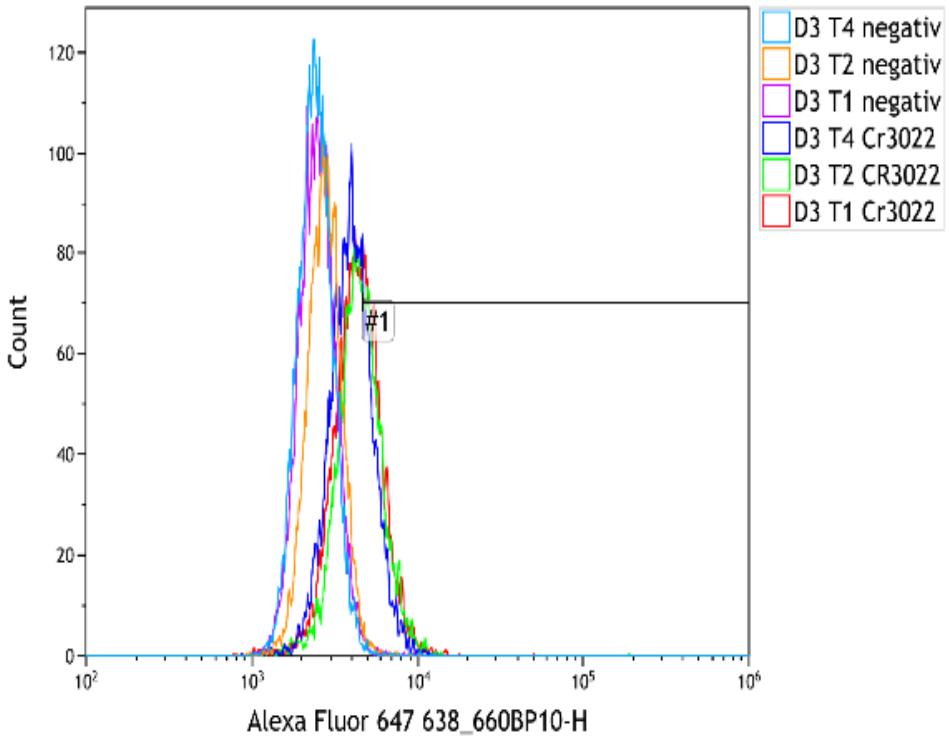

Figure 80: Histogram of fluorescence intensity to cell count on process day 3; CR3022-biotin (1:100) conjugated to Streptavidin-Alexa 647 (1:100)

Table 15: Sample data of Figure 80; Total %: percentage of cells gated; X-Gmean: geometric mean of the fluorescence intensity; Marker #1 %: percentage of cells with a higher fluorescence intensity than the marker setpoint at the negative control; Marker #1 gmean: geometric mean of the fluorescence intensity of the cells within Marker #1.

Data set	Total [%]	X-GMean	Marker #1 [%]	Marker #1 X-Gmean
D3 T4 negativ	76	2406	0	6150
D3 T2 negativ	61	2723	1	5258
D3 T1 negativ	72	2471	1	5885
D3 T4 Cr3022	69	3951	20	5613
D3 T2 CR3022	60	4420	26	5829
D3 T1 Cr3022	68	4303	28	5831

CR3022 binding to the cell also showed good results, with a higher percentage (compared to Anti-His and HyperimmuneIgG binding) of cells having more fluorescence than the control (see Figure 80 and Table 15

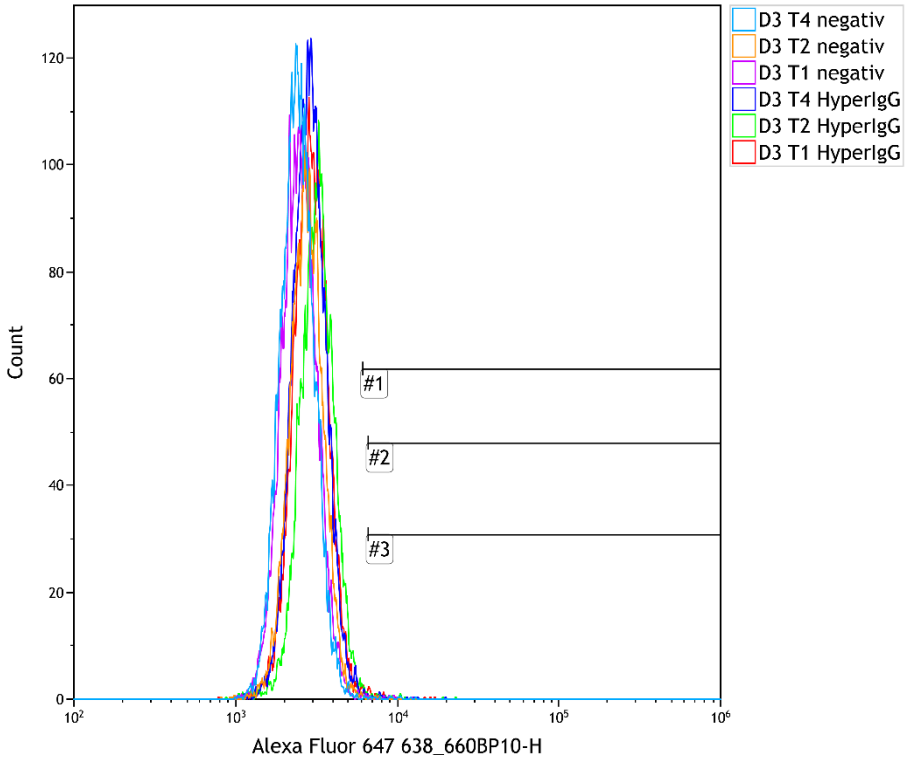

Figure 81: Histogram of fluorescence intensity to cell count on process day 3; HyperimmuneIgG-Biotin (1:10) conjugated to Streptavidin-Alexa 647 (1:100)

Table 16 Sample data of Figure 81; Total %: percentage of cells gated; X-Gmean: geometric mean of the fluorescence intensity; Marker #1 %: percentage of cells with a higher fluorescence intensity than the marker setpoint at the negative control; Marker #1 gmean: geometric mean of the fluorescence intensity of the cells within Marker #1.

Data set	Total [%]	X-Gmean	Marker #1 [%]	Marker #1 X-Gmean
D3 T4 negativ	76	2406	0	8375
D3 T2 negativ	61	2723	0	6804
D3 T1 negativ	72	2471	0	7764
D3 T4 HyperIgG	75	2845	0	7301
D3 T2 HyperIgG	61	3164	0	8945
D3 T1 HyperIgG	70	2888	0	7187

Altogether we can propose that Anti-His and CR3022 showed similarly good binding (Figure 79 and Figure 80), although anti-His has a higher mean fluorescence (Table 14 and Table 15). HyperimmuneIgG showed only very weak binding, barely distinguishable from the negative control and not significant (Figure 81).

By process day 9, well into the stationary phase, the picture changes. T4, which featured a lower reactor temperature(32°C) and the highest titer in the supernatant, has significantly lower mean

fluorescence compared to T1 and T2(see Figure 82), pointing to a lower intracellular CSs content.

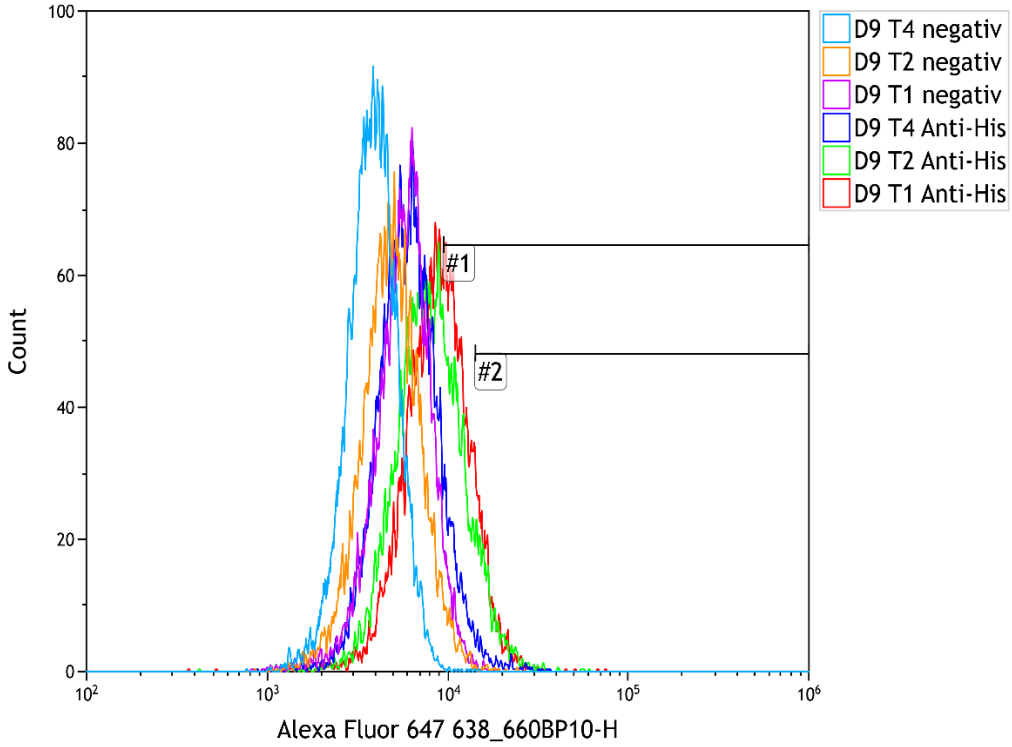

Figure 82: Histogram of fluorescence intensity to cell count on process day 9; Anti-His-Biotin (1:100) conjugated to Streptavidin-Alexa 647 (1:100)

Table 17: Sample data of Figure 82: Total %: percentage of cells gated; X-Gmean: geometric mean of the fluorescence intensity; Marker #1 %: percentage of cells with a higher fluorescence intensity than the marker setpoint at the negative control; Marker #1 gmean: geometric mean of the fluorescence intensity of the cells within Marker #1. The same applies for the columns with Marker #2.

Data set	Total [%]	X-Gmean	Marker #1 [%]	Marker #1 X-Gmean	Marker #2 [%]	Marker #2 X-Gmean
D9 T4 negativ	72	3799	0	11782	0	14897
D9 T2 negativ	65	4797	2	11115	0	17426
D9 T1 negativ	65	5592	4	10769	0	15569
D9 T4 Anti-His	71	6026	8	11792	1	18000
D9 T2 Anti-His	67	7887	22	12591	6	17395
D9 T1 Anti-His	66	8644	28	12395	7	16886

Due to the T1 negative and the T2 negative having very similar datapoints, data of T2 was omitted in Table 17.

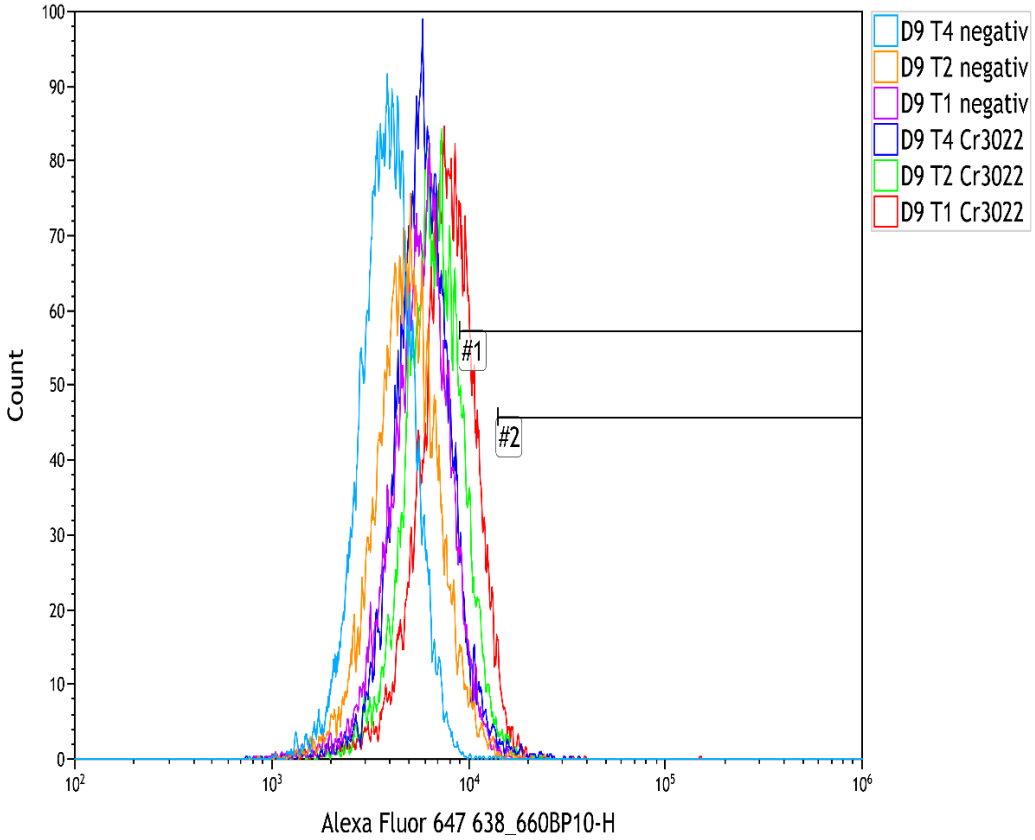

Figure 83: Histogram of fluorescence intensity to cell count on process day 9; CR3022-biotin(1:100) conjugated to Streptavidin-Alexa 647 (1:100)

Table 18: Sample data of Figure 83: Total %: percentage of cells gated; X-Gmean: geometric mean of the fluorescence intensity; Marker #1 %: percentage of cells with a higher fluorescence intensity than the marker setpoint at the negative control; Marker #1 gmean: geometric mean of the fluorescence intensity of the cells within Marker #1. The same applies for the columns with Marker #2.

Data set	Total [%]	X-Gmean	Marker #1 [%]	Marker #1 X-Gmean	Marker #2 [%]	Marker #2 X-Gmean
D9 T4 negativ	72	3799	0	10704	0	14463
D9 T2 negativ	65	4797	3	10548	0	17018
D9 T1 negativ	65	5592	5	10255	0	15458
D9 T4 CR3022	70	5822	6	10989	1	17883
D9 T2 CR3022	66	6549	12	10515	1	15723
D9 T1 CR3022	68	7604	23	10860	2	15880

As was the case with Anti-His binding, negative points of T1 and T2 are very similar and the data for negative T2 omitted from Table 18.

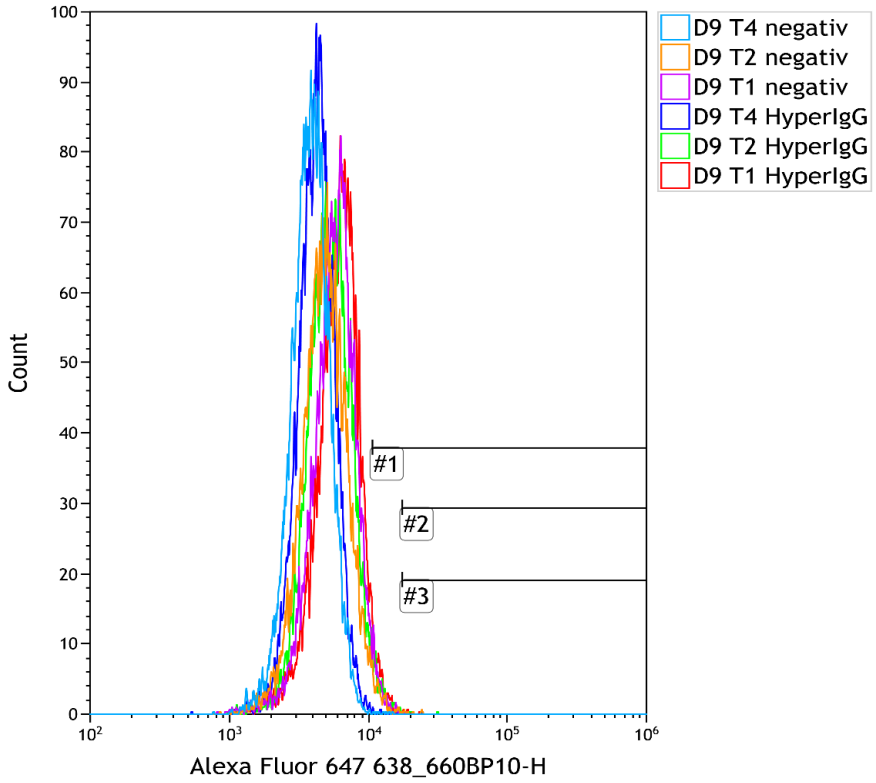

Figure 84: Histogram of fluorescence intensity to cell count on process day 9; HyperimmuneIgG-Biotin (1:10) conjugated to Streptavidin-Alexa 647 (1:100)

Table 19: Sample data of Figure 84Figure 83: Total %: percentage of cells gated; X-Gmean: geometric mean of the fluorescence intensity; Marker #1 %: percentage of cells with a higher fluorescence intensity than the marker setpoint at the negative control; Marker #1 gmean: geometric mean of the fluorescence intensity of the cells within Marker #1. The same applies for the columns with Marker #2.

Data set	Total [%]	X-Gmean	Marker #1 [%]	Marker #1 X-Gmean	Marker #2 [%]	Marker #2 X-Gmean
D9 T4 negativ	72	3799	0	12662	0	N/A
D9 T2 negativ	65	4797	1	12426	0	20540
D9 T1 negativ	65	5592	2	11882	0	18536
D3 T4 HyperIgG	71	4173	0	13804	0	19814
D3 T2 HyperIgG	68	5227	2	12279	0	23192
D3 T1 HyperIgG	64	5991	2	12101	0	19417

As was the case with Anti-His binding and CR3022 binding before, negatives of T1 and T2 were on very similar points. Data of negative T2 was therefore omitted from Table 19.

Binding-wise we can again observe that the HyperimmuneIgG is almost not discernible from the control. Only a few percentages of cells pass the marker point #1. Anti-His binding and CR3022 binding give similar Histograms, with a slightly higher mean fluorescence by Anti-His.

On process day 15, the remaining reactors T1 and T4 were in the decline phase, with high product titers. In resulting cytometry histograms T1 both control and sample have wider peaks and higher mean fluorescence, although we can see with both reactors that there is only a minor difference to the control (Figure 87). This observation suggests that there is practically no intracellular product in the decline phase of the process.

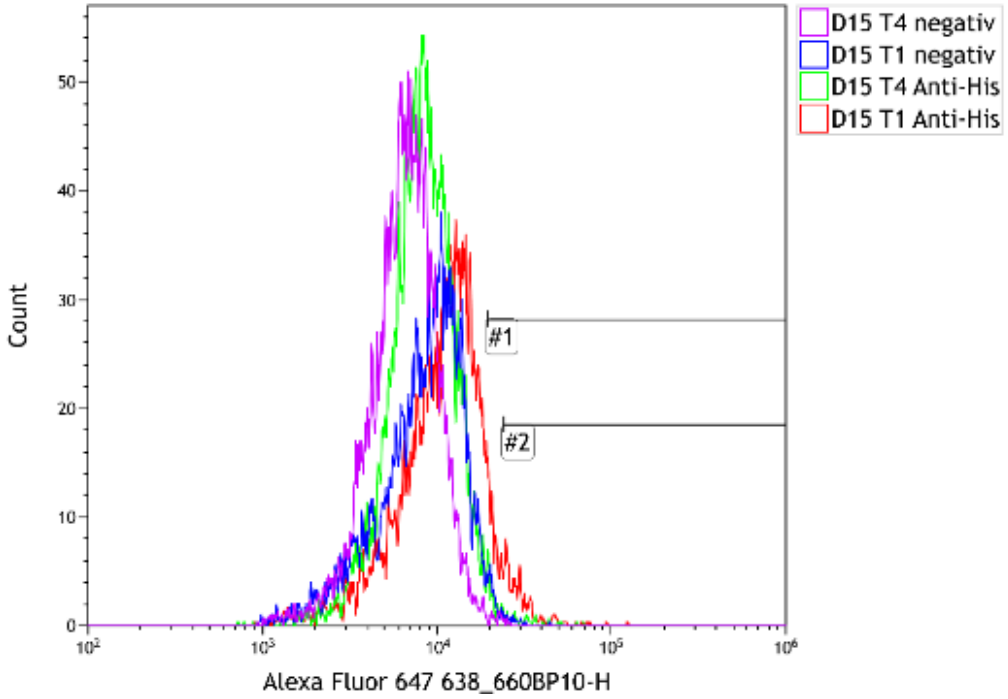

Figure 85: Histogram of fluorescence intensity to cell count on process day 15; Anti-His-Biotin (1:100) conjugated to Streptavidin-Alexa 647 (1:100)

Table 20: Sample data of Figure 85: Total %: percentage of cells gated; X-Gmean: geometric mean of the fluorescence intensity; Marker #1 %: percentage of cells with a higher fluorescence intensity than the marker setpoint at the negative control; Marker #1 gmean: geometric mean of the fluorescence intensity of the cells within Marker #1. The same applies for the columns with Marker #2.

Data set	Total [%]	X-Gmean	Marker #1 [%]	Marker #1 X-Gmean	Marker #2 [%]	Marker #2 X-Gmean
D15 T4 negativ	50	6405	2	22363	0	24895
D15 T1 negativ	39	7977	1	22152	0	27967
D15 T4 Anti-His	52	8120	1	24818	0	32520
D15 T1 Anti-His	40	10447	4	25365	2	30647

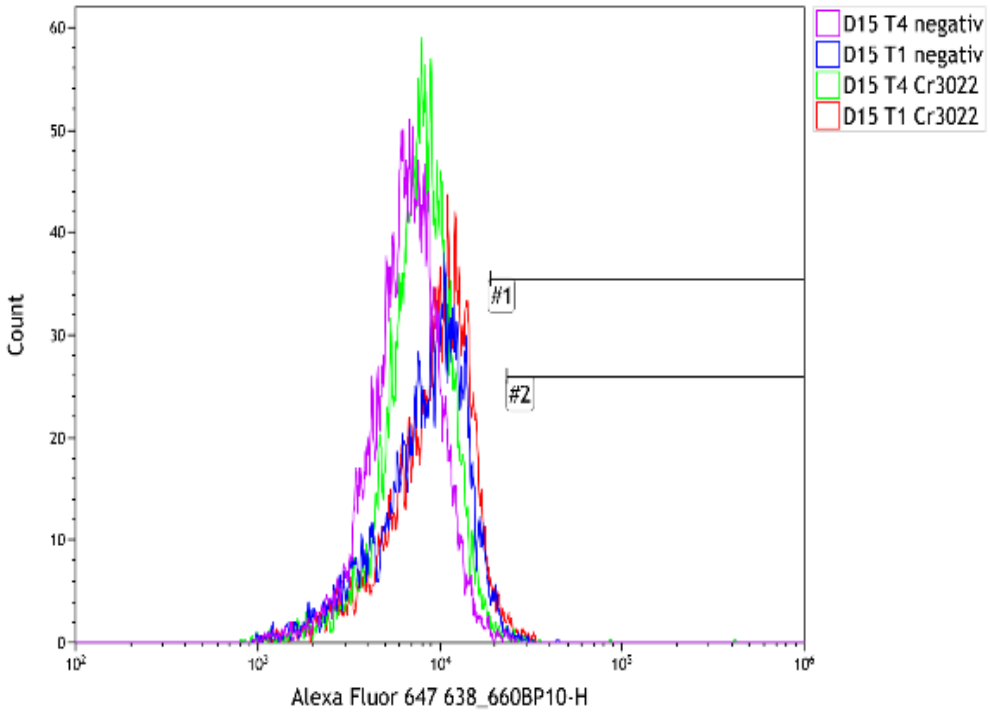

Figure 86: Histogram of fluorescence intensity to cell count on process day 15; CR3022-biotin (1:100) conjugated to Streptavidin-Alexa 647 (1:100)

Table 21: Sample data of Figure 86: Total %: percentage of cells gated; X-Gmean: geometric mean of the fluorescence intensity; Marker #1 %: percentage of cells with a higher fluorescence intensity than the marker setpoint at the negative control; Marker #1 gmean: geometric mean of the fluorescence intensity of the cells within Marker #1. The same applies for the columns with Marker #2.

Data set	Total [%]	X-Gmean	Marker #1 [%]	Marker #1 X-Gmean	Marker #2 [%]	Marker #2 X-Gmean
D15 T4 negativ	50	6405	0	21897	0	24244
D15 T1 negativ	39	7977	1	21644	0	26851
D15 T4 Cr3022	50	7558	0	24659	0	33571
D15 T1 Cr3022	40	8866	1	22191	0	26393

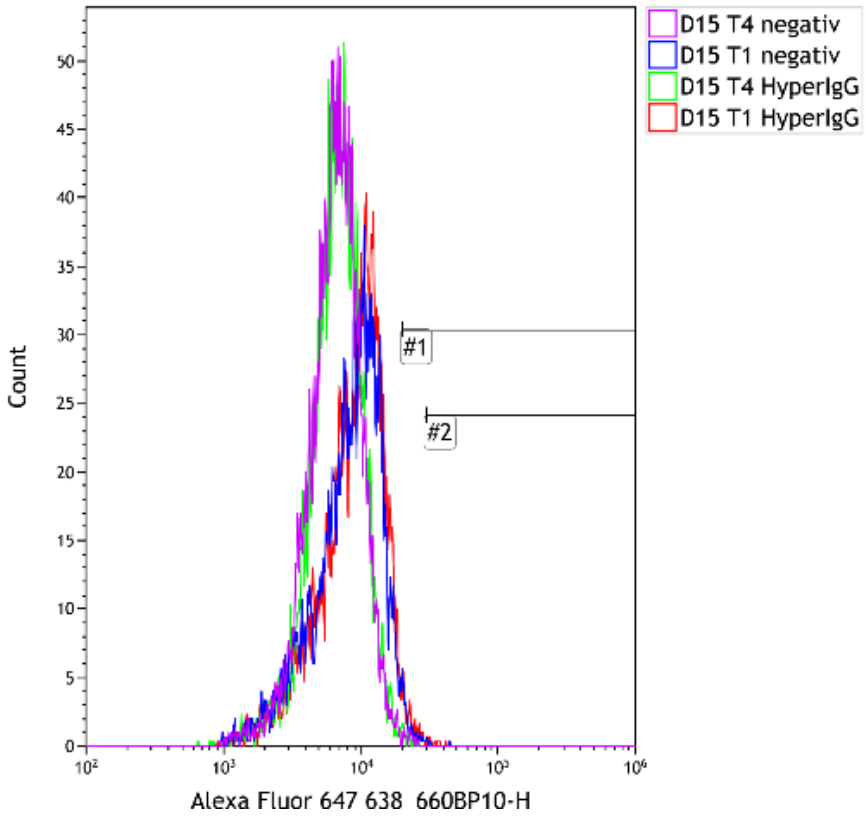

Figure 87: Histogram of fluorescence intensity to cell count on process day 15; HyperimmuneIgG-Biotin (1:10) conjugated to Streptavidin-Alexa 647 (1:100)

Table 22: Sample data of Figure 87: Total %: percentage of cells gated; X-Gmean: geometric mean of the fluorescence intensity; Marker #1 %: percentage of cells with a higher fluorescence intensity than the marker setpoint at the negative control; Marker #1 gmean: geometric mean of the fluorescence intensity of the cells within Marker #1. The same applies for the columns with Marker #2.

Data set	Total [%]	X-Gmean	Marker #1 [%]	Marker #1 X-Gmean	Marker #2 [%]	Marker #2 X-Gmean
D15 T4 negativ	50	6405	0	22362	0	N/A
D15 T1 negativ	39	7977	1	22898	0	33384
D15 T4 HyperIgG	48	6570	0	21658	0	N/A
D15 T1 HyperIgG	41	8513	1	23439	0	35067

Although CR3022 and anti-His give very similar histograms, anti-His has an overall higher mean fluorescence. There is only weak binding for HyperimmuneIgG, compared to its control (Figure 87).

To compare the reactor histograms with each other, I chose the anti-His conjugate, as it has the highest mean fluorescence compared to CR3022 and HyperimmuneIgG (see Figure 79, Figure 80,

Figure 81 and corresponding tables).

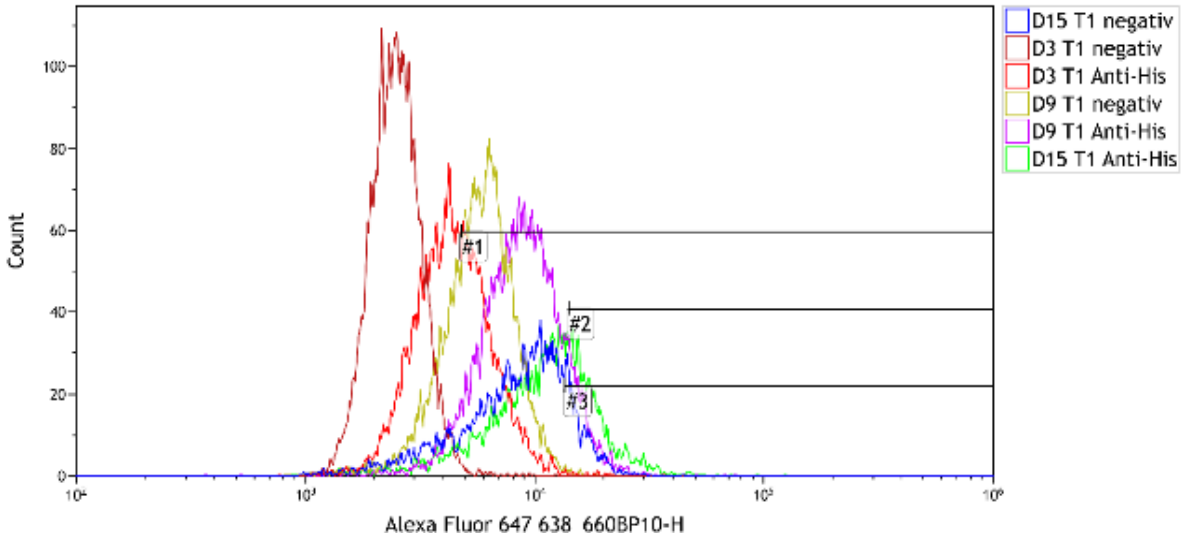

Figure 88: Histogram of fluorescence intensity to cell count of reactor T1 on process day 3, 9 and 15; Anti-His-Biotin (1:100) conjugated to conjugated to Streptavidin-Alexa 647 (1:100)

Table 23: Sample data of Figure 88: Total %: percentage of cells gated; X-Gmean: geometric mean of the fluorescence intensity; Marker #1 %: percentage of cells with a higher fluorescence intensity than the marker setpoint at the negative control; Marker #1 gmean: geometric mean of the fluorescence intensity of the cells within Marker #1. The same applies for the columns with Marker #2.

Data set	Total [%]	X-GMean	Marker #1 [%]	Marker #1 X-Gmean	Marker #2 [%]	Marker #2 X-Gmean	Marker #3 [%]	Marker #3 X-Gmean
D15 T1 negativ	39	7977	32	9702	5	16609	6	15901
D3 T1 negativ	72	2471	0	6021	0	N/A	0	N/A
D3 T1 Anti-His	64	4363	26	6255	0	17801	0	16964
D9 T1 negativ	65	5592	46	6655	0	15458	0	14660
D9 T1 Anti-His	66	8644	62	9183	7	16685	9	16091
D15 T1 Anti-His	40	10447	36	11803	13	18354	14	17787

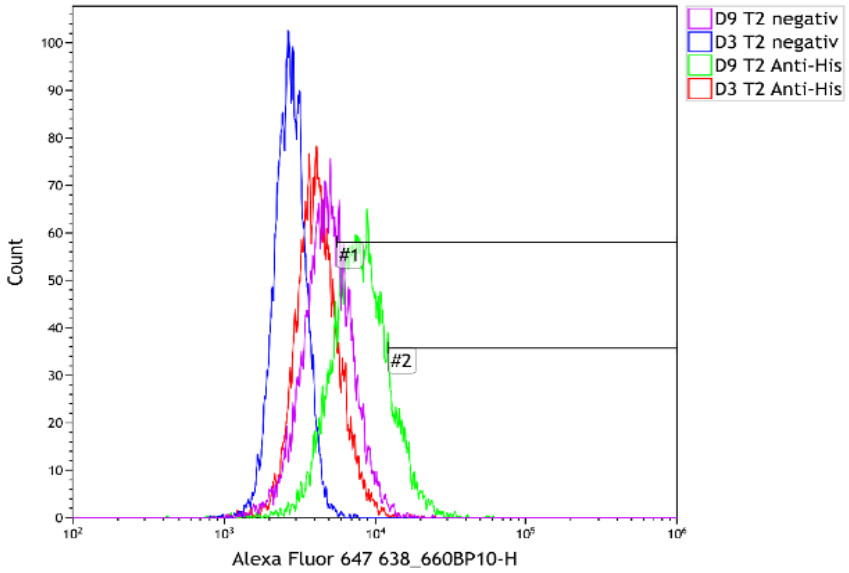

Figure 89: Histogram of fluorescence intensity to cell count of reactor T2 on process day 3 and 9; Anti-His-Biotin (1:100) conjugated to conjugated to Streptavidin-Alexa 647 (1:100)

Table 24: : Sample data of Figure 89: Total %: percentage of cells gated; X-Gmean: geometric mean of the fluorescence intensity; Marker #1 %: percentage of cells with a higher fluorescence intensity than the marker setpoint at the negative control; Marker #1 gmean: geometric mean of the fluorescence intensity of the cells within Marker #1. The same applies for the columns with Marker #2.

Data set	Total [%]	X-GMean	Marker #1 [%]	Marker #1 X-Gmean	Marker #2 [%]	Marker #2 X-Gmean
D9 T2 negativ	65	4797	22	7100	0	14468
D3 T2 negativ	61	2723	0	6346	0	N/A
D9 T2 Anti-His	67	7887	54	9155	10	15584
D3 T2 Anti-His	60	4158	11	6884	0	16245

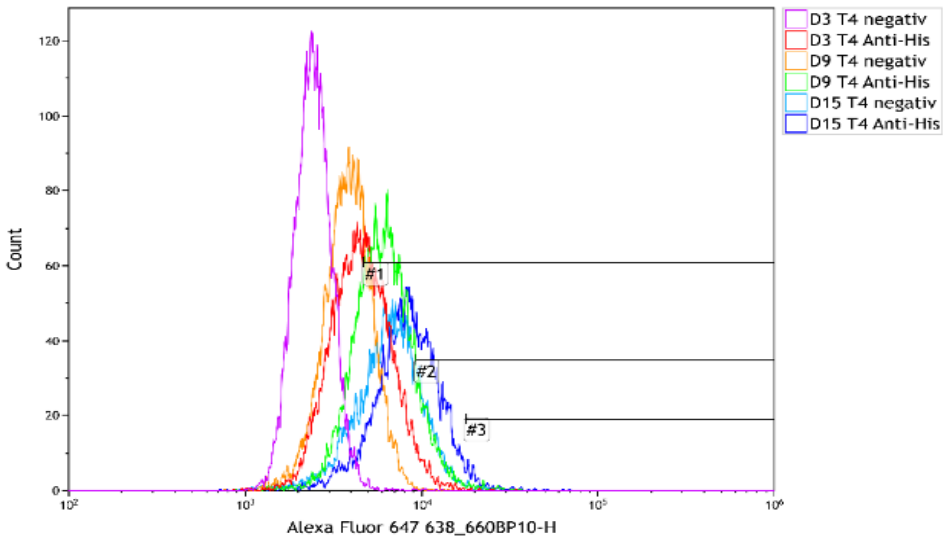

Figure 90 Histogram of fluorescence intensity to cell count of reactor T4 on process day 3, 9 and 15; Anti-His-Biotin (1:100) conjugated to conjugated to Streptavidin-Alexa 647 (1:100)

Table 25: : Sample data of Figure 90: Total %: percentage of cells gated; X-Gmean: geometric mean of the fluorescence intensity; Marker #1 %: percentage of cells with a higher fluorescence intensity than the marker setpoint at the negative control; Marker #1 gmean: geometric mean of the fluorescence intensity of the cells within Marker #1. The same applies for the columns with Marker #2.

Data set	Total [%]	X-GMean	Marker #1 [%]	Marker #1 X-Gmean	Marker #2 [%]	Marker #2 X-Gmean	Marker #3 [%]	Marker #3 X-Gmean
D3 T4 negativ	76	2406	0	6034	0	10797	0	N/A
D3 T4 Anti-His	73	4514	34	6290	3	11137	0	22348
D9 T4 negativ	72	3799	19	5544	0	11158	0	N/A
D9 T4 Anti-His	71	6026	54	7026	9	11576	1	22546
D15 T4 negativ	50	6405	40	7556	10	11352	0	20471
D15 T4 Anti-His	52	8120	48	8876	21	12241	1	22289

T1 seems to have to highest overall mean fluorescence, on all process days measured. The peaks are also spread wider from each other and the control, suggesting it has the highest intracellular product content. T4, despite having a 10fold higher product titer than the other reactors, shows decreased mean fluorescence compared to the others.

4. Discussion

4.1 RBD

The RBD expressing clone 2P7 was subcloned to generate a high producer clone, as 2P7 was generally fast-growing, but relatively low-producing, reaching titer maximums of 20 mg/L in routine culture.

After selection with semi-quantitative and quantitative ELISAs the three top-clones F8, F3 and G7 were chosen. G7 was fastest-growing, reaching a specific growth rate of over 0.9 in the exponential phase, and having 2.5-fold higher productivity than 2P7, but at later passages seemed to decline in productivity and titer to nearly the level of the parental clone (Figure 41). This is a commonly seen result of very fast-growing clones, as epigenetic changes in favor of better cell growth and lower desired protein production take place[36]. F3 and F8 performed growth-and productivity-wise very similar, with only a slightly lower growth rate compared to the parental clone but having a nearly 6-fold higher average qP in routine culture compared to the parental clone (Figure 41).

Under semi-perfusion conditions in 200 mL shaking tubes, the parental clone reached VCDs with nearly 60E6 cells/mL, until sudden culture death which was probably caused by a lack of oxygen.

The purified supernatant of the semi-perfusion was compared with the same steps purified HEK produced RBD. The silver staining on the LDS-PAGE showed fewer bands on the CHO-K1 produced

RBD product than on the HEK produced (Figure 31). Due to the main purification step being a HisTrap column, we can assume that the HEK cells produce more host cell proteins that bind to the HisTrap, therefore the production of the RBD could be favorable in CHO-K1 cells for ease of purification.

Anti-His-biotin Western blots of the supernatant from the 3 top clones confirmed the expression of RBD, as every clone showed a band at the 30kDa marker line (Figure 53). A second band between the 50kDa and the 65 kDa marker line suggests the formation of RBD dimers. The smears over the 185 kDa marker point to a buildup of RBD aggregates with other endogenous proteins.

On a Western blot with HyperimmuneIgG, F3 showed a weak band present at the 30 kDa marker line, further confirming the biological activity of our recombinant RBD (Figure 54).

From our flow cytometry experiment for the intracellular RBD content, we can conclude that HyperimmuneIgG is not suitable as primary conjugate for the RBD clones, as there is only a small difference to the negative control (Figure 75). Binding to CR3022 was also only minimal compared to the control with only one conjugate skipped (Figure 78). With both conjugates skipped in the control sample preparation, the CR3022 FACS for intracellular protein content of the three RBD clones showed uniform monopeaks for every clone (Figure 78). This strongly suggests that the subcloning process was a success, as more than one peak or a high difference in the fluorescence median and the G-mean would point to a population of cells with higher or lower intracellular product content. That would mean the subclone arose from more than one cell and signify a further need for another round of subcloning.

Altogether we can say clones F8 and F3 performed very similar in routine culture and batch. As F3 reached sometimes higher titers and specific productivity (Figure 40, Figure 42) than F8 as well as showing a band on the HyperimmuneIgG Western blot(Figure 54), it is the top-performer.

4.2 CSs

Generally, the CSs is a protein difficult to express as it has a high amount of glycosylation, reported titers ranging to a maximum of 53 mg/L[37], with the addition of VPA to improve expression. To improve on this and to get a stably producing top clone, subcloning of the parental clone C131A4 was performed.

Semi-perfusion of the parental clone showed that VPA had a major effect on productivity (Figure 17 II), increasing it up to 5-fold compared to the control on process day 9. The titer was also greatly increased by VPA, reaching 30 µg/mL on day 9 (Figure 17 I), 3 days after first VPA addition, compared to the maximum titer of 13 µg/mL of the control on day 5. This effect on productivity could not be reproduced in the fed-batch of the subclone C11. As one of the reasons VPA increases productivity is its function as an unspecific histone deacetylase inhibitor, basically reverting epigenetic changes in its genome which could hinder the production of the recombinant protein[6], we can assume that yet no epigenetic changes happened in C11 with a negative impact on CSs production.

The three final subclones had an up to 5-fold higher productivity than the parental clone in routine culture (see Figure 47), with C11 being the top-performer, even though it initially displayed a low µ of only 0.5 (see Figure 43). The low growth rate is common for high producers, as the metabolic burden is higher, and therefore the growth rate is negatively influenced. Over later passages, the growth rate of C11 increased, reaching µs of 0.7 and being on the same level in growth as the rest of the subclones. Regardless of the increase in growth rate and VCD over passage number, the CSs titer and productivity of the subclones did not decrease (see Figure 45 and Figure 46).

Western blot of the routine culture supernatant confirmed the expression of the Anti-His binding CSs at the 185kDa marker line (Figure 53), which is the projected molecular weight of our CSs [15].

Interestingly, only the C11 clone showed a band (around the 185kDA marker line) in a HyperimmuneIgG Western blot (Figure 54). This could point to a lower biological activity or wrong expression of the CSs in the F4 and the G3 cell lines, even though it has to be considered that the total amount of protein loaded on the gel was twice as much on the C11 wells. But compared to the Anti-His Western blot, in which the same amount of supernatant was loaded from the same routine culture passage, there should be a signal band for the F4 and G3 as well (Figure 53).

In the FACS assay for intracellular product content, the low binding of F4 to the HyperimmuneIgG (as well as CR3022) was confirmed, as there is only a minuscule difference to the negative control (Figure 75). The FACS assay with CR3022 of all clones in different days of cultivation showed homogeneous peaks for every cell line (Figure 78), supporting the thesis that the subcloning process was successful, as more than one major subpopulation would give double or more peaks. Even though C11 had substantially higher product titers than F4 and G3 (nearly double the CSs titer) in the supernatant (Figure 58), there is no significant difference in fluorescence signal between them. This could either point to a better product transport out of the cell by C11, or that the cells have an inner 'fixed' concentration equilibrium of CSs and to support it, the product gets ejected if over the concentration limit.

4.3 CSs C11 Fed-batch

The CDM4HEK medium which was used for the fed-batch was already expired for 2 years according to the packaging. A test batch with every CSs clone showed that, surprisingly, the productivity in this medium was even significantly higher than in the previously used CDCHO medium (Figure 56). The addition of G418 in the routine culture medium is unlikely to have caused the lower productivity, as G418 can increase the metabolic load by overexpression of the neomycin resistance gene but has shown no effect on the recombinant protein production[38] .

VPA addition to a process is known to inhibit cell proliferation, so to minimize the negative effect, a common strategy is a biphasic process[5,37], essentially delaying the VPA addition until a high VCD is reached and the exponential growth phase over. VPA, a histone deacetylase inhibitor, is thought to increase productivity in some cell lines by increasing the amount of mRNA for the POI by reversing methylation[39] and reducing chromatin compactness[40] , which could suggest that VPA addition is more effective after several passages, i.e., if the cell line has undergone epigenetic changes, like gene silencing and loss of recombinant gene copy number[41,42], due to the generally high plasticity of the CHO genome[43]. In our Fed-batch, the VPA addition in T1 did not increase productivity or titer of CSs compared to the control reactor (Figure 61). It decreased cell proliferation dramatically, as after VPA addition the viability and the VCD constantly decreased, although compared to the control reactor survived 4 days longer (Figure 60). This could be explained by the generally lower VCD of the VPA reactor, as the initial supply of macronutrients lasted longer. Furthermore, VPA addition decreased the specific glucose consumption of the cells (Figure 62, II), which coincided with a higher lactate consumption (Figure 63, II) and despite several glucose-only feedings, apparently no net lactate was produced daily. It seems that VPA facilitates or supports the metabolic shift from mainly glucose consumption to lactate consumption, which would be contradictory to findings suggesting an accumulation of lactate by VPA[44]. It could also have been influenced or have been the result of inhibited cell proliferation, as lactate is mainly produced as a metabolite in high energy requirement settings (i.e., cell growth) with an abundance of oxygen and glucose available, called the Warburg effect[45]. Lower lactate concentration and lactate consumption is a desired process parameter, as high lactate lowers the pH and therefore requires pH adjustments by base addition, as well as inhibiting cell proliferation[46,47]. Because of the apparent detrimental of lactate effects on cell culture, multiple efforts to curb lactate production through cell engineering and process parameter optimization [33,47,48] were performed. We tried to reduce lactate production by setting the pH in the reactor to 6.8, as

well as setting the DO to a minimum of 30%. Reduced lactate production might be a desirable side effect of VPA. Ammonia, another crucial cell metabolite in cell culture which is known to severely impede cell proliferation, productivity, and product quality[49–51], increased slightly slower in T1 to the end of the process compared to the control T2 (Figure 66). This could be the result of the slower metabolic activity and lower ATP levels of VPA impacted cells [52,53], delaying the onset of higher ammonia production associated with the 'death phase' in the process cell cycle. Intriguingly, after process day 8, T1 had the highest specific oxygen consumption of all reactors (Figure 67 II), despite the reported decreasing effect on oxygen consumption of VPA[53]. The general trend of specific oxygen consumption was simply calculated as a function of the gas inlet flow, which was constant, and the percentage of oxygen added to it. Due to this simplistic approach, the calculated values do not represent oxygen consumption rate (OCR) but rather give a general impression of the oxygen requirement the cultures had. CO_2 requirement of T1 was nearly as high as the control group (Figure 68), even though it had lower VCD. As CO_2 was mainly supplied to lower the pH, the high CO_2 percentages were required to offset the missing lactate in T1.

SEC-MALS of the T1 harvest showed that the average of molar mass 1 (for the trimeric CSs, around 600kDa) in the main peak was elevated compared to T2(607 kDa) and T4(589 kDa) harvest to 610 kDa, which coincides with the steep Molar Mass slope in the main peak (see Figure 73). The higher mean and broad main peak could point to a higher formation of tetrameric aggregates and general product aggregation, which influences product quality negatively and impedes purification. Even though some studies show no negative impact in product quality (in antibodies) by VPA addition[5], there are reports of VPA increasing aggregation and hampering N-glycosylation[54] which could be detrimental for CSs production, as CSs features 22 N-glycosylation sites.

Western blot of the T1 reactor supernatant of process day 3 and process day 9 showed that, as was the case with the control T2, the CSs is expressed correctly in the reactor. The smear above the 185 kDa signal band on process day 9 (Figure 74) suggest the presence of high kDa proteins or aggregates which bind the His-tag antibody as well as CSs aggregates. This could point to the formation of aggregates in the reactor over the course of time.

FACS assay for intracellular product content was done for process day 3, 9 and 15. As expected, there are no major differences in g-mean fluorescence intensity on day 3 between the reactors (Figure 79, Figure 80, Figure 81 and corresponding tables). On day 9, cells of T1 show the highest g-mean fluorescence intensity of all reactors, even though if we subtract the negative control for all, the Fluorescence intensity is the same for cells of T1 and the T2 control reactor (Table 17, Table 18, Table 19). At day 15 the T1 samples showed only minor difference in fluorescence intensity compared to the control, even though it steadily increased over the reactor time (Figure 85, Figure 86, Figure 87 and corresponding tables). Interestingly, not only did the prepared samples have increased fluorescence over the process, but also the negative control samples (Figure 88, Figure 89, Figure 90 and corresponding tables). This could point to either a higher binding of the Alexa Fluor conjugate in the cells as they age, or the accumulation of unspecific streptavidin binding proteins in the cells[55] .

In Reactor T4 the biphasic process consisted of the induction of mild hypothermia (MH) after high cell densities were reached, in our case over 10E6 cells/mL on process day 6 (see Figure 60). MH conditions were achieved by reducing the reactor temperature to 32°C. Only one day after temperature reduction there is a significant decrease in growth rate compared to the control reactor T2, even though at process day 9 the VCD of control and T4 is on the same level (see Figure 60), an interesting phenomenon which has been reported before[37]. So even though a decrease in temperature should decrease the growth rate dramatically [56], the late induction of MH seems to mostly counteract the negative effects on growth associated with MH. As expected[57,58], the viability

of T4 lasted the longest over 80%, which can be attributed mainly due to the delayed onset of apoptosis [59].

CSs titer and the productivity of T4 were highly increased compared to T2 and T1, reaching over 500 mg/L at the peak on process day 14 (see Figure 61). The exact mechanism behind this 10-fold increase in titer by mild hypothermia is still not fully understood, even though most of the findings point to a cell cycle arrest in the G1/G0 phase 60,[8].

Specific Glucose consumption was slightly decreased in T4 compared to control (see Figure 62, II). The average glucose consumption in T4 was 217 pg/c/d (from day 7 to day 12) while the control consumed 302 pg/c/d (from day 7 to day 12) on average. The discrepancy (see Figure 62, II) can be attributed to the lower carbon and energy requirements under MH[59,61,62]. The lowest average glucose consumption had T1(+VPA) with only 192 pg/c/d from day 7 to day 12.

Probably due to a lower glutamate consumption[8] and a shift from glutamine consumption to glutamine generation[9] by cells under MH, the increase and accumulation of ammonia were delayed until day 10, which coincides with the decrease in specific glutamate consumption of the culture (see Figure 65, II). We can assume the accumulation is triggered by the reduced glutamate conversion to glutamine as less glutamine is needed for cell growth at the end of the process.

Reduced lactate production and consumption is a common side effect of MH[63], correlating with the lower glucose consumption and less energy need of the culture [62,64] In T4 we could see the lowest lactate consumption of all reactors (see Figure 63 II), even though it had the same daily glucose concentration as T1 with VPA. But the metabolic shift is clearly visible with the steady decrease of lactate concentration from day 8 until day 12 (see Figure 63 I), even though it never reached zero, as was the case with the other reactors.

T4 had the lowest oxygen requirement of all reactors (see Figure 67 II), slowly decreasing over process time. We can assume this is the result of generally less energy requirement of the cells under MH. T4 also had the lowest CO_2 requirement (Figure 68), which we can attribute to the lactate concentration in the reactor, as CO_2 was used to lower the pH if over the setpoint of 6.8.

SEC-MALS of the purified CSs harvest revealed 2 peaks(Figure 71, Figure 72, Figure 73), one main peak with an average molar mass of 589 kDa, which fits a lower estimate of the molecular weight of the CSs homotrimer. Interestingly, the T4 harvest gave the sharpest peak of all reactors (Figure 72), which, combined with relatively low variation of molar mass inside the peak, points to a homogenic formation of the desired trimers. The T4 harvest was also the only one that showed a distinct small peak for the aggregates over 620 kDa at 1094 kDa. In the T2 and T1 harvest on the other hand (Figure 71, Figure 73) the peak for the aggregates was not discernible from the main peak. The smaller peak points to an aggregation of 2 homotrimer together. We can assume that in the T4 harvest the amount of pure homotrimers is higher than in the control and T1 with VPA. This might be caused by several factors. For one, the total process time of T4 was the longest, and the time to form trimers therefore elongated. The high titer of CSs in T4, which is 10-fold higher than the control, might promote the formation of trimers to, as there is a higher chance of the monomers reacting with each other. The lower reactor temperature might also have had a stabilizing effect on the CSs trimers[65].

Anti-His-Western blot of the T4 reactor supernatant of day 3 and day 9 showed (Figure 74), as was the case with the other reactors, the formation of trimers over the course of time. The smear above the 185kDa marker line, which is most pronounced on the T4 supernatant, suggests the formation of CSs aggregates, but could also be only a side effect of the high amount of product.

FACS assay for internal protein content showed that cells of T4 had generally the same if not less mean fluorescence compared to the control and T1(Figure 85, Figure 82). This is unexpected, as it points to a similar internal CSs content in all the cells, even though T4 had a 10-fold higher titer in the supernatant in the later stages of the process. There is apparently no significant relation between internal protein content and titer in the supernatant with this protein, even though day 9 and 15 had vastly more mean fluorescence intensity (and day 15 more than day 9), the difference to the negative control was not higher than with T2 or T1 cells (Table 14, Table 17, Table 20). There are some factors to be considered: due to the signal sequence fused to the CSs, a high level of secretion is possible, which could make it difficult to quantitatively analyze internal protein content. Therefore, it might be beneficial to block the Golgi-apparatus with Brefeldin A, to inhibit secretion[66].

4.4 CD19-AD2

The clone D19 expressing CD19-AD2 was used for the subcloning process. It had known problems after thawing from liquid nitrogen cold storage, severely lagging behind in growth and viability. One goal of the subcloning was therefore to increase the vitality of the subclones in standard routine culture, next to increased productivity of CD19-AD2.

In a semi-perfusion setting, in an experimental 200 mL shaking tube, the parental clone D19 was tested on VPA response, but due to a failure in the air supply in the control tube no exact conclusion can be drawn to the influence of VPA to the productivity of the clone (Figure 23). Although we can assume that the VPA addition reduced the amount of oxygen required by the culture, which is an observed side effect[53].

The three final clones C2, F9 and E10 were chosen by several rounds of semi-quantitative and quantitative ELISAs. They all performed very similarly in CD19-AD2 production, and in routine culture have a nearly 3-fold higher average productivity than the parental clone D19 (Figure 52). Compared to the parental clone the subclones showed a generally higher growth rate of over 0.8 (Figure 49), and F9 managed to reach VCDs of nearly 8E6 cells/mL (Figure 48). It can be assumed that the subclones have been adjusted to the CDCHO medium better. In monitoring the routine culture, we can discern an increase of product titer and productivity over passage number (Figure 51). This could be also caused by a better adaption to the culture conditions, but it is also worth noticing that the CD19-AD2 standard used for the ELISA (always the same batch used, stored at -20°C) seemed to have declining absorption after 3-4 months, skewing the results. Even though a partial degradation of the standard cannot be excluded, we can at least assume that there is no decline in titer nor productivity after 24 passages, rather the opposite.

To further confirm that our top-clones produce the desired fusion protein, a Western blot was done (Figure 53). CD19-AD2 has a molecular weight of 64kDA[28], but on the western blot we can discern 2 bands in every row of the clones: one slightly under the 65kDA marker, which is our product, and one directly under it. This could point to a partial degradation of the product, either in storage or even already during production.

FACS measurements of the intracellular product content suggest that the subcloning was a success in isolating the clones from a single cell, as only one peak is discernable per clone, and the G-mean doesn't differ greatly from the median (Figure 76, Table 11). The CD19-AD2 clones had nearly double the G-mean value (conjugated with Anti-His) in the routine culture samples compared to RBD and CSs(compare Table 10, Table 11), which might be caused by an easier accumulation of the CD19-AD2 in the intracellular space as it is a transmembrane protein.

Due to the improved vitality compared to the parental clone and a consistently qP (Figure 51) subclone CD19-AD2 F9 is the top performer.

5. Conclusion

Subcloning of the CHO-K1 cell lines expressing different proteins (RBD, CD19-AD2, CSs) increased the productivity without decreasing growth rate or vitality, and in the case of the CD19-AD2 subclones, it increased the general vitality and decreased recovery time after cryogenic freezing and rethawing.

C11, the CSs top-producer subclone was outperforming its parental clone by a 5-fold increased productivity in the routine culture.

In a biphasic reactor process C11, under mild hypothermia conditions, was able to reach titers of 500 mg/L of CSs product, which is nearly 10-fold higher than in the control setup.

The addition of VPA had no positive effect on productivity, with the exception of the parental CSs clone in semi-perfusion, although it increased the culture time and delayed apoptosis in all experiments.

Our FACS assay for internal protein content gave no clear conclusion to the CSs or titer in the supernatant, nor the productivity of a clone, so a revision of the staining protocol with possible addition of Brefeldin A might be necessary.

6. Bibliography

1. Takagi, Y., Kikuchi, T., Wada, R. & Omasa, T. The enhancement of antibody concentration and achievement of high cell density CHO cell cultivation by adding nucleoside. *Cytotechnology* **69**, 511 (2017).
2. Clausen, H., Wandall, H. H., Steentoft, C., Stanley, P. & Schnaar, R. L. Glycosylation Engineering. *Chemical and Engineering News* **84**, 13–22 (2017).
3. Frye, C. *et al.* Industry view on the relative importance of "clonality" of biopharmaceutical-producing cell lines. *Biologicals* **44**, 117–122 (2016).
4. Weinguny, M. *et al.* Subcloning induces changes in the DNA-methylation pattern of outgrowing Chinese hamster ovary cell colonies. *Biotechnology Journal* **16**, 2000350 (2021).
5. Yang, W. C. *et al.* Addition of Valproic Acid to CHO Cell Fed-Batch Cultures Improves Monoclonal Antibody Titers. *Molecular Biotechnology 2013 56:5* **56**, 421–428 (2014).
6. Wulhfard, S., Baldi, L., Hacker, D. L. & Wurm, F. Valproic acid enhances recombinant mRNA and protein levels in transiently transfected Chinese hamster ovary cells. *Journal of Biotechnology* **148**, 128–132 (2010).

7. Becerra, S., Berrios, J., Osses, N. & Altamirano, C. Exploring the effect of mild hypothermia on CHO cell productivity. *Biochemical Engineering Journal* **60**, 1–8 (2012).

8. Wulhfard, S. *et al.* Mild Hypothermia Improves Transient Gene Expression Yields Several Fold in Chinese Hamster Ovary Cells. *Biotechnology Progress* **24**, 458–465 (2008).

9. Torres, M. *et al.* Mild hypothermia upregulates myc and xbp1s expression and improves anti-TNFα production in CHO cells. *PLoS ONE* **13**, (2018).

10. Fan, Y., Ley, D. & Andersen, M. R. Fed-Batch CHO Cell Culture for Lab-Scale Antibody Production. *Methods in Molecular Biology* **1674**, 147–161 (2018).

11. Xu, C. *et al.* Conformational dynamics of SARS-CoV-2 trimeric spike glycoprotein in complex with receptor ACE2 revealed by cryo-EM. *Science Advances* **7**, (2021).

12. Cai, Y. *et al.* Distinct conformational states of SARS-CoV-2 spike protein. *Science (1979)* **369**, (2020).

13. Du, L. *et al.* The spike protein of SARS-CoV — a target for vaccine and therapeutic development. *Nature Reviews. Microbiology* **7**, 226 (2009).

14. Huang, Y., Yang, C., Xu, X., Xu, W. & Liu, S. Structural and functional properties of SARS-CoV-2 spike protein: potential antivirus drug development for COVID-19. *Acta Pharmacologica Sinica 2020 41:9* **41**, 1141–1149 (2020).

15. Watanabe, Y., Allen, J. D., Wrapp, D., McLellan, J. S. & Crispin, M. Site-specific glycan analysis of the SARS-CoV-2 spike. *Science (1979)* **369**, 330–333 (2020).

16. Tian, W. *et al.* O-glycosylation pattern of the SARS-CoV-2 spike protein reveals an "O-Follow-N" rule. *Cell Research* **31**, 1123 (2021).

17. Walls, A. C. *et al.* Structure, Function, and Antigenicity of the SARS-CoV-2 Spike Glycoprotein. *Cell* **181**, 281 (2020).

18. Tortorici, M. A. & Veesler, D. Structural insights into coronavirus entry. *Advances in Virus Research* **105**, 93 (2019).

19. Gui, M. *et al.* Cryo-electron microscopy structures of the SARS-CoV spike glycoprotein reveal a prerequisite conformational state for receptor binding. *Cell Research* **27**, 119 (2017).

20. Hwang, S. S. *et al.* Cryo-EM structure of the 2019-nCoV spike in the prefusion conformation. *Science (New York, N.y.)* **367**, 1260 (2020).

21. Amanat, F. *et al.* A serological assay to detect SARS-CoV-2 seroconversion in humans. *Nature Medicine 2020 26:7* **26**, 1033–1036 (2020).

22. Mayrhofer, P., Hunjadi, M. & Kunert, R. Functional Trimeric SARS-CoV-2 Envelope Protein Expressed in Stable CHO Cells. *Frontiers in Bioengineering and Biotechnology* **9**, (2021).

23. Hoffmann, M., Kleine-Weber, H. & Pöhlmann, S. A Multibasic Cleavage Site in the Spike Protein of SARS-CoV-2 Is Essential for Infection of Human Lung Cells. *Molecular Cell* **78**, 779-784.e5 (2020).

24. Lan, J. *et al.* Structure of the SARS-CoV-2 spike receptor-binding domain bound to the ACE2 receptor. *Nature 2020 581:7807* **581**, 215–220 (2020).

25. Tai, W. *et al.* Characterization of the receptor-binding domain (RBD) of 2019 novel coronavirus: implication for development of RBD protein as a viral attachment inhibitor and vaccine. *Cellular & Molecular Immunology 2020 17:6* **17**, 613–620 (2020).

26. Law, J. L. M. *et al.* SARS-COV-2 recombinant Receptor-Binding-Domain (RBD) induces neutralizing antibodies against variant strains of SARS-CoV-2 and SARS-CoV-1. *Vaccine* **39**, 5769 (2021).

27. Wang, K., Wei, G. & Liu, D. CD19: a biomarker for B cell development, lymphoma diagnosis and therapy. *Experimental Hematology & Oncology 2012 1:1* **1**, 1–7 (2012).

28. Lobner, E. *et al.* Getting CD19 Into Shape: Expression of Natively Folded "Difficult-to- Express" CD19 for Staining and Stimulation of CAR-T Cells. *Frontiers in Bioengineering and Biotechnology* **8**, 49 (2020).

29. Young, C. L., Britton, Z. T. & Robinson, A. S. Recombinant protein expression and purification: A comprehensive review of affinity tags and microbial applications. *Biotechnology Journal* **7**, 620–634 (2012).

30. Joung, C. H. *et al.* Production and characterization of long-acting recombinant human albumin–EPO fusion protein expressed in CHO cell. *Protein Expression and Purification* **68**, 137–145 (2009).

31. Kunert, R. & Casanova, E. Recent advances in recombinant protein production. *http://dx.doi.org/10.4161/bioe.24060* **4**, 258–261 (2013).

32. Kempken, R., Berthold, W. & Thomse, K. Significance of Specific Productivity for the Effectiveness and Consistency of Mammalian Cell Cultivation. *Animal Cell Technology: Developments Towards the 21st Century* 561–565 (1995) doi:10.1007/978-94-011-0437-1_88.

33. Zagari, F., Jordan, M., Stettler, M., Broly, H. & Wurm, F. M. Lactate metabolism shift in CHO cell culture: the role of mitochondrial oxidative activity. *New Biotechnology* **30**, 238–245 (2013).

34. Brunner, M., Doppler, P., Klein, T., Herwig, C. & Fricke, J. Elevated pCO2 affects the lactate metabolic shift in CHO cell culture processes. *Engineering in Life Sciences* **18**, 204–214 (2018).

35. Watanabe, Y., Allen, J. D., Wrapp, D., McLellan, J. S. & Crispin, M. Site-specific glycan analysis of the SARS-CoV-2 spike. *Science (1979)* **369**, 330–333 (2020).

36. Yang, Y., Mariati, Chusainow, J. & Yap, M. G. S. DNA methylation contributes to loss in productivity of monoclonal antibody-producing CHO cell lines. *Journal of Biotechnology* **147**, 180–185 (2010).

37. Johari, Y. B. *et al.* Production of trimeric SARS-CoV-2 spike protein by CHO cells for serological COVID-19 testing. *Biotechnology and Bioengineering* **118**, 1013–1021 (2021).

38. Yallop, C. A. & Svendsen, I. The effects of G418 on the growth and metabolism of recombinant mammalian cell lines. *Cytotechnology* **35**, 101 (2001).

39. SARKAR, S. *et al.* Histone Deacetylase Inhibitors Reverse CpG Methylation by Regulating DNMT1 through ERK Signaling. *Anticancer Research* **31**, (2011).

40. Rountree, M. R., Bachman, K. E., Herman, J. G. & Baylin, S. B. DNA methylation, chromatin inheritance, and cancer. *Oncogene 2001 20:24* **20**, 3156–3165 (2001).

41. Paredes, V., Park, J. S., Jeong, Y., Yoon, J. & Baek, K. Unstable expression of recombinant antibody during long-term culture of CHO cells is accompanied by histone H3 hypoacetylation. *Biotechnology Letters* **35**, 987–993 (2013).

42. Bailey, L. A., Hatton, D., Field, R. & Dickson, A. J. Determination of Chinese hamster ovary cell line stability and recombinant antibody expression during long-term culture. *Biotechnology and Bioengineering* **109**, 2093–2103 (2012).

43. Feichtinger, J. *et al.* Comprehensive genome and epigenome characterization of CHO cells in response to evolutionary pressures and over time. *Biotechnology and Bioengineering* **113**, 2241–2253 (2016).

44. Doval, M. *et al.* Effect of valproate on lactate and glutamine metabolism by rat renal cortical tubules. *Proc Soc Exp Biol Med* **190**, 357–364 (1989).

45. Buchsteiner, M., Quek, L. E., Gray, P. & Nielsen, L. K. Improving culture performance and antibody production in CHO cell culture processes by reducing the Warburg effect. *Biotechnology and Bioengineering* **115**, 2315–2327 (2018).

46. Lao, M. S. & Toth, D. Effects of ammonium and lactate on growth and metabolism of a recombinant Chinese hamster ovary cell culture. *Biotechnology Progress* **13**, 688–691 (1997).

47. Pérez-Rodriguez, S., Ramírez-Lira, M. de J., Trujillo-Roldán, M. A. & Valdez-Cruz, N. A. Nutrient supplementation strategy improves cell concentration and longevity, monoclonal antibody production and lactate metabolism of Chinese hamster ovary cells. *Bioengineered* **11**, 463–471 (2020).

48. Xu, S., Hoshan, L. & Chen, H. Improving lactate metabolism in an intensified CHO culture process: productivity and product quality considerations. *Bioprocess Biosyst Eng* **39**, 1689–1702 (2016).

49. Chitwood, D. G. *et al.* Characterization of metabolic responses, genetic variations, and microsatellite instability in ammonia-stressed CHO cells grown in fed-batch cultures. *BMC Biotechnology 2021 21:1* **21**, 1–16 (2021).

50. Lao, M.-S. & Toth, D. Effects of Ammonium and Lactate on Growth and Metabolism of a Recombinant Chinese Hamster Ovary Cell Culture. *Biotechnology Progress* **13**, 688–691 (1997).

51. Kim, D. Y. *et al.* Fed-batch CHO cell t-PA production and feed glutamine replacement to reduce ammonia production. *Biotechnology Progress* **29**, 165–175 (2013).

52. Salsaa, M. *et al.* Valproate inhibits mitochondrial bioenergetics and increases glycolysis in Saccharomyces cerevisiae. *Scientific Reports 2020 10:1* **10**, 1–11 (2020).

53. Komulainen, T. *et al.* Sodium valproate induces mitochondrial respiration dysfunction in HepG2 in vitro cell model. *Toxicology* **331**, 47–56 (2015).

54. Fischer, S. *et al.* miR-2861 as novel HDAC5 inhibitor in CHO cells enhances productivity while maintaining product quality. *Biotechnology and Bioengineering* **112**, 2142–2153 (2015).

55. Norton, R., Heuzenroeder, M. & Manning, P. A. Non-specific serum binding to streptavidin in a biotinylated peptide based enzyme immunoassay. *J Immunoassay* **17**, 195–204 (1996).

56. Chen, Z.-L., Wu, B.-C., Liu, H., Liu, X.-M. & Huang, P.-T. Temperature shift as a process optimization step for the production of pro-urokinase by a recombinant Chinese hamster ovary cell line in high-density perfusion culture. *J Biosci Bioeng* **97**, 239–243 (2004).

57. Vergara, M. *et al.* Endoplasmic Reticulum-Associated rht-PA Processing in CHO Cells: Influence of Mild Hypothermia and Specific Growth Rates in Batch and Chemostat Cultures. *PLoS ONE* **10**, (2015).

58. E, T. *et al.* Process parameter shifting: Part I. Effect of DOT, pH, and temperature on the performance of Epo-Fc expressing CHO cells cultivated in controlled batch bioreactors. *Biotechnol Bioeng* **94**, 1033–1044 (2006).

59. Moore, A. *et al.* Effects of temperature shift on cell cycle, apoptosis and nucleotide pools in CHO cell batch cultues. *Cytotechnology* **23**, 47 (1997).

60. Bedoya-López, A. *et al.* Effect of Temperature Downshift on the Transcriptomic Responses of Chinese Hamster Ovary Cells Using Recombinant Human Tissue Plasminogen Activator Production Culture. *PLoS ONE* **11**, 151529 (2016).

61. SK, Y. *et al.* Adaptation of Chinese hamster ovary cells to low culture temperature: cell growth and recombinant protein production. *J Biotechnol* **122**, 463–472 (2006).

62. Fogolín, M. B., Wagner, R., Etcheverrigaray, M. & Kratje, R. Impact of temperature reduction and expression of yeast pyruvate carboxylase on hGM-CSF-producing CHO cells. *J Biotechnol* **109**, 179–191 (2004).

63. M, B.-F. *et al.* Temperature reduction in cultures of hGM-CSF-expressing CHO cells: effect on productivity and product quality. *Biotechnol Prog* **21**, 17–21 (2005).

64. Yoon, S. K., Choi, S. L., Song, J. Y. & Lee, G. M. Effect of culture pH on erythropoietin production by Chinese hamster ovary cells grown in suspension at 32.5 and 37.0 degrees C. *Biotechnol Bioeng* **89**, 345–356 (2005).

65. Martí, D., Torras, J., Bertran, O., Turon, P. & Alemán, C. Temperature effect on the SARS-CoV-2: A molecular dynamics study of the spike homotrimeric glycoprotein. *Computational and Structural Biotechnology Journal* **19**, 1848–1862 (2021).

66. Chardin, P. & McCormick, F. Brefeldin A: The Advantage of Being Uncompetitive. *Cell* **97**, 153–155 (1999).

7. Appendix

7.1 Abbreviations and units

°C - degree Celsius

Aa – amino acid

AD2 - albumin domain 2

BSA - bovine serum albumin

CC – cell count

CD19 – cluster of differentiation 19

CHO – Chinese hamster ovary cells

CSs – Covid spike soluble

D – days

Da – Dalton

DTT - dithiothreitol

EDTA - ethylenediaminetetraacetic acid

ELISA – enzyme linked immunsorbent assay

EtOH - ethanol

Fc - Fragment crystallizable

HPLC – high-pressure liquid chromatography

G - gram

g-mean – geometric mean

H - hour

HEK – human embryonic kidney cells

HRP - horse-radish peroxidase

HSA – Human serum albumin

IgG – immunoglobin G

kDa - Kilodalton [g/mol]

L - liter

LDS - lithium dodecyl sulfate

M - molarity [mol/L]

Mg - milligram

MH – mild hypothermia

Min - minute

mL - milliliter

Ng - nanogram

Nm - nanometer

PAGE - Polyacrylamide gel electrophoresis

PBS - phosphate buffered saline

PBST - phosphate buffered saline + Tween

Pg - picogram

PVP - Polyvinylpyrrolidone

RBD - receptor binding domain

RC – routine culture

Rpm - revolutions per minute

SARS-COV-2 - severe acute respiratory syndrome coronavirus type 2

Sec -second

TFF - tangential flow filtration

TMB - 3,3',5,5'-Tetramethylbenzidine

TRIS - Tris(hydroxymethyl)-aminomethane

UV - ultraviolet

VCD – viable cell density

W - watt

WV - working volume

µ - specific growth rate [d-1]

µg - Microgram

µL - Microliter

7.2 Construct sequences:

RBD amino acid sequence | 243 aa

MFVFLVLLPLVSSQRVQPTESIVRFPNITNLCPFGEVFNATRFASVYAWNRKRISNCVADYSVLYNSASFSTFKCYGV
SPTKLNDLCFTNVYADSFVIRGDEVRQIAPGQTGKIADYNYKLPDDFTGCVIAWNSNNLDSKVGGNYNYLYRLFRKS
NLKPFERDISTEIYQAGSTPCNGVEGFNCYFPLQSYGFQPTNGVGYQPYRVVVLSFELLHAPATVCGPKKSTNLVKN
KCVNFHHHHHH

S protein Signal peptide
CoV-2 RBD S sequence
6x His-tag

CSs amino acid sequence| 1256 aa

MFVFLVLLPLVSSQCVNLTTRTQLPPAYTNSFTRGVYYPDKVFRSSVLHSTQDLFLPFFSNVTWFHAIHVSGTNGTKR
FDNPVLPFNDGVYFASTEKSNIIRGWIFGTTLDSKTQSLLIVNNATNVVIKVCEFQFCNDPFLGVYYHKNNKSWMES
EFRVYSSANNCTFEYVSQPFLMDLEGKQGNFKNLREFVFKNIDGYFKIYSKHTPINLVRDLPQGFSALEPLVDLPIGINI
TRFQTLLALHRSYLTPGDSSSGWTAGAAAYYVGYLQPRTFLLKYNENGTITDAVDCALDPLSETKCTLKSFTVEKGIY
QTSNFRVQPTESIVRFPNITNLCPFGEVFNATRFASVYAWNRKRISNCVADYSVLYNSASFSTFKCYGVSPTKLNDLC
FTNVYADSFVIRGDEVRQIAPGQTGKIADYNYKLPDDFTGCVIAWNSNNLDSKVGGNYNYLYRLFRKSNLKPFERDI
STEIYQAGSTPCNGVEGFNCYFPLQSYGFQPTNGVGYQPYRVVVLSFELLHAPATVCGPKKSTNLVKNKCVNFNFN

GLTGTGVLTESNKKFLPFQQFGRDIADTTDAVRDPQTLEILDITPCSFGGVSVITPGTNTSNQVAVLYQDVNCTEVPV
AIHADQLTPTWRVYSTGSNVFQTRAGCLIGAEHVNNSYECDIPIGAGICASYQTQTNSPASVASQSIIAYTMSLGAE
NSVAYSNNSIAIPTNFTISVTTEILPVSMTKTSVDCTMYICGDSTECSNLLLQYGSFCTQLNRALTGIAVEQDKNTQEV
FAQVKQIYKTPPIKDFGGFNFSQILPDPSKPSKRSFIEDLLFNKVTLADAGFIKQYGDCLGDIAARDLICAQKFNGLTVL
PPLLTDEMIAQYTSALLAGTITSGWTFGAGAALQIPFAMQMAYRFNGIGVTQNVLYENQKLIANQFNSAIGKIQDS
LSSTASALGKLQDVVNQNAQALNTLVKQLSSNFGAISSVLNDILSRLDPPEAEVQIDRLITGRLQSLQTYVTQQLIRAA
EIRASANLAATKMSECVLGQSKRVDFCGKGYHLMSFPQSAPHGVVFLHVTYVPAQEKNFTTAPAICHDGKAHFPRE
GVFVSNGTHWFVTQRNFYEPQIITTDNTFVSGNCDVVIGIVNNTVYDPLQPELDSFKEELDKYFKNHTSPDVDLGDI
SGINASVVNIQKEIDRLNEVAKNLNESLIDLQELGKYEQYIKWPSGRLVPRGSPGSGYIPEAPRDGQAYVRKDGEWV
LLSTFLGHHHHHH

S protein Signal peptide
CoV-2 S sequence
Thrombin cleavage site
T4 Trimer-Foldon Domain
6x His-tag

CD19-AD2
Amino acid sequence:
MPPPRLLFFLLFLTPMEVRPEEPLVVKVEEGDNAVLQCLKGTSDGPTQQLTWSRESPLKPFLKLSLGLPGL
GIHMRPLAIWLFIFNVSQQMGGFYLCQPGPPSEKAWQPGWTVNVEGSGELFRWNVSDLGGLGCGLKN
RSSEGPSSPSGKLMSPKLYVWAKDRPEIWEGEPPCLPPRDSLNQSLSQDLTMAPGSTLWLSCGVPPDSVS
RGPLSWTHVHPKGPKSLLSLELKDDRPARDMWVMETGLLLPRATAQDAGKYYCHRGNLTMSFHLEITA
RP VLWHWLLRTGGWKGGGGSGGGGSGGGGSDEGKASSAKQRLKCASLQKFGERAFKAWAVARL
SQRFPKAEFAEVSKLVTDLTKVHTECCHGDLLECADDRADLAKYICENQDSISSKLKECCEKPLLEKSHCIAE
VENDEMPADLPSLAADFVESKDVCKNYAEAKDVFLGMFLYEYARRHPDYSVVLLLRLAKTYETTLEKCCAA
ADPHECYAKVFDEFKPGTSHHHHHHHHHHHH

Native leader
CD19-ECD
HAS-AD2
His-tag

7.3 List of figures and tables